الجمهورية الجزائرية الديمقراطية الشعبية

République Algérienne Démocratique et Populaire

Ministère de l'Enseignement Supérieur et de la Recherche Scientifique
Ecole Supérieure des Sciences Appliquées d'Alger

وزارة التعليم العالي والبحث العلمي
المدرسة العليا في العلوم التطبيقية بالجزائر

Département du second cycle

Mémoire de Fin d'Etudes

En vue de l'obtention du diplôme d'ingéniorat d'état

Filière **: Electrotechnique**

Spécialité : **Traction électrique**

Thème :

La commande prédictive à base de modèle (MPC) et les réseaux de neurones (NN), application à l'entrainement électrique et aux convertisseurs de puissance

Présenté par : HATTABI Intissar
Et par : BOUBERGOUG Aya

Encadré (e) par : Dr. BENACHOUR Ali
Co-encadré(e) par : Dr. Dali Ali

Soutenu le : 17/07/2021

Devant le jury composé de :

M	**ARBID Mahmoud**	**Président**
M	**TEFFAHI Abdelkader**	**Examinateur**
M	**BENACHOUR Ali**	**Encadreur**
M	**DALI Ali**	**Co-Encadreur**

Binôme N° : 07/PFE /TR/ 2021

ملخص:

إن الهدف الرئيسي من هذا الموضوع يتلخص في دراسة وتنفيذ التحكم التنبؤي استنادا على النموذج (MPC) ثم على الشبكات العصبونية الاصطناعية المطبقة على المحركات الكهربائية ومحولات الطاقة الكهربائية بغرض تحسين أداء أنظمتنا. نبدأ دراستنا بنبذة حول المحولات المصفوفية والتحكم التنبؤي من خلال تقديم بعض الطوبولوجيات من MC، بعض تطبيقات التحكم التنبؤي وتحسيناته وأخيرا لمحة على الشبكات العصبونية الاصطناعية. تم تطبيق التحكم التنبؤي المستند على النموذج MPCCثم على الشبكات العصبونية الاصطناعية على شحنة RL التي يغذيها مموج في البداية، ثم طوبولوجيتين من MC. ثم تم تطبيق التحكم التنبؤي القائم على النموذج (MPTC) و (ANN-MPTC) أيضاً على آلة تحفيز تعمل بواسطة مموج ثلاثي الدور ثم أجريت مقارنة بين التحكمين المقترحين لكل اختبار.

كلمات مفتاحية:

مموج مصفوفي (MC)،آلة لا تزامنية،التحكم التنبؤي (MPC)،دالة التكلفة، الشبكات العصبونية الاصطناعية

Abstract:

The main objective of this topic is to study and implement predictive control based (MPC) model, neural networks applied to electrical drive and power converters, in order to improve performances of ours systems. We begin our study with a state of the art on matrix converters and predictive control by presenting some topologies of the MC, some applications of predictive control and its improvements and finally a glimpse into artificial neural networks. Then, the model predictive current control (MPCC) and artificial neural networks based MPCC (ANN-MPCC) were applied to an RL charge fed by an inverter then by two topologies of the MC. Furthermore, a model predictive torque control (MPTC) and ANN-MPTC were also applied to the induction machine fed by a three-phase inverter. A comparison between the two proposed strategies was introduced for each test.

Key words:

Matrix Converter (MC), induction machine, Model Predictive Control (MPC), cost function, artificial neural network.

Résumé :

L'objectif principal de ce sujet est d'étudier et implémenter la commande prédictive à base du model (MPC) puis à base des réseaux de neurones appliqué à l'entrainement électrique et aux convertisseurs de puissance pour améliorer les performances de nos systèmes. Nous commençons notre étude par un état de l'art sur les convertisseurs matriciels et sur la commande prédictive en présentant quelques topologies du MC, quelques applications de la commande prédictive et ses améliorations et finalement un aperçu sue les réseaux de neurones artificiels. Ensuite, la commande prédictive du courant à

base du modèle (MPCC) puis à base des réseaux de neurones artificiels a été appliquée à une charge RL alimentée par un onduleur au premier temps, et puis par deux topologies du MC. Ensuite la commande prédictive à base du modèle (MPTC) et ANN-MPTC a été aussi appliquée sur une machine à induction alimentée par un onduleur triphasé. Une comparaison entre les deux commandes proposées a été établie pour chaque essai.

Mots clés :

Convertisseur Matriciel (MC), machine asynchrone, la commande prédictive à base du modèle (MPC), fonction de coût, les réseaux de neurones artificiels.

Acknowledgment

Foremost, we would like to give our sincere gratitude to Allah Almighty for giving us ability, knowledge and strength to complete our research study. Without His continuous blessings, it would not be possible.

We would like to express our sincere and deepest appreciationto our advisor Dr.BENACHOUR Ali and to our co-advisor Dr. DALI Ali, for their help and continuous invaluable support, for their patience, and their infinite constructive guidance and advices. For their motivation and their belief in us and the final fruit we have been working on.

We also like to extent our heartfelt thanks to the members of the board of examiners for proofreading and examining our thesis. We would like to thank Dr. ARBID Mahmoud who give us the honor of chairing the committee. Our thanks also go to
Mr.TEFFAHI Abd el kader who gave us the honor of participating in the committee.
We are also grateful to the staff at the Higher School of Applied Sciences of Algiers especially those from the Electrical Engineering department especially
Dr. HAMACHE Amar and Dr. ABERBOUR Adel.

Our extended deep thanks to MEKHILEF Aymen for his help during this work. It would not possible to conclude this work. Without mentioning our families and their unconditional love and support, our friends and their meaningful backup, and everyone who has believed in us.

Dedication

First of all , I would like to thank the person who never stopped to support me, to believe in me, to watch over my success from a very young age, to whom I owe what I became today, and what I will become in the future, my precious mother.

I dedicate this work

To my late father, whom I hope to be proud of me, may God welcomes him into his vast paradise.

To my Grandmother, May Allah prolongs her life and grants her health.

To my brother KARIM, my confident, the person who always takes care of me, may god bless him.

To my sisters CHAYMA and NOOR who are always there for me.

To my late childhood friend Imane , may God welcomes her into his vast paradise

To my best friend Aya who never stopped believing in me and for her precious help as partner.

To My friends Maroua and Sonia

INTISSAR

Dedication

I dedicate this project

To my dear parents MOHAMMED and SONIA this is for that look on your faces when I told you the good news , thank you to never stopped, to say prayers for me, to support me , make me happy and believe on me so that I can achieve my goals.

To my lovely brothers, IYED and ABD EL OUADOUD this is for your permanent support, you were in my sides in every step

To my dear grandparents AMAR, BRAHIM and my force DALILA, Whom I wish good health, this is for your support indefectible.

To my dear partner and best friend, Intissar for her understanding and her sympathy.

To my best friend YOUSRA, thank you to be in my life

To my dear friends, AMIRA, NARIMEN, MANEL, MAROUA, SONIA who helped me and supported me in difficult time.

To all those I love and those who love me

AYA

Table of contents

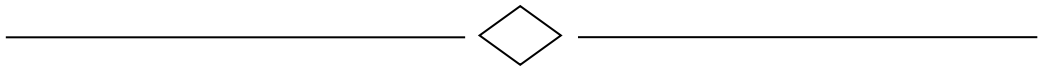

Table of content

LIST OF TABLES

TABLE OF FIGURES

LIST OF SYMBOLS AND ACRONYMS

GENERAL INTRODUCTION 1

CHAPTER ONE

INTRODUCTION 3

I.1 STATE OF THE ART OF THE INVERTERS 3

I.2 THREE PHASE INVERTER 3

I.3 STATE OF THE ART OF MATRIX CONVERTERS 4

I.3.1 Direct matrix converter 5

I.3.2 Indirect matrix converters 6

I.3.3 Different structures of indirect matrix converters 7

I.4 STATE OF THE ART OF MODEL PREDICTIVE CONTROL 9

I.4.1 Introduction 9

I.4.2 Development of MPC (History) 9

I.4.3 Working Principal of MPC 10

I.4.4 MPC Strategy 11

I.4.5 MPC's Elements 12

I.4.6 Prediction Model 12

I.4.7 Objective Function 13

I.4.8 Obtaining the control law 13

I.4.9 The major problem of the MPC 14

I.4.10 Different methods of improving MPC's performance 14

I.5 MODEL PREDICTIVE CONTROL BASED ON NEURAL NETWORK 16

I.5.1 Overview of neural networks 16

I.5.2 How ANN Systems are applied 20

I.6 CONCLUSION 21

CHAPTER TWO

INTRODUCTION 22

II.1 ARTIFICIAL NEURAL NETWORK BASED MPCC 22

II.2 SYSTEM MODELING 23

II.2.1 Inverter model 23

II.2.2 Load model 25

II.2.3 Model predictive control 25

II.3 THE PROPOSED ARTIFICIAL NEURAL NETWORKS ARCHITECTURES 29

II.3.1 Perceptron neural network 30

II.3.2 Artificial Neural Network Fitting (fitnet) 31

II.4 ANN TRAINING PROCEDURE 31

II.5 SIMULATION RESULTS AND ANALYSIS 34

II.6 COMPARISON OF THE THREE METHODS 40

II.7 IMPLEMENTATION OF ANN-MPCC 41

II.8 CONCLUSION 44

CHAPTER THREE

INTRODUCTION 45

III.1ARTIFICIAL NEURAL NETWORK BASED MPTC 45

III.2SYSTEM MODELING 46

III.2.1 Electrical equations 48

III.2.2 Magnetic equations 48

III.2.3 Mechanical equation 49

III.2.4 Cost function 52

III.2.5 Working principle 53

III.3 IMPLEMENTATION 56

III.4 ARTIFICIAL NEURAL NETWORK TRAINING PRINCIPLE 57

III.5SIMULATION AND RESULTS 61

III.6CONCLUSION 68

CHAPTER FOUR

INTRODUCTION 69

IV.1 MODELING OF THE INPUT FILTER 69

IV.2 MODELING OF THE DIRECT MATRIX CONVERTER (DMC) 71

IV.3 MODELING OF THE INDIRECT MATRIX CONVERTER (IMC) 73

IV.4 WORKING PRINCIPLE OF MPCC 75

IV.5 IMPLEMENTATION OF THE MPC 76

IV.6 TRAINING PROCEDURE 77

IV.7 SIMULATION AND RESULTS 79

IV.8 CONCLUSION 88

GENERAL CONCLUSION…. 89

APPENDIX A 96

APPENDIX B 97

APPENDIX C 99

List of figures

List of figures

Figure I- 1 : Three phase inverter topology 4
Figure I- 2: Classification of power converters.....5
Figure I- 3: Direct matrix converter (DMC) 6
Figure I- 4: Indirect Matrix Converter (IMC) 6
Figure I- 5: Structure of a conventional indirect matrix converter 7
FigureI-6:Sparse matrix converter (SMC).....8
Figure I- 7: Very sparse matrix converter 8
Figure I- 8: Ultra sparse matrix converter (USMC) 8
Figure I- 9: Multi level IMC 9
Figure I- 10: Classification of predictive control methods used in power electronic 10
Figure I- 11: Working principle of MPC 11
Figure I- 12: Basic structure of MPC.....12
Figure I- 13: A three-layer neural network system 17
Figure I- 14: The feed-forward neural network.....19
Figure I- 15: Simple recurrent neural network.....19
Figure I- 16: Diagram of a Self-Organizing Map.....20
Figure I- 17: An overview of the proposed control strategy 21
Figure II- 1 : Three phase inverter topology.....24
Figure II- 2 : Voltage source inverter power circuit 23
Figure II- 3 : Flow diagram of MPCC.....27
Figure II- 4 : Voltage vectors in the complex plane 29
Figure II- 5 : (a) perceptron neural network scheme, (b) the activation function hard-lim.30
Figure II- 6 : General topology of the 15-neuron hidden layer feed-forward ANN 32
Figure II- 7 : General topology of single layer perceptron neural network 32
Figure II- 8 : (a) fitting neural network performances,(b)fitting neural network regression33
Figure II- 9: (a) confusion matrix of PNN, (b) training performance of PNN 33
Figure II- 10 : Simulation results of current control of a two-level inverter-fed RL-load: Reference and output current of phase A and their zoom. (a): MPCC, (b): PNN, (c): fitnet35

Figure II- 11 : Simulation results of current control of a two level inverter-fed RL-load Output current and output voltage spectra expressed as percentages of fundamental magnitude,$|I*| = 3$ A and $f* = 50$ Hz with (a) MPC, (b) fitnet, (c) PNN 36
Figure II- 12: Simulation results of current control of a two-level inverter-fed RL-load: Output voltage of the inverter and $50 \times$the load current of phase A with: (a) MPC, (b) fitnet, (c) PNN 37
Figure II- 13: Simulation results of current control of a two-level inverter-fed RL-load: output current of phase A with PNN and fitnet (NFTOOL) for different magnitude and different frequencies 38
Figure II- 14 : Comparison of the THD of the output current obtained by the three proposed control strategies, for some cases, under different operating conditions. 38
Figure II- 15 : laboratory materials 42
Figure II- 16 : The blocs used for implementation Test 43
Figure II- 17 : the blocs that will be used for real implementation 43
Figure II- 18 : the PWM signals (a) 44
Figure III- 1 : Schematic representation of the three-phase asynchronous machine 47
Figure III- 3 : Coordinate transformation 50
Figure III- 4 : MPTC scheme 53
Figure III- 5 : Flow diagram of the MPTC 55
Figure III- 6 : PI speed controller 57
Figure III- 7 : General topology of multilayer Feed Forward Back-propagation neural network of MPC 59
Figure III- 8 : General topology of multilayer Feed Forward Back propagation neural network of PI 59
Figure III- 9 : performance of Feed forward back-propagation neural network based 60
Figure III- 10 : Regression training of: (a) MPC, (b) PI 60
Figure III- 11: Simulation results (rotor speed and its reference) of an inverter-fed induction machine with: (a) ANN-MPTC, (b) MPTC 62
Figure III- 12: Simulation results (rotor speed and its reference) of an inverter-fed induction machine with: (a) ANN-MPTC, (b) MPTC and theirs zoom (c) ANN-MPTC, (d) MPTC 62

Figure III- 13: Simulation results of stator flux of an inverter-fed induction machine with (a) ANN-MPTC, (b) MPTC and theirs zoom (c) ANN-MPTC, (d) MPTC.....63
Figure III- 14: Simulation results of output voltage of an inverter-fed induction machine with (a) ANN-MPTC, (b) MPTC and theirs zoom (c) ANN-MPTC, (d) MPTC.....64
Figure III- 15 : Simulation results of stator current of an inverter-fed induction machine with (a) ANN-MPTC, (b) MPTC and theirs zoom (c) ANN-MPTC, (d) MPTC.....65
Figure III- 16: Simulation results of the THD of the stator current of an induction machine: (a) ANN-MPTC, (b) MPTC and theirs zoom (c) ANN-MPTC, (d) MPTC.....65
Figure III- 17 : Comparison of the THD of the stator current obtained by the two proposed control strategies, for some cases, under different operating conditions. 66
Figure IV- 1: Input filter.....70
Figure IV- 2 : topology of (3×3) direct matrix converter.....71
Figure IV- 3 : (3×3) Indirect Matrix Converter.....73
(b) Figure IV- 4 : General topology of multilayer Feed Forward Back-propagation neural network of MPCC of : (a) DMC , (b) IMC.....78
Figure IV- 5: Performance of Feed forward back-propagation neural network based MPCC of: (a) DMC, (b) IMC.....79
Figure IV- 6: Regression of Feed forward back-propagation neural network based MPCC of: (a) DMC, (b) IMC.....79
Figure IV- 7 : Simulation results of a DMC-fed RL-load: Reference and output current of phase A and their zoom with: (a) ANN-MPCC, (b) MPC 80
Figure IV- 8 : Simulation results of a DMC-fed RL-load of load currents with: (a) ANN-MPCC, (b) MPC 81
Figure IV- 9 : Simulation results of a DMC-fed RL-load of load voltage and currents of phase A with: (a) ANN-MPCC, (b) MPC.....81
Figure IV- 10 : Simulation results of a DMC-fed RL-load of supply current and of phase A with: (a) ANN-MPCC, (b) MPC.....81
Figure IV- 11 : Simulation results of a DMC-fed RL-load of input current and voltage of DMC of phase A with: (a) ANN-MPCC, (b) MPC.....82
Figure IV- 12: Simulation results of a DMC-fed RL-load of the input reactive power and its moving average value with: (a) ANN-MPCC, (b) MPC.....82

Figure IV- 13 : Simulation results of a DMC-fed RL-load of Output current spectra expressed as percentages of fundamental magnitude with: (a) ANN-MPCC, (b) MPCC 82
Figure IV- 14: Simulation results of a DMC-fed RL-load of Output voltage spectra expressed as percentages of fundamental magnitude with: (a) ANN-MPCC, (b) MPCC 83
Figure IV- 15 : Simulation results of an IMC-fed RL-load: Reference and output current of phase A and their zoom with: (a) ANN-MPCC, (b) MPC 83
Figure IV- 16: Simulation results of an IMC-fed RL-load of load currents with: (a) ANN-MPCC, (b) MPC 84
Figure IV- 17: Simulation results of an IMC-fed RL-load of load voltage and currents of phase A with: (a) ANN-MPCC, (b) MPC.....84
Figure IV- 18 : Simulation results of an IMC-fed RL-load of supply current and of phase A with: (a) ANN-MPCC, (b) MPC.....85
Figure IV- 19 : Simulation results of an IMC-fed RL-load of input current and voltage of DMC of phase A with: (a) ANN-MPCC, (b) MPC.....85
Figure IV- 20: Simulation results of an IMC-fed RL-load of the input reactive power and its moving average value with: (a) ANN-MPCC, (b) MPC 85
Figure IV- 21 : Simulation results of an IMC-fed RL-load of Output current spectra expressed as percentages of fundamental magnitude with: (a) ANN-MPCC, (b) MPCC 86
Figure IV- 22: Simulation results of an IMC-fed RL-load of Output voltage spectra expressed as percentages of fundamental magnitude with: (a) ANN-MPCC, (b) MPCC 86

List of tables

List of tables

Table II- 1: Feasible switching states of the two-level four-leg inverter 24
Table II- 2: Possible switching states and output vector voltage 28
Table II- 3 : the training parameters 32
Table II- 4 : A comparison between the two proposed control strategies under different operating conditions 39
Table III- 1 : training parameters 61
Table III- 2 : Comparison of the THD of the stator current obtained by the two proposed control strategies, for some cases 66
Table IV- 1: Possible switching states for the rectifierstage 74
Table IV- 2: Possible switching states for the inverter stage 75
Table IV- 3 : Training parameters of DMC and IMC 78
Table A- 1 : Simulation parameters forMPCC / PNN / Fitnet of an inverter fed RL load 96
Table B- 1: Machine parameters 98
Table B- 2 : Simulation parameters for the MPTC of an inverter fed IM 98
Table C- 1: Simulation parameters for the MPCC of a MC-fed RL-load 101
Table C- 2 : Filter parameters 101

List of symbols and acronyms

List of symbols and acronyms

MC : Matrix Converter

IMC : Indirect Matrix Converter

DMC : Direct Matrix Converter

SMC : Sparse Matrix Converter

MIMC : Multilevel Indirect Matrix Converter

2LVSI : Two-Level Voltage Source Inverter

MPC : Model Predictive Control

MHPC : Model Heuristic Predictive Control

DMC : Dynamic Matrix Control

GPC : Generalized Predictive Control

P-DPC : Predictive Direct Power Control

MPCC : Model Predictive Current Control

MPTC : Model Predictive Torque Control

ANN : Artificial neural network

ANN-MPC : Artificial neural network based model predictive control

ANN-MPCC: Artificial neural network based model predictive current control

ANN-MPTC: Artificial neural network based model predictive torque control

FNN : Feed forward back-propagation neural network

PNN : Perceptron neural network

FITNET : Fitting application neural network

NFTOOL : Network-fitting tool

NNTOOL : Neural network tool

T_s : Sampling period

FCS-MPC : Finite Control Set-Model Predictive Control

FACTS : Flexible AC Transmission Systems

StatComps : Static synchronous compensators

APF : Active Power Filter

THD : Total Harmonic Distortion

V_{DC} : DC source voltage

M : Neutral point of the inverter

N : Neutral point of the load

PMSG : Permanent Magnet Synchronous Generator

φ_r : Rotor flux

φ_s : Stator flux

i_s : Stator current

i_r : Rotor current

v_s : Stator Voltage

v_r : Rotor voltage

L_m : Magnetizing inductance

L_s : Stator inductance

R_s : Stator resistance

L_r : Rotor inductance

R_r : Rotor resistance

M_s : Mutual inductance between two stator windings

M_r : Mutual inductance between two rotor windings

M_{sr} : Magnitude of the inductance between the stator and the rotor

Ω : Mechanical speed

J : Moment of inertia of the mechanical shaft

T_{em} : Electromagnetic torque

T_L : load torque

k_f : Dry friction coefficient

ω : Rotor angular speed

p : Number of pole pairs

ξ : damping coefficient

ω_n : Natural circular pulse

Q : Reactive Power

R_f : Filter resistance

L_f : Filter inductance

C_f : Filter capacitance

α : Temperature coefficient

T : Temperature

λ : weighting factor

General introduction

General introduction

In the last few decades, power electronic systems and electrical drives have drawn significant revolution in a broad range of industrial applications. This is mainly due to the advancement in power semiconductor devices, converter topologies, control methods, and micro-controller resources [1]. The control of power converters has been extensively studied, and new control schemes are presented every year. Most prominently, the development of control methods is progressing well for the newly emerged sophisticated applications which may have multiple control targets, system constraints, and functionalities, …etc.[2].The overall revolution in power electronic systems and electrical drive applications become possible because of the migration of control platform from analog to digital system. At first microprocessor technology was introduced as a digital platform in the early 1970s, and then become popular during the 1990s [3]. Nowadays, digital signal processors (DSPs) and field programmable gate arrays (FPGAs) have emerged as powerful technology that allow us to implement the advanced control methods [4], [5] ,

Three-phase induction motors (IMs) were used for high power, variable speed drives and traction systems in railways replacing DC machines[6] due to their increased robustness and reduced cost and maintenance requirements. In addition, precise control of the IM torque/speed is perfectly possible thanks to the development of new power devices and digital signal processors [7].

Several control schemes have been proposed for the control of power converters and drives among these control schemes, Model predictive control (MPC). The MPC was originally introduced in the process industry with success for several decades [8]. The complex model and slow dynamics of the process industry made it compatible with the available control platform for the implementation [9], [10], however, there are many disadvantages with this control method. Among these disadvantages are relatively low computation efficiency [11] and huge amount of real-time calculations [1]. For this reason, most of the methods used to overcome these disadvantages are accomplished by replacing another strategy more preferment.

Recently, several studies have suggested the application of the technique of artificial intelligence like neural networks, fuzzy logic and genetic algorithms to replace hysteresis controller of the inverter[12][6]. The artificial neural networks (ANNs) are capable of

learning the desired mapping between the inputs and outputs signals of the system without knowing the exact mathematical model of the system. The ANNs are excellent estimators in nonlinear systems [11]

Artificial neural networksare introduced also to replace the model predictive control. The ANN are used for their properties of learning capability and generalization to improve the control performance of the system and to overcome the disadvantages of the MPC.

This thesis is organized into four chapters;they are summarized as follows:

The first chapter is dedicated to an overview of the matrix converters by citing the different topologies proposed in the literature then,the model predictive torque control (MPC) is introduced and its main drawbacks are presented.The chapter is concluded with an overview of artificial neural network.

The second chapter is devoted to the analysis and the simulation of neural network based predictive current control applied to a two-level three-phase inverter feeding an RL-load.An evaluation of its performance is proposed. Then a comparison between the two strategies is established. The chapter is concluded by a real time implementation of the ANN-MPC.

In the third chapter, a neural network model predictive torque control (MPTC) of an induction machine driven by an inverter is developed. The chapter is started by presenting the MPTC and its working principle. After that, the modeling of the induction machine then,the presentation the training steps withdetails is introduced. This chapter is concluded with a comparison between the two strategies.

The last chapter of this thesis is dedicated to the analysis and the simulation of the two topologies of the matrix converter (direct and indirect).A neural network based predictive current control is applied to the matrix converter-fed RL load. The performance of proposed strategy is evaluated. This chapter is also concluded with a comparison between the two strategies.

The general conclusion concerns a brief synthesis of the work carried out with the main obtained results and some perspectives.

Chapter one

State of the art: model predictive control based on neural network

CHAPTER ONE

Introduction

Model predictive control (MPC) has become one of the well-established modern control methods for converter topologies, where a high-quality voltage with low total harmonic distortion (THD) is needed. Although it is an intuitive controller, easy to understand and implement, it has the significant disadvantage of requiring a large number of online calculations for solving the optimization problem. On the other hand, the application of model-free approaches such as those based on artificial neural networks approaches is currently growing rapidly in the area of power electronics and drives. Broadly speaking, the use of neural networks for the control of dynamical systems was proposed in the early nineties[13].

This chapter is divided into two main parts, the first is devoted to the state of the art of the converter, and the second part is devoted to the state of the art of the Model Predictive Control (MPC) based on neural network. Where some converter topologies, some applications of the control strategy were presented, and an overview of the neural network as an enhancement of MPC.

I.1 State of the art of the inverters

An inverter refers to a power electronic device that converts power in DC form to AC form at the required frequency and voltage output.

I.2 Three Phase Inverter

A three-phase inverter converts a DC input into a three-phase AC output. Its three arms are normally delayed by an angle of 120° so as to generate a three-phase AC supply. The inverter switches each has a ratio of 50% and switching occurs after every T/6 of the time T. The switches S1 and S4, the switches S2 and S5 and switches S3 and S6 complement each other.

The figure below shows a circuit for a three phase inverter. It is nothing but three single phase inverters put across the same DC source. The pole voltages in a three phase inverter are equal to the pole voltages in single phase half bridge inverter.[14]

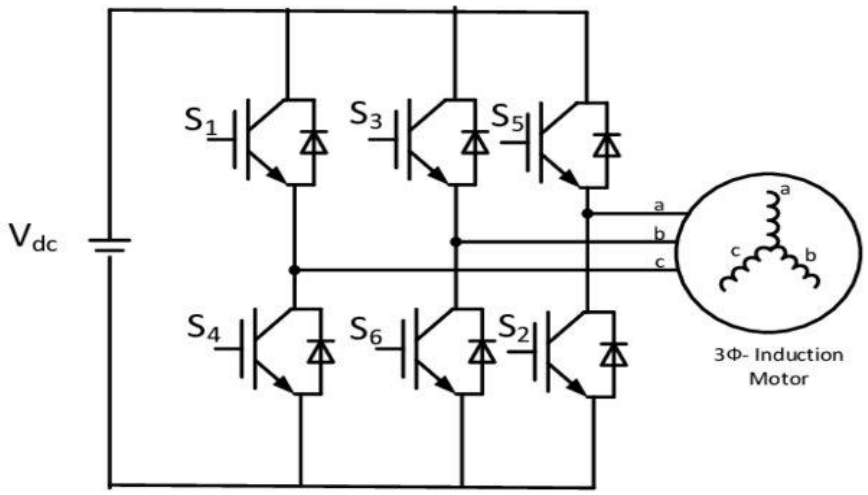

Figure I- 1 : Three phase inverter topology

I.3 State of the art of matrix converters

The majority of industrial application request AC-AC power conversion, this necessity is exponentiallyincreasing. For generating variable amplitude, frequency, phase voltages and currents , power electronics converters are involved[15]. Matrix converter (MC) is an all-switch power converter with interesting properties such as controllable input power factor, bidirectional power flow, and high quality sinusoidal input and output current waveforms. The absence of a huge electrolytic capacitor in matrix converters is considered as a more reliable and compact solution for AC-AC power conversion[16] , it benefits from the possibility of a compact design [17]. There are two main types for the MC, direct matrix converter (DMC) and indirect matrix converter (IMC). The appliance of those converters are extensive: motor drive, FACTS devices, distributed generation systems, and wind energy conversion systems. [18]

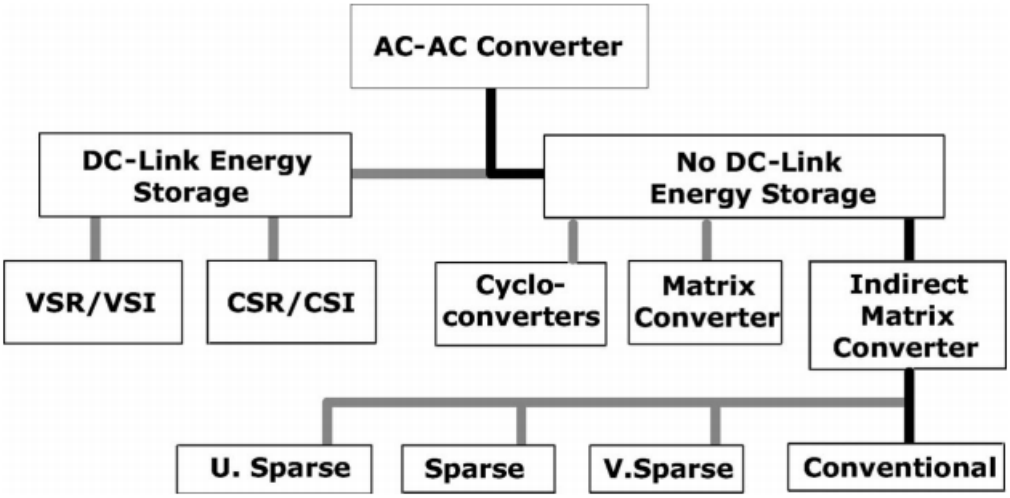

Figure I- 2: Classification of power converters

I.3.1 Direct matrix converter

Direct Matrix converter, which uses the principle of single stage AC- AC conversion without the need of energy storage elements, it is able to convert AC voltage into another AC voltage [19]. They offer inherent advantages such as bi-directional power flow, nearly sinusoidal input and output waveform Also the input power factor, output current amplitude , frequency are controllable .Finally they have a compact design and they do not need DC-link capacitors for energy storage [20].

Using the fully controlled bi-directional switches, that perform direct energy conversion without any energy storage elements in an intermediate link, to connect directly the inputs to the outputs. The matrix converter is also able to generate an adjustable input power factor regardless of the load [21]

The concept of a direct MC appeared in the literature as early as the 1970. Research started more extensive with the work of Venturini and Alesina in the 1980 [22]

The absence of the DC-link capacitor reduces the volume, enhances the efficiency, increases the lifetime and simplifies the control schemes. It only requires small filters to suppress the ripples generated by the switching actions [23]

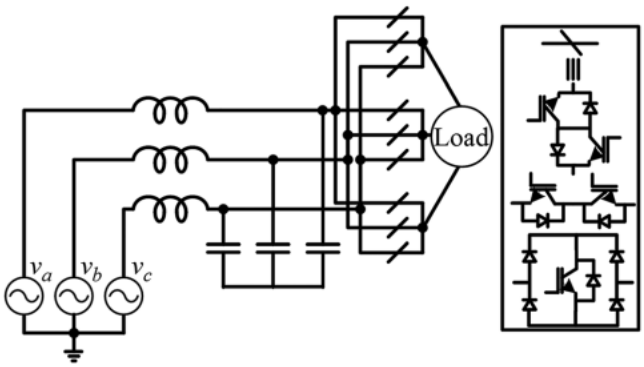

Figure I- 3: Direct matrix converter (DMC)

I.3.2 Indirect matrix converters

The IMC offers a set of advantages such as simpler commutation [24] , clamp circuit for overvoltage protection [25] , possibility of reducing the rectifier-stage switch count, while providing similar performance as that of direct matrix converter. Multi-modular topologies for IMC have been proposed that they allow for modification of output stage to meet different application requirements. Modern variable frequency drives powered by high switching frequency power converters, such as MC, have made it possible to an accurately and efficiently control AC machines.

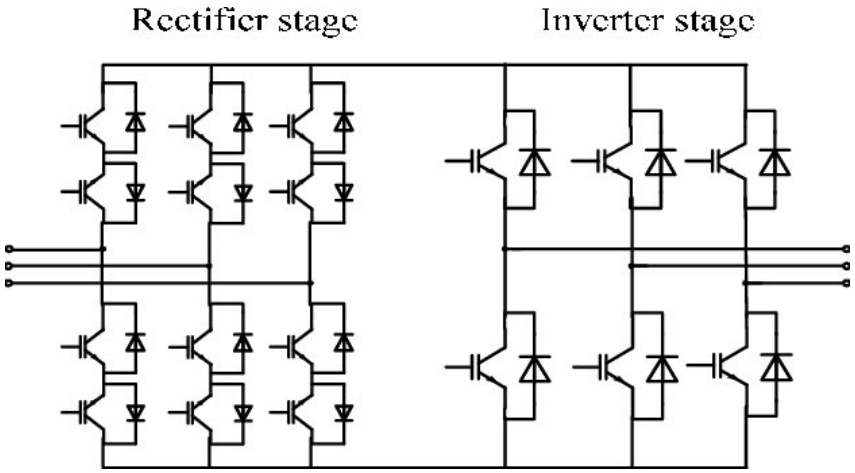

Figure I- 4: Indirect Matrix Converter (IMC)

I.3.3 Different structures of indirect matrix converters

I.3.3.1 Conventional indirect matrix converters

The conventional IMC perform AC/DC/AC power conversion in two stages, namely, rectification and inversion stages in addition to a storage element which can be either a capacitor or an inductor [26].The rectifier stage, which is formed by six bidirectional switching, provides a fictitious DC link voltage with a variable average. The other six unidirectional switching forming the inverter stage, are synthesizes three-phase output voltages. [18]

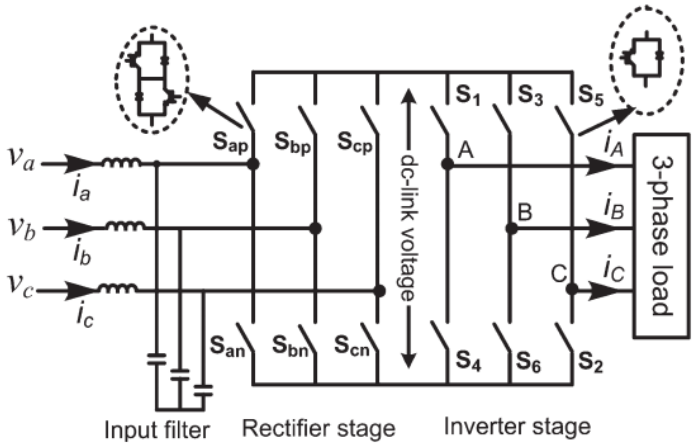

Figure I- 5: Structure of a conventional indirect matrix converter

I.3.3.2 Sparse indirect matrix converters

The IMC topology has a complex control for the number of switches to handle. In order to reduce the number of transistors, one IGBT from each leg of the rectifier is eliminated, compared to the previous configuration to be sparse indirect matrix converters (SMC).

By an implementation of bidirectional IGBT switches connected to a diode bridge, where the number of the controlled components in the rectifier is reduced, a very sparse IMC structure is created .[27]

In ultra-sparse indirect matrix converters configuration, minimum number of switches are employed. There is a single switch by input. It does not allow bidirectional power flow due to the structure of the rectifier, which limits its practical application like aerospace. [27]

The main advantage of minimizing number of switches is to simplify the development of the control of the converter. [28]

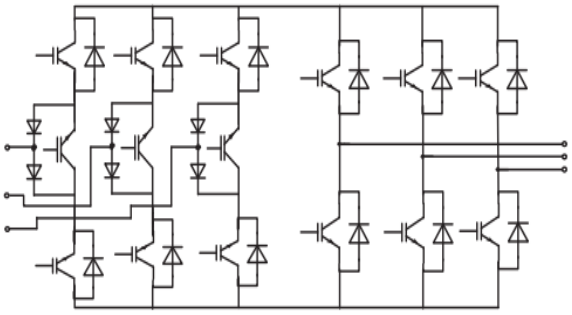

Figure I- 6: Sparse matrix converter (SMC)

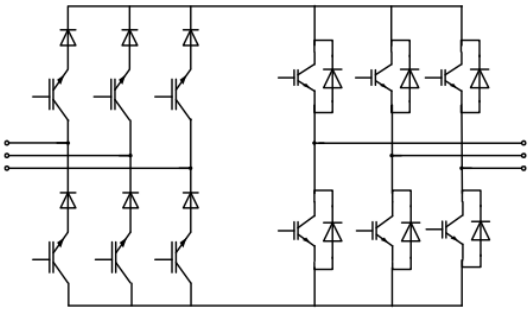

Figure I- 7: Very sparse matrix converter

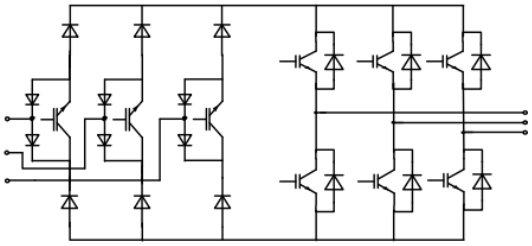

Figure I- 8: Ultra sparse matrix converter (USMC)

I.3.3.3 Multilevel indirect matrix converters

The multilevel MC can synthesize more than two-level output voltage to improve output performance in terms of reduced harmonic content. [29] .The conventional multilevel IMC topology was firstly based on the traditional IMC, but with six-switch inverter in the back replaced by a three-level neutral-point-clamped (NPC) inverter [30] . Then, the new multilevel IMC based on the combination of conventional NPC and cascaded-rectifier [31] in order to improve the voltage transfer ratio.

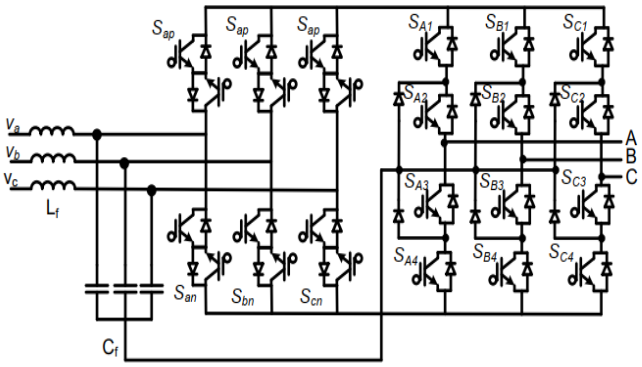

Figure I- 9: Multi level IMC

I.4 State of the art of model predictive control

I.4.1 Introduction

Model predictive control (MPC) has a long history in the field of control engineering. It is one of the few areas that has received on-going interest from researchers in both the industrial and academic communities [32] . The term Model Predictive Control does not designate a specific control strategy but a very ample range of control methods which make an explicit use of a model of the process to obtain the control signal by minimizing an objective function[33]. There are many applications of predictive control successfully in use at the present time, not only in the industrial process but also in the applications on the control of a diversity of processes ranging , from robot manipulators [34] to clinical anesthesia[35],power converters and drives [36]. Thanks to the evolution of high processing microprocessors which surpassed the drawback of computational burden of the MPC [37].

I.4.2 Development of MPC (History)

The author in [38] reviewed three decades of the MPC development. According to his research, the MPC was first used in industry such as oil and petrochemical industry, which dates back to the 1950s as a computer based supervisory control. At that time, MPC was a promising control strategy yet it was not widely embraced by other industrial process due to the computational power needed for the MPC until the mid-1970s, when several other techniques were introduced like Model Heuristic Predictive Control (MHPC) and Dynamic

Matrix Control (DMC). These two control algorithms are developed into Generalized Predictive Control (GPC), which is more robust, compared to the MHPC and DMC.

In the second decade of the MPC development, during the late 1980s, researchers founded a theoretical approach for the MPC: the discrete-time state-space representation model:

$$\begin{cases} x[i+1] = Ax[i] + Bu[i] \\ y[i+1] = Cx[i] + Du[i] \end{cases}$$

During this decade, researchers showed interest in studying the stability of the MPC for the first time. Which can be proven by considering the cost function of the MPC as a Lyapuno function [38].

I.4.3 Working Principal of MPC

Predictive control covers a very wide class of controllers that have found rather recent application in power converters. A classification for different predictive control methods is shown in the following Figure:

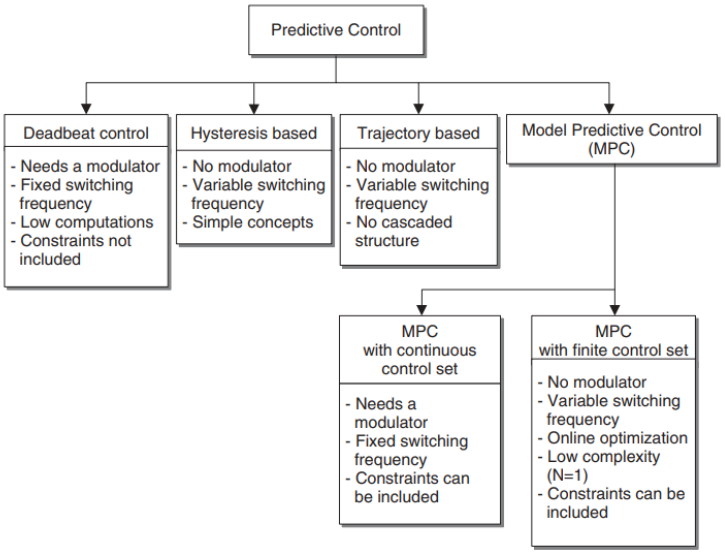

Figure I- 10: Classification of predictive control methods used in power electronic

The optimization criterion in hysteresis-based predictive control is to keep the controlled variable within the boundaries of a hysteresis area, while in trajectory-based control the variables are forced to follow a predefined trajectory. In deadbeat control, the optimal actuation is the one that makes the error equal to zero in the next sampling instant. A more flexible criterion is used in model predictive control (MPC), expressed as a cost function to be minimized [39].

The difference between these groups of controllers is that deadbeat control and MPC with continuous control set need a modulator in order to generate the required voltage. This will result in having a fixed switching frequency. The other controllers directly generate the switching signals for the converter, do not need a modulator, and present a variable switching frequency [39].

Nonlinearities in the system can be included in the model, avoiding the need to linearize the model for a given operating point, and improving the operation of the system for all conditions. It is also possible to include restrictions on some variables when designing the controller. These advantages can be very easily implemented in some control schemes, such as MPC, but are very difficult to obtain in schemes like deadbeat control [39].

I.4.4 MPC Strategy

The methodology of all the controllers belonging to the MPC family is characterized by the following strategy, represented in figure

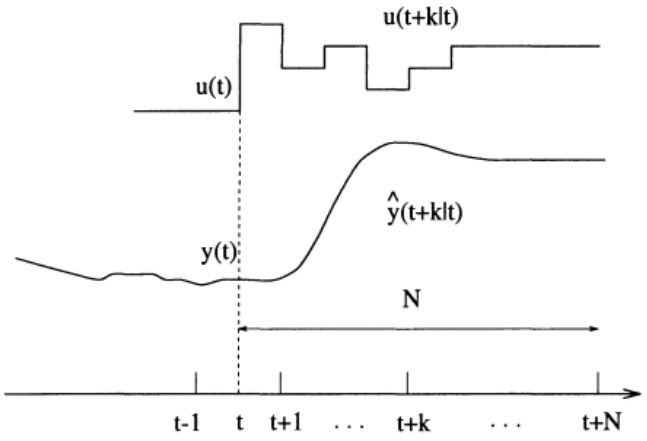

Figure I- 11: Working principle of MPC

MPC defines the control action by minimizing a cost function that describes the desired system behavior. This cost function compares the predicted system output with a reference. The predicted outputs are computed from the system model. In general, for each sampling time, the MPC controller calculates a control action sequence that minimizes the cost function, but only the first element of this sequence is applied to the system. Although MPC controllers solve an open-loop optimal control problem, the MPC algorithm is

repeated in a forward horizon fashion at every sampling time, thus, providing a feedback loop and potential robustness with respect to system uncertainties [36].

I.4.5 MPC's Elements

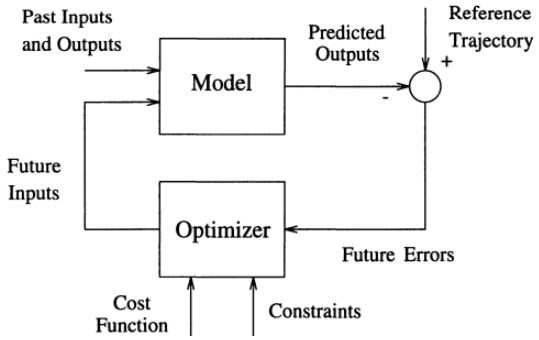

Figure I- 12: Basic structure of MPC

All the MPC algorithms possess common elements and different options can be chosen for each one of these elements giving rise to different algorithms. These elements are:

- Prediction Model
- Objective Function
- Obtaining the control law

I.4.6 Prediction Model

The model is the corner-stone of MPC [33]; a complete design should include the necessary mechanisms for obtaining the best possible model, which should be complete enough to fully capture the process dynamics and should also be capable of allowing the predictions to be calculated and at the same time, to be intuitive and to permit theoretic analysis.

Practically every possible form of modeling a process appears in a given MPC formulation, the following being the most commonly used:

• Transfer function.

• State space.

Non-linear models can also be used to represent the process but the problem of their use springs from the fact that they cause the optimization problem to be more complicated.

Neural nets [40]as well as fuzzy logic [41] are other forms of representation used in some applications.

I.4.7 Objective Function

The various MPC algorithms propose different cost functions for obtaining the control law. The cost function definition is one of the most important stages in the design of an MPC, since it allows not only to select the control objectives of the application, but also to include any required constraints that represents the desired behavior of the system [42]. This function considers the references, future states (or predicted states), and future actuations. In case of a multivariable system, the cost function may be written as

$$J=\sum_i^n \lambda_i \left|x_i^* - x_i^p\right|$$

While:

n : is the number of controlled variables

x_i : is the controlled variable(It is not written in the function but , it is just to mention the controlled variable)

x_i^* : is the reference value of the controlled variable

x_i^p: is the predicted value of the controlled variable

λ_i: is the weighting factor

The weighting factor allows for adjusting the importance of each controlled variable according to its priority in the scope statement

The selected actuation is the one that minimizes the cost function, it is stored so that it can be applied to the converter in the upcoming sampling period [43]

I.4.8 Obtaining the control law

In order to obtain values u (t + k | t) which is mentioned in Figure I-11 it is necessary to minimize functional *J*. To do this the values of the predicted outputs y(t + k | t) are calculated in function of past values of inputs and outputs and of future control signals, making use of the model chosen and substituted in the cost function, obtaining an

expression whose minimization leads. An analytical solution can be obtained for the quadratic criterion if the model is linear and there are not constraints, otherwise an iterative method of optimization should be used [44].

If the system is not linear but nonlinear, we can use linear MPC and still benefit from the proprieties of the convex optimization problem , the available method to use this case are the adaptive and gain scheduled MPC , the way these controllers deal with a nonlinear system is based on linearization. If the system is nonlinear and that cannot be approximated well then we have to use nonlinear MPC, this method is the most powerful on as, it uses the most powerful on as, it uses the most accurate representation of plant.

I.4.9 The major problem of the MPC

The Model Predictive Control (MPC) is a well-established technique for process control that has been applied to electrical systems, so after the three decades of the gradual development, so what remains now? [45]

At present, the MPC suffer from many problems, such as the lack of systematic handling of uncertainty. Therefore, it is necessary to improve the predictionaccuracy for mismatched prediction models. The other problem is howto design the cost functions and the weight coefficients [46][47] .One of the other drawback of MPC is that it requires the optimization problem to be solved online

All this makes the existing MPC algorithms suffer from a major challenge: relatively low computation efficiency [48] and huge amount of real-time calculations [13].

I.4.10 Different methods of improving MPC's performance

a- The authors proposed in [46] Luenberger model-based predictive torque control (LM-PTC) of induction machine to compensate the prediction error caused by the mismatched parameters. The prediction error is eliminated actively by modifying the prediction model itself with a correction compensation term based on an open-loop predictive model of traditional (T-PTC). Inspired by the idea of closed-loop Luenberger observer, in the torque and flux prediction, the feedback correction part is introduced into the prediction equations

for LM-PTC. Secondly, the steady prediction errors of T-PTC and LM-PTC are respectively analyzed with mismatched parameter.

b- In [49], the author studied the possibility of reducing the MPC incertitude by proposing a predictive-control-based direct power control (DPC) with an adaptive online parameter identification technique for AC-DC active front ends (AFEs). This approach calculates the input inductance and the resistance in the model parameters using the sampled input currents and input voltages every sampling period based on least-squares estimation. Therefore, the AFE generates sinusoidal input currents, and it mitigates a performance degradation resulting from the model uncertainty of the MPC.

c- In the paper [50] a discrete-time model for an induction machine with time varying components was proposed to improve the accuracy of the MPC control strategy compared to the Euler discretization approach. The machine model is updated at every sampling instant and used to predict the future current and flux values for each voltage vector produced the least torque and stator flux magnitude errors , then it will be applied during the next sampling time. It is also possible to include additional constraints in the cost function such as reduction of the switching frequency [51] and imposed spectrum [52].

d- In order to solve the parameter dependence problem in model predictive control, an improved model predictive current control (MPCC) method based on the incremental model for surface-mounted permanent magnet synchronous motor (SPMSM) drives is proposed in paper [53], where the results of simulation show that it can effectively reduce the parameter sensitivity of the MPCC. Firstly, an analysis of the parameter sensitivity of the conventional MPCC method is established. Then,an incremental prediction model is introduced to eliminate the use of permanent magnetic flux linkage in the prediction model. Therefore, in order to improve the anti-parameter-disturbance capability of the MPCC method, an inductance disturbance controller is presented to update accurate inductance information for the whole control system in real time.

e- In paper [54] , the combination of a finite-control-set MPC (FCS-MPC) with a system identification is proposed. The method does not require high-frequency signal

injection, but uses the measured values already required for the FCS-MPC. An evaluation of the least squares-based identification on a laboratory test showed that the model accuracy and thus the control performance could be improved by an online update of the prediction models.

I.5 Model predictive control based on neural network

In the last few decades, there has been a significant evolution of traditional control techniques in parallel with the appearance of modern tools associated with artificial intelligence. It should be noticed that most of classical model-based control methods, including nonlinear ones, require the knowledge of the controlled system by means of set of algebraic and differential equations, Moreover, complete mathematical models describing the systems are often very complex and their parameters need to be known. In real applications, some parameters may be hard to measure or their identification is very complicated. In order to overcome these problems, it is beneficial to use artificial intelligence techniques, such as neural networks, fuzzy logic and genetic algorithms , which do not need the controlled system models and use expert knowledge or experimental data for controller training [55].

Recently, based on a biological prototype of the human brain, the neural networks have attracted considerable attention for modeling uncertain, nonlinear, and complex systems, owing to their learning and adaptation capabilities [56], [57]. In general, the structures of neural networks can be classified as feed-forward NN and recurrent NN [58]

I.5.1 Overview of neural networks

In general, ANN systems are capable of “learning” trends in a given data set and establishing input–output relationships based strictly on a “test” set of data.

I.5.1.1 The construction of ANN systems

The basic element in neural network systems is called a neuron. The neuron accepts one input$x$, and produces an output value y, based on the (generally) nonlinear function. However, there is no way to determine beforehand which choice of this function will produce the best results for a particular problem. A complete multilayer neural network

system is constructed by combining neurons in series (from left to right) and parallel (from top to bottom). [59]

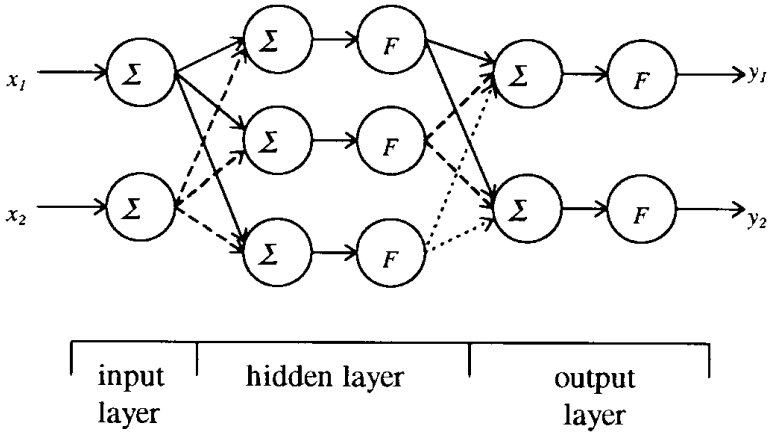

Figure I- 13: A three-layer neural network system

A layer is defined to be a set of parallel-connected neurons, or "nodes." The hidden and output layers are identical in both form and functionality; they give the network its ability to "learn" complex nonlinear relationships between inputs and outputs. [59]

I.5.1.2 The ANN's working principle

ANN's perform their calculations using the nonlinear functions and simple multiplying factors, called weights that are associated with a pathway between any two neurons.In its basic form, this model can be expressed as an iterative composition of input-output functions of the form [60]

$$f(\vec{x}) = h\left(w_0 + \sum_{i=1}^{M} w_i x_i\right)$$

Where $h(x)$ is an activation function , $\vec{x}= \{x_1, x_2, \cdots, x_M\}$ is the input vector of the ANN with M elements, w_i are the weights for each input xi , and w_0 is a bias or correction factor. The objective of the ANN training phase is to optimize some cost function by finding optimal values for the w_i and w_0 [60]. The weights are updated in a manner such that the complete network "learns" to produce a specific output for a specific input. The process of adjusting the weights to achieve a specified accuracy level is referred to as "training." [61]

I.5.1.3 The training of ANN

The major justification for the use of ANN's is their ability to "see" and "learn" relationships in complex data sets that may not be easily perceived by human engineers. An ANN system performs this function as a result of "training" which, in words, is a process of repetitively presenting a set of training data (typically a representative subset of the complete set of data available) to the network and adjusting the weights so that each input data set produces the desired output[61].

I.5.1.4 Learning Algorithm Categorization

Neural networks are trained by two main types of learning algorithms: supervised and unsupervised learning algorithms.

Supervised Learning: a supervised learning algorithm adjusts the strengths or weights of the inter-neuron connections according to the difference between the desired and actual network outputs corresponding to a given input. Thus, supervised learning requires a "teacher" or "supervisor" to provide desired or target output signals. The network employs a special one-step procedure during "learning" and an iterative procedure during recall.[62]

Unsupervised Learning: unsupervised learning algorithms do not require the desired outputs to be known. During training, only input patterns are presented to the neural network which automatically adapts the weights of its connections to cluster the input patterns into groups with similar features. [62]

I.5.1.5 Classes of neural network

a- The feed-forward neural net

FNN tend to be straightforward networks that allow signals to travel one way only, from input to output. There are no feedback (loops); i.e. the output of any layer does not affect that same layer. Most of the works on nonlinear MPC (NMPC) use FNN, for example In [63] , S.Tiwari, R. Naresh, and R. Jha realize a neural network model predictive controller, by using the FNN, for predictive control of the power system to improve its transient stability. Yan and Wang in [64] introduce a robust MPC based on a FNN The results show that this robust MPC could improve computational efficiency and shed a light for real-time

implementation. However, the main drawback of FNN that their capability for representing nonlinear systems is limited [58]

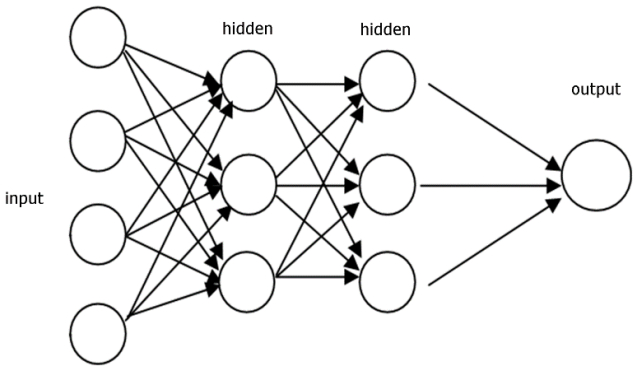

Figure I- 14: The feed-forward neural network

b- The recurrent neural net

RNN can have signals traveling in both directions by introducing loops in the network. They are capable of providing long-range predictions even in the presence of measurements noise due to their structures. Therefore, RNN are better suited to model nonlinear systems for MPC. Pan and Wang in [65] use an echo state network to identify unknown nonlinear dynamical systems for NMPC. The results show that the echo state network-based NMPC can reach the global convergence. RNN improved performance in terms of global convergence and reduced model complexity [66].Examples of recurrent networks include the Hopfield network [Hopfield, 1982], the Elman network [Elman, 1990] and the Jordan network [Jordan, 1986]. [62]

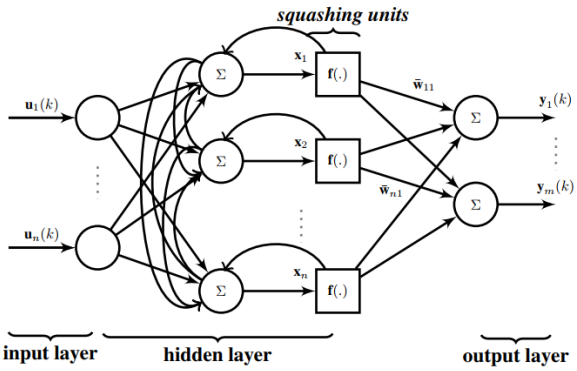

Figure I- 15: Simple recurrent neural network

c- Self-organizing neural network

The class of methods that have been often termed "self-organizing maps" (SOM) involve iterative procedures for associating a finite number of object vectors (inputs) with a finite number of representational points [67]. A self-organizing neural network consists of two parts: main part and control part. The main part, structurally, is the same as an ordinary 3-layered feed-forward neural network, but each neuron in its hidden layer contains a signal from the control part, the main part is trained by a supervised learning and learns input-output mapping. The control part consists of a self-organizing map (SOM) network [68] whose outputs associate with the hidden neurons in the main part one by one and control the firing strength; the control part is trained by an unsupervised learning [69].

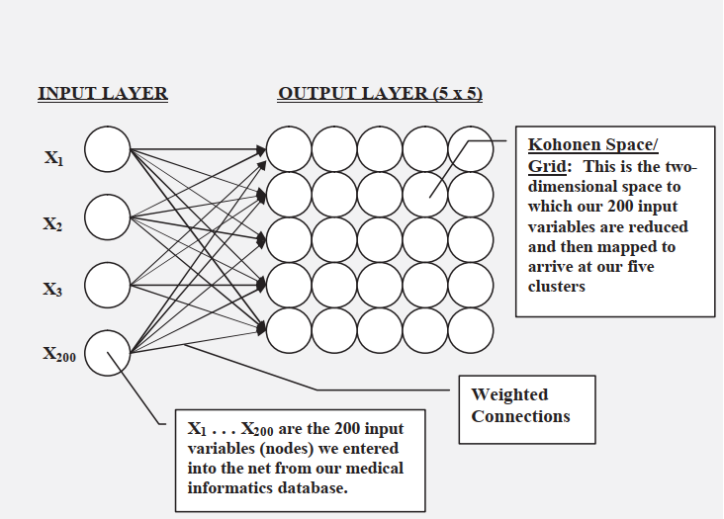

Figure I- 16: Diagram of a Self-Organizing Map

I.5.2 How ANN Systems are applied

ANN systems must be applied to problems for which a suitable amount of training data exists; it may come from historical records from measured data. The system will only perform as well as it has been trained [61]. In our case, the objective is to drive a three-phase's inverter. Therefore, we use MPC as an expert or a teacher for generating the data required for training off-line the proposed neural network using standard supervised learning, under full state observation of the system, once the off-line training is performed,

the trained ANN can successfully control the output voltage of the inverter, without the need of using MPC at test time.

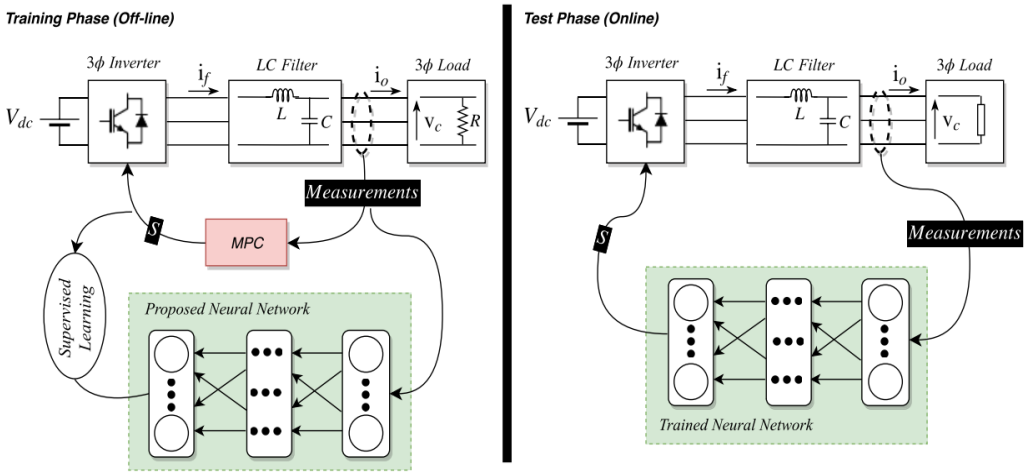

Figure I- 17: An overview of the proposed control strategy

I.6 Conclusion

In this chapter, a state of the art of the major elements of our work is presented.

At the beginning, we talked about the AC-AC converters which are divided into direct and indirect converters, which have different structures where each one has its special requirements and issues.

Secondly, a section briefly describes the model predictive control, including a historical development, its working principle with some examples of its applications. The MPC suffers from the concern of the relatively low computation efficiency. Therefore, we highlight the methods of performance's improvement of the MPC.The neural network is one of the most promoted solutions.The last section was dedicated to present an overview of ANN and how it could improve the model predictive control.

Chapter two

Artificial neural network based on Model Predictive Current Control of a Three-Phase, Two Level, Inverter-Fed RL-Load

CHAPTER TWO

Introduction

In recent years, model predictive current control (MPC) has been proposed as an interesting alternative for the control of power converters and drives. This control technique uses a model of the system to calculate predictions of the future behavior of the system for a given set of possible actuations for a predefined time horizon[70].Inother hand, a major drawback of MPC is that it requires the optimization problem to be solved online, which involves a huge amount of real-time calculations. However, different solutions have been introduced in order to address this problem [13].In particular, ANN-based controllers and estimators which have been widely used in identification and control of power converters and motor drives.

This chapter presents a neural network based on MPC scheme for a three-phase, two-level, inverter-fed RL-load. The modeling of the two-level voltage source inverter (2LVSI) and of the load will be presented, the working principle, procedure training will be explained and simulation results will be shown.

II.1Artificial neural network based MPCC

In this chapter we present a new control scheme for a two-level converter based on combining MPC and feed-forward ANN, with the aim of getting lower THD and improving the steady and dynamic performance of the system. First, MPCC is used, as an expert in the training phase to generate data required to train the proposed neural network. Then, once the neural network is fine-tuned, it can be successfully used online for controlling, without the need of using MPCC. The proposed ANN-based control strategy is validated through simulation, using MATLAB/Simulink tools, taking into account different conditions.

II.2System modeling

II.2.1 Inverter model

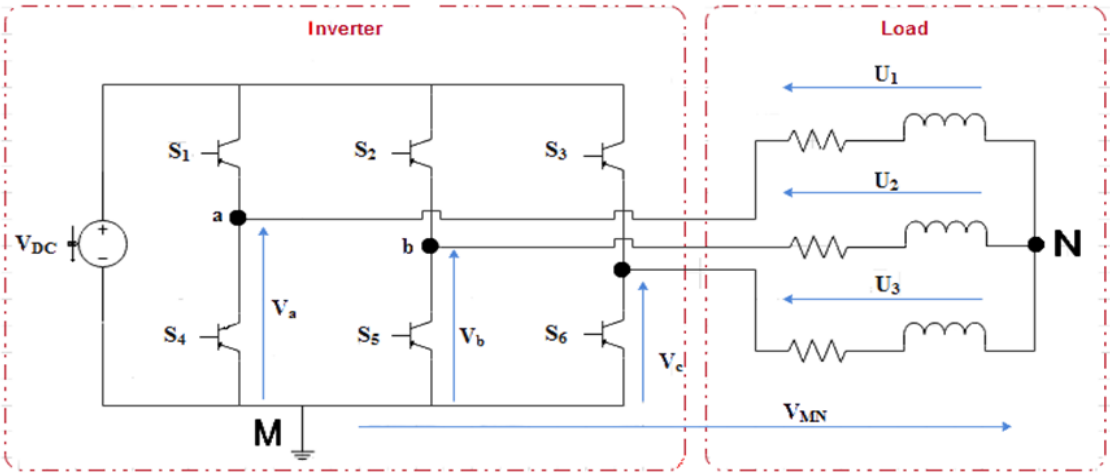

Figure II- 1 : Voltage source inverter power circuit

Considering a generic two-level, three-phase power inverter, there are six switches that generate the output. Moreover, the two switches of each leg of the converter operate in a complementary mode, in order to avoid the occurrence of short-circuit conditions. The three control signals named Sa, Sb, Sc forms a total of 2^3=8 feasible switching states of the converter. The valid switching states with the corresponding phase and line voltages are presented in Table I

Where

- $V_{DC}$is the DC source voltage.
- v_a, v_b and v_c are the phase-to-neutral (M) voltages of the inverter
- u_1, u_2 and u_3 are the phase-to-neutral (N) voltages of the load
- S_1, …, S_6 are the gate signals

Thus, eight switching states can be determined by three main gating signals: Sa, Sb, and Sc, expressed as follows:

$$S_a = \begin{cases} 1 \text{ if} S_1 \text{on and} S_4 \text{off} \\ 0 \text{ if} S_1 \text{off and} S_4 \text{on} \end{cases}$$

$$S_b = \begin{cases} 1 \text{ if} S_2 \text{on and} S_5 \text{off} \\ 0 \text{ if} S_2 \text{off and} S_5 \text{on} \end{cases} \quad \text{(II.1)}$$

$$S_c = \begin{cases} 1 \text{ if} S_3 \text{on and} S_6 \text{off} \\ 0 \text{ if} S_3 \text{off and} S_6 \text{on} \end{cases}$$

By applying Kirchhoff's first law we get:

$$\begin{cases} u_1 = v_{MN} + v_a \\ u_2 = v_{MN} + v_b \\ u_3 = v_{MN} + v_c \end{cases} \quad \text{(II.2)}$$

Adding the three equations we get:

$$v_{MN} = -\frac{1}{3}(v_a + v_b + v_c) \quad \text{(II.3)}$$

Replacing v_{MN} in (II.2) and considering that the load is balanced, we result in the following system that will be implemented in MATLAB:

$$\begin{pmatrix} u_1 \\ u_2 \\ u_3 \end{pmatrix} = \frac{1}{3} V_{DC} \begin{pmatrix} 2 & -1 & -1 \\ -1 & 2 & -1 \\ -1 & -1 & 2 \end{pmatrix} \begin{pmatrix} S_a \\ S_b \\ S_c \end{pmatrix} \quad \text{(II.4)}$$

Table II- 1: Feasible switching states of the two-level four-leg inverter

S_a	S_b	S_c	u_1	u_2	u_3
0	0	0	0	0	0
1	0	0	$\frac{2}{3}V_{DC}$	$\frac{-1}{3}V_{DC}$	$\frac{-1}{3}V_{DC}$
1	1	0	$\frac{1}{3}V_{DC}$	$\frac{1}{3}V_{DC}$	$\frac{-2}{3}V_{DC}$
0	1	0	$\frac{-1}{3}V_{DC}$	$\frac{2}{3}V_{DC}$	$\frac{-1}{3}V_{DC}$
0	1	1	$\frac{-2}{3}V_{DC}$	$\frac{1}{3}V_{DC}$	$\frac{1}{3}V_{DC}$
0	0	1	$\frac{-1}{3}V_{DC}$	$\frac{-1}{3}V_{DC}$	$\frac{2}{3}V_{DC}$
1	0	1	$\frac{1}{3}V_{DC}$	$\frac{-2}{3}V_{DC}$	$\frac{1}{3}V_{DC}$
1	1	1	0	0	0

II.2.2 Load model

The application of Kirchhoff's first law to the RL-load in Figure II.1 gives:

$$\begin{cases} u_1 = L\dfrac{di_a}{dt} + Ri_a \\ u_2 = L\dfrac{di_b}{dt} + Ri_b \\ u_3 = L\dfrac{di_c}{dt} + Ri_c \end{cases} \quad \text{(II.5)}$$

By transforming (II.5) into Laplace domain as transfer functions, to get a model for this RL load for simulation in MATLAB/Simulink environment we get:

$$\begin{cases} \dfrac{i_a}{u_1} = \dfrac{1}{sL+R} \\ \dfrac{i_b}{u_2} = \dfrac{1}{sL+R} \\ \dfrac{i_c}{u_3} = \dfrac{1}{sL+R} \end{cases} \quad \text{(II.6)}$$

To achieve a precise control strategy, a forward Euler method discretization of the system (II.5) is used to accurately predict the future values of the output current at the sampling period Ts. So $\frac{\mathrm{di}}{\mathrm{dt}}$ is replaced by $\frac{\mathrm{i[k+1]-i[k]}}{\mathrm{T_s}}$ and after some arrangements, (II.5) becomes:

$$\begin{cases} i_a[k+1] = \left(1 - \dfrac{RT_s}{L}\right) i_a[k] + \dfrac{u_1 T_s}{L} \\ i_b[k+1] = \left(1 - \dfrac{RT_s}{L}\right) i_b[k] + \dfrac{u_2 T_s}{L} \\ i_c[k+1] = \left(1 - \dfrac{RT_s}{L}\right) i_c[k] + \dfrac{u_3 T_s}{L} \end{cases} \quad \text{(II.7)}$$

Where, in the control algorithm, $\mathrm{i_a[k]}$ is evaluated as the measured current of phase a at the sample k and $\mathrm{i_a[k+1]}$ is evaluated as the predicted value of the current of phase a at the sample$k+1$.

II.2.3 Model predictive control

In this section, the goal is to control the load current. MPC exploits the discrete-time model of the inverter to predict the future behavior of the current, for each switching state.

Thereafter, the optimum switching statex_{opt} is selected, based on the minimization of the cost function, and directly fed to the power switches of the converter in each sampling interval Ts.[71]

We choose the cost function to be minimized to achieve the lowest error between the predicted current and the reference values; which is expressed as:

$$J = |i_a[k+1] - i_a^*[k+1]| + |i_b[k+1] - i_b^*[k+1]| + |i_c[k+1] - i_c^*[k+1]| \qquad \text{(II.8)}$$

Where $i_a^*[k+1], i_b^*[k+1]$ and $i_c^*[k+1]$ are the reference values of the phase currents at the sample $k+1$.

The MPC steps can be described in the algorithm shown in Figure II.2. The algorithm starts with the measurement current at the beginning of the sampling time. Once the variables are available, the model is evaluated for the first switching state obtaining the predicted variables, which are used in the cost function. Depending on the result, the switching state is selected or discarded and the loop is repeated. Once the switching states were evaluated, the selected one is applied to the converter.

The MPCC scheme uses finite number of valid switching states of the inverter in order to find the x_opt by using the following steps:

1) Measure the controlled variable $i[k]$and estimate $i^*[k+1]$.
2) Apply the optimal switching state (computed in the previous sampling period) to calculate the output voltage of the inverter $v[k]$ using the inverter model.
3) For every switching state of the converter, predict (using the mathematical model) the behavior of current in the next sampling interval $i[k+1]$
4) Evaluate the cost function, or error, for each prediction as, for instance:
$$J = |i[k+1] - i^*[k+]1]|$$
5) Select the switching state that minimizes the cost function, $Sopt$, and store it so that it can be applied to the converter in the next sampling period

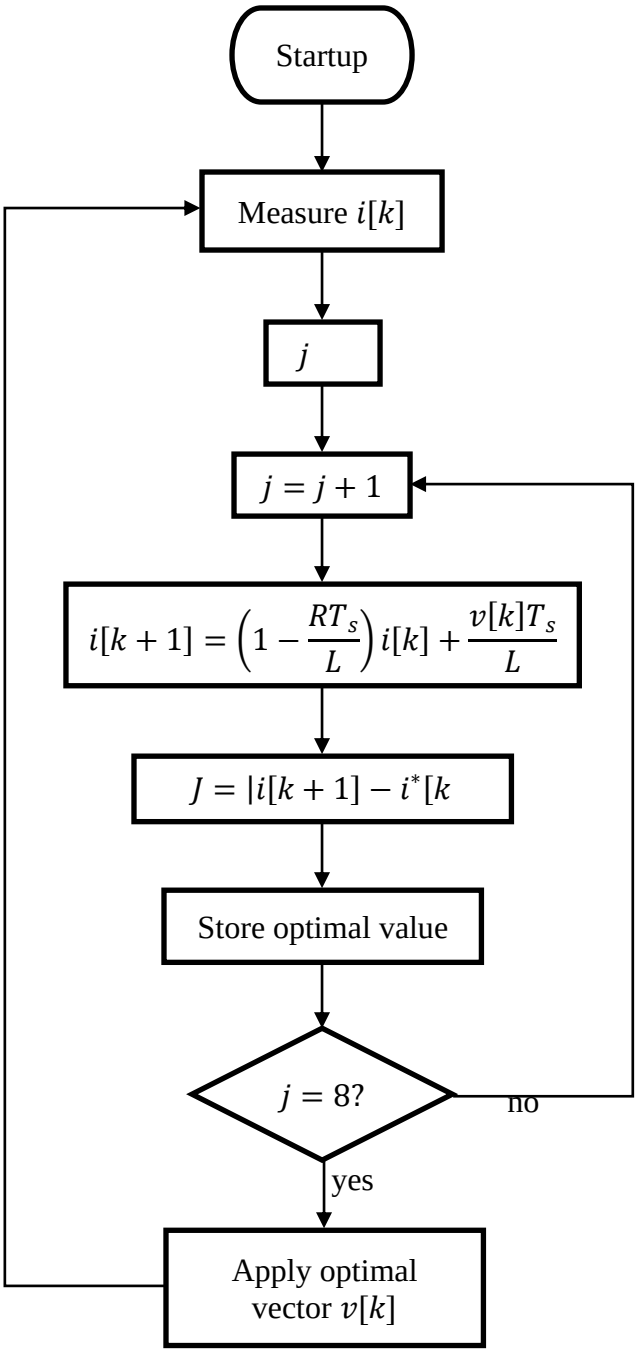

Figure II- 2 : Flow diagram of MPCC

Then in implementation, we should express, the currents and the output voltage of the inverter in $\alpha\beta$ coordinate system, to simplify and minimize the computation time as follow

$$v = \frac{2}{3}(v_a + av_b + a^2 v_c) \quad \text{(II.9)}$$

$$i = \frac{2}{3}(i_a + ai_b + a^2 i_c) \quad \text{(II.10)}$$

Where:

$$a = e^{\frac{j2\pi}{3}} = -\frac{1}{2} + j\frac{\sqrt{3}}{2}$$

$$i_\alpha = Re(i)$$

$$i_\beta = Im(i)$$

Instead of calculating the output voltage of the inverter for each possible switching state at every iteration, we can calculate them in advance and apply them to the load model.

Table II- 2: Possible switching states and output vector voltage

S_a	S_b	S_c	v
0	0	0	$v_0 = 0$
1	0	0	$v_1 = \frac{2}{3}V_{DC}$
1	1	0	$v_2 = \frac{1}{3}V_{DC} + j\frac{\sqrt{3}}{2}V_{DC}$
0	1	0	$v_3 = \frac{-1}{3}V_{DC} + j\frac{\sqrt{3}}{2}V_{DC}$
0	1	1	$v_4 = \frac{-2}{3}V_{DC}$
0	0	1	$v_5 = \frac{-1}{3}V_{DC} - j\frac{\sqrt{3}}{2}V_{DC}$
1	0	1	$v_6 = \frac{1}{3}V_{DC} - j\frac{\sqrt{3}}{2}V_{DC}$
1	1	1	$v_7 = 0$

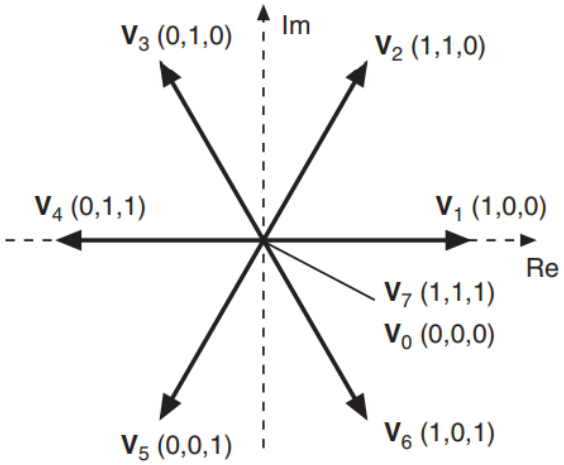

Figure II- 3 : Voltage vectors in the complex plane

In order to reduce the number of calculations for the output current, we can transform the three equations in (II.1) into one equation using (II.1). We obtain:

$$i[k+1] = \left(1 - \frac{RT_s}{L}\right) i[k] + \frac{vT_s}{L} \qquad \text{(II.11)}$$

Thus, the cost function (II.1) becomes:

$$J = |i[k+1] - i^*[k+1]| \qquad \text{(II.12)}$$

The output voltage vectors of the inverter are stored and selected rather than calculated each sampling period of the algorithm. The calculation of the cost function is a subtraction of two one-dimensional complex variables rather than three-dimensional variables. So, the number of calculations is considerably reduced.

II.3The proposed artificial neural networks architectures

The ANN based on MPCC combinesthe advantages of both neural network and model predictive control, for current control and it undergoes two main steps: (i) we use MPC as an expert or a teacher for generating the data required for training off-line the proposed neural network using standard supervised learning, under full-state observation of the system; (ii) once the off-line training is performed, the trained ANN can successfully control the switching, without the need of using MPC at test time.

In this chapter, we focus on two different types, perceptron neural network using the hard-limit as active function and feed forward back-propagation which use as activation function Levenberg-Marquardt (trainLm). Though the training data collected from MPC algorithm are the same for both networks, their data processing varies due to the different requirement of NN outputs. [13]

II.3.1 Perceptron neural network

The perceptron is a linear combiner that quantizes its output to one of two discrete values. In single-layer perceptron, the input signals p_k are scaled by a set of adjustable weights$w_k$to generate an intermediate output signal$y$, which is then processed by a hard limiter, resulting in the quantized binary output a. This binary output is then compared to the desired response (target), which is also a binary signal, generating an error that is used in a feedback strategy to adapt the weights. The input signals can be binary-valued or they can be drawn according to a continuous distribution. [72]

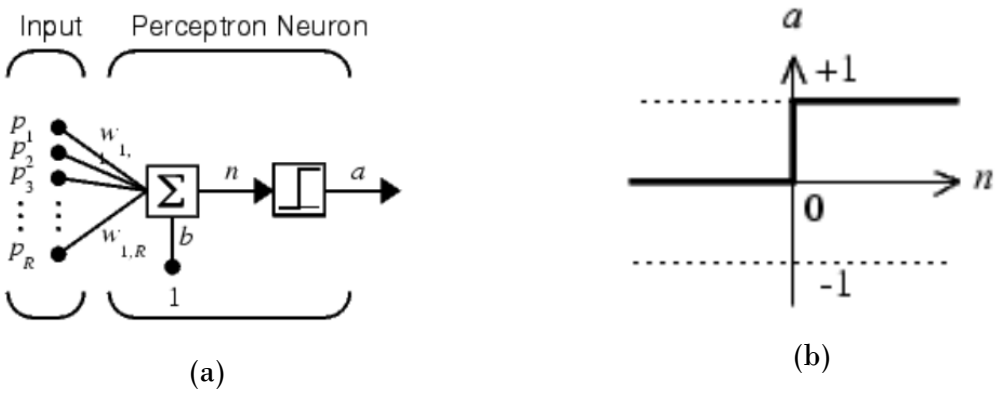

Figure II- 4 : (a) perceptron neural network scheme, (b) the activation function hard-lim

The output unit uses the Hard-limit (threshold) function as an activation function, thus implementing a two-class classification task onto the space {0, 1}

$$a = hardlim(n)\begin{cases}1 & if\ y > 0\\ 0 & if\ y < 0\end{cases}$$

Where: y is the output of the trained ANN.

II.3.2 Artificial Neural Network Fitting (fitnet)

MATLAB R2015a [nnstart] wizard has been used to create and train a network and afterward test the network. Neural network is trained by using Levenberg-Marquardt (trainlm), unless there is not enough memory, in which case scaled conjugate gradient back-propagation (trainscg) will be used. These algorithms display competitive advantages over one another.

Artificial Neural Network Fitting (fitnet) is used for static fitting problems with standard two layer feed forward neural network trained with Levenberg- Marquardt (LM) algorithm, denoted by 'trainlm', works faster when it trains a moderate-sized feed forward neural network that can hold up to several hundred weights [23] and supports the training with validation and test vectors, The data are randomly divided into 70% training, 15% testing and 15 % validation. The training data are used to adjust network weight as per error. The validation data are used for network generalization and to halt training when generalization stops improving. The testing data have no effect on training and it provides an independent measure of network performance during and after training. The hidden layer neurons are increased when network is not performing well after training. The training stops automatically when generalization stops improving as indicated by an increase in the mean square error (MSE) of the validation data samples. [72]

II.4ANN training procedure

The ANN takes as inputs the measured current i , the reference current i^* , all expressed in $\alpha\beta$ coordinates. The real and imaginary parts of these variables are separately fed to the neural network, bringing the total number of input features to four i.e., *inputs* =4. The outputs of the ANN are the three control signals Sa, Sb, Sc.

The training data, which have been collected by MPC, comprises10 experimental conditions; in each experience we choose a specific value of resistance (R= 5, 10, 15, 20, 25, 30, 35, 40, 45, 50 Ω) with different values of current of reference i^*,

For each experimental condition, the simulation is run using MPC. Then, the input features of the neural network and their targets are stored for training.

As a consequence, the total dataset consists of 500010 instances, which is the same for both networks. This dataset has been divided into two parts: 70% randomly selected for training purposes, and 30% for testing and validation when we used a fitnet training, as opposed to the perceptron method where 100% of the data has been used for training purposes. Their data processing varies due to the different requires of NN outputs. NN fitting net has no limits for the output elements so we had to add a saturation + round blocks on Simulink compared with NN perceptron which provide binary outputs (0 and 1).

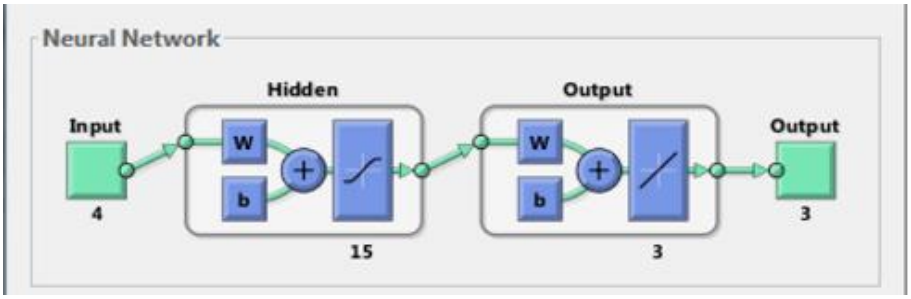

Figure II- 5 : General topology of the 15-neuron hidden layer feed-forward ANN

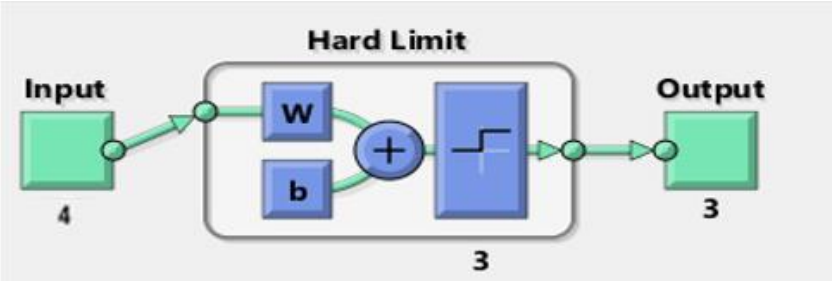

Figure II- 6 : General topology of single layer perceptron neural network

The following table presents the NN training parameters

Table II- 3 : the training parameters

	Perceptron	Feed forward back-propagation
Epochs	1	1000
iterations	1	278
Training time	48 mn	27mn
MSE	0.78262	0.058118
regression	-	0.81175
Hidden layers	Single layer	One hidden layer (15 nodes)

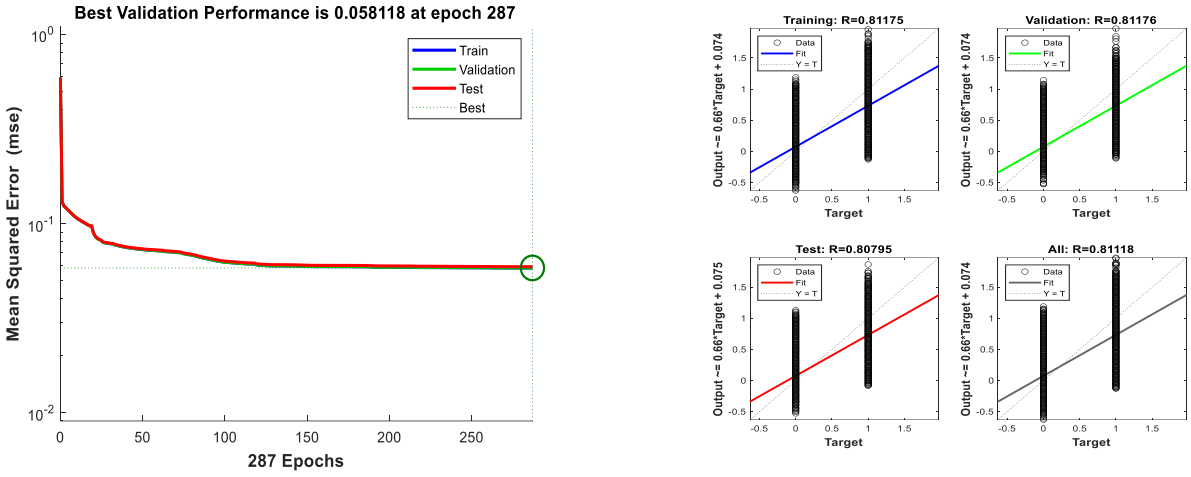

(a) (b)

Figure II- 7 : (a) fitting neural network performances, (b) fitting neural network regression

Figures (II-7) and (II-8) indicate the best validation performance, which was taken, for the fitnet training case, from epoch 278 with the lowest validation error of 0.058118, while for the perceptron neural network the best validation was taken from the first training iteration with the lowest validation error of 0.78262.

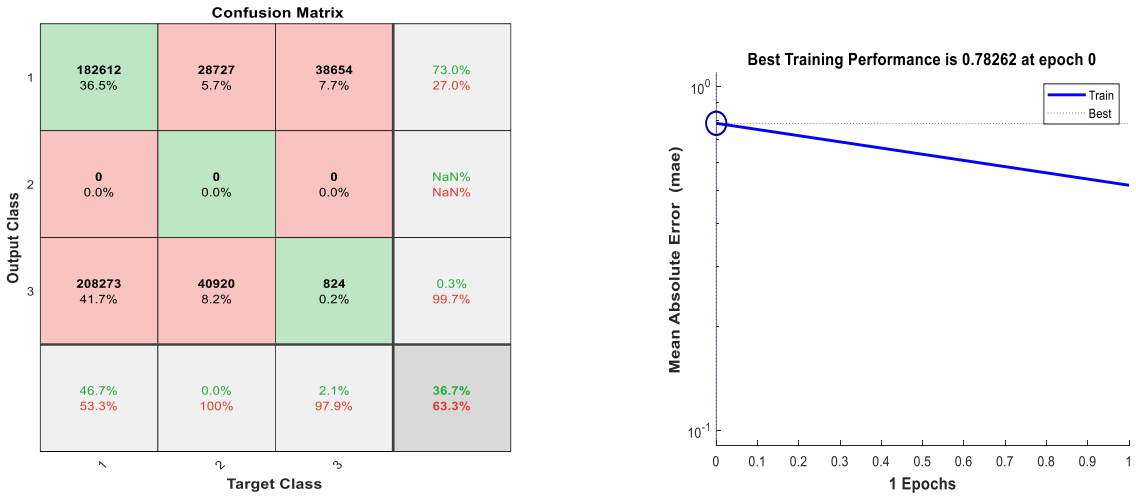

(a) **(b)**

Figure II- 8: (a) confusion matrix of PNN, (b) training performance of PNN

To clearly improve the training performance of perceptron neural network, it gives a confusion matrix shown in Figure II-8 which is obtained from the training code, each row in matrix corresponds to an output class (i.e. Sa, Sb and Sc), and the columns are the target classes which are taken from the sample data. The green cells in the diagonal of the matrix identify the number and percentage of correctly classified data points (at the final training iteration), while all other red cells indicate the incorrect classifications. On the other hand, five light-grey blocks in the last column, row include the specific prediction accuracies for every class/feature. As shown in FigureII.8, the 2nd and 3rd classes have very low accuracies so, we may adjust the training data set of 2ndand 3rd classes to pursue a better training performance. However, in this study, we cannot change to the data affected becauseall training data are obtained under certain conditions with sinusoidal references thus; it is very hard to manually determine which inputs can get its data.

II.5Simulation Results and analysis

This section provides a comprehensive study and evaluation of the two proposed control strategies, taking into account different loads under various operating conditions.

To verify the proposed ANN-based control strategy (model predictive current control) and compare its performance with the conventional MPC, we used MATLAB (R2020a)/SIMULINK software components to implement the SIMULINK model and the simulations results of the system are shown in the figures bellow

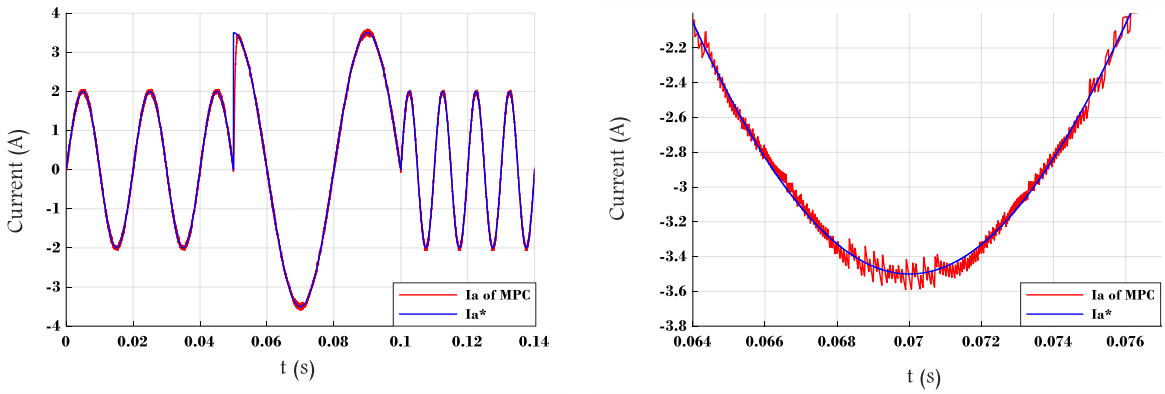

(a)

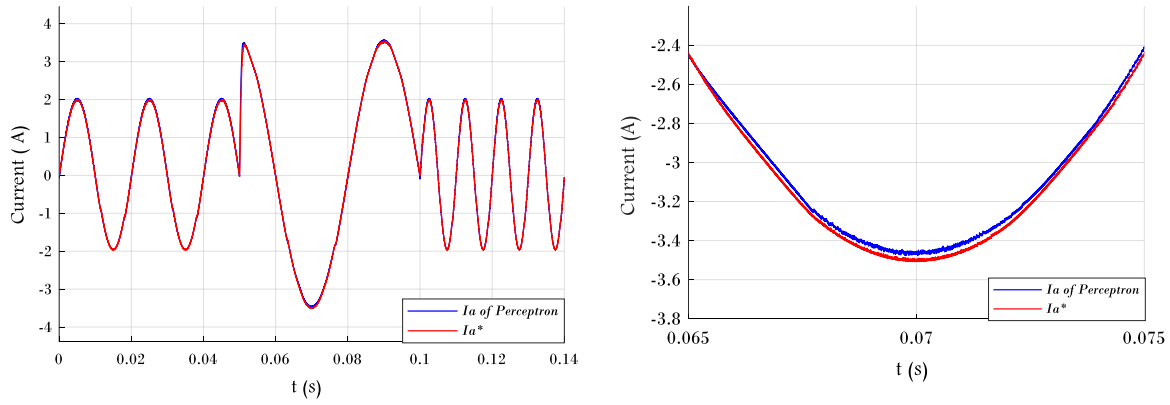

(b)

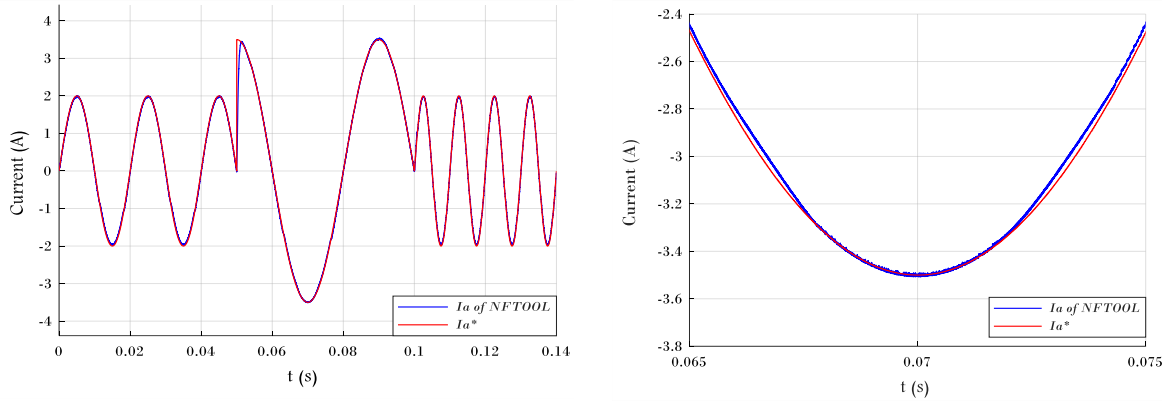

(c)

Figure II- 9 : Simulation results of current control of a two-level inverter-fed RL-load: Reference and output current of phase A and their zoom. (a): MPCC, (b): PNN, (c): fitnet

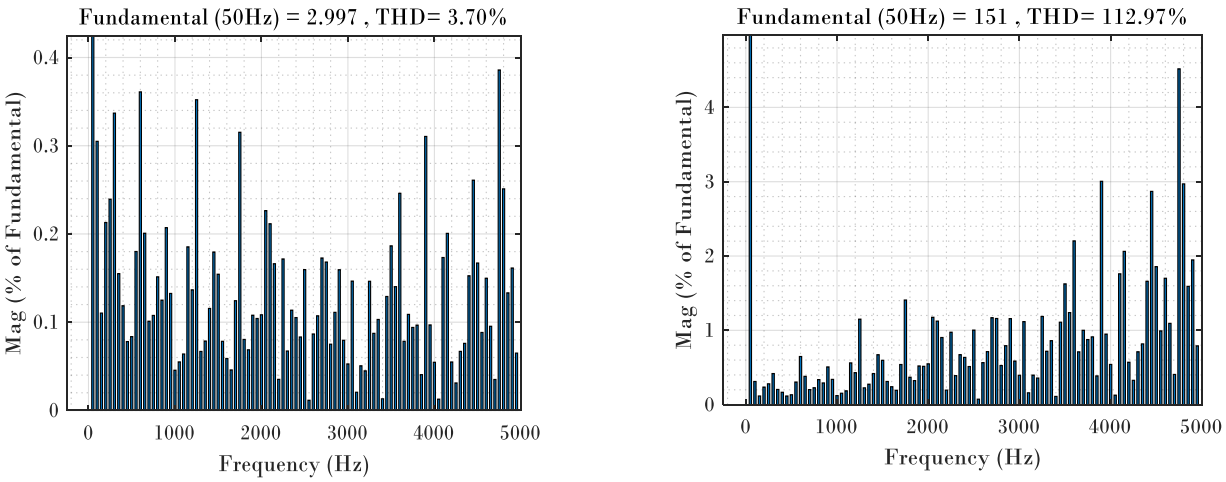

(a)

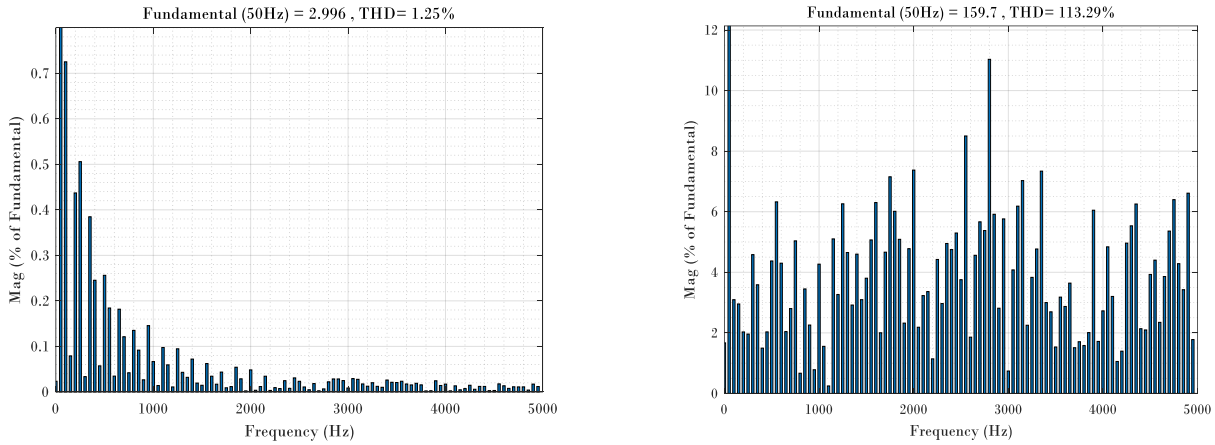

(b)

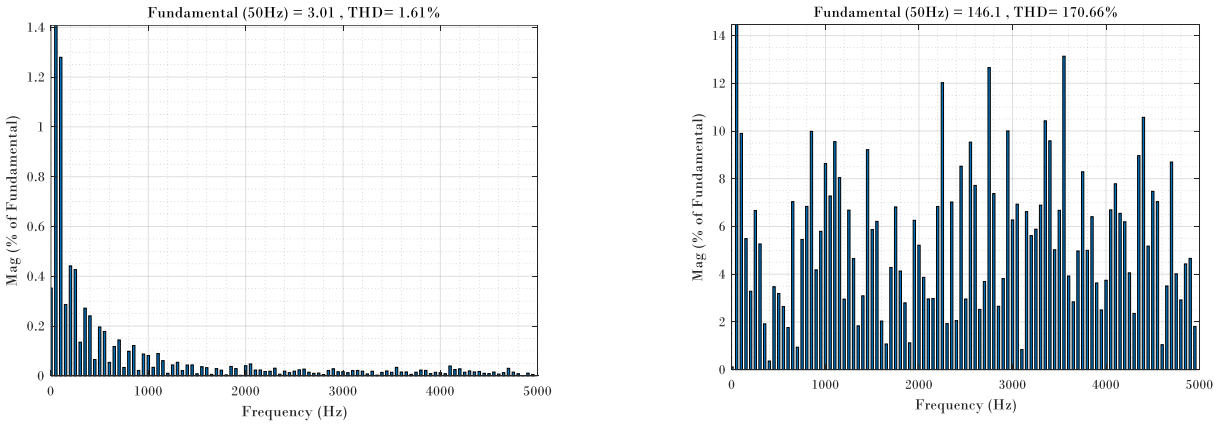

(c)

Figure II- 10 : Simulation results of current control of a two level inverter-fed RL-load Output current and output voltage spectra expressed as percentages of fundamental magnitude,$|\mathbf{I}^*| = \mathbf{3\ A}$ and $\mathbf{f}^* = \mathbf{50\ Hz}$ with (a) MPC, (b) fitnet, (c) PNN

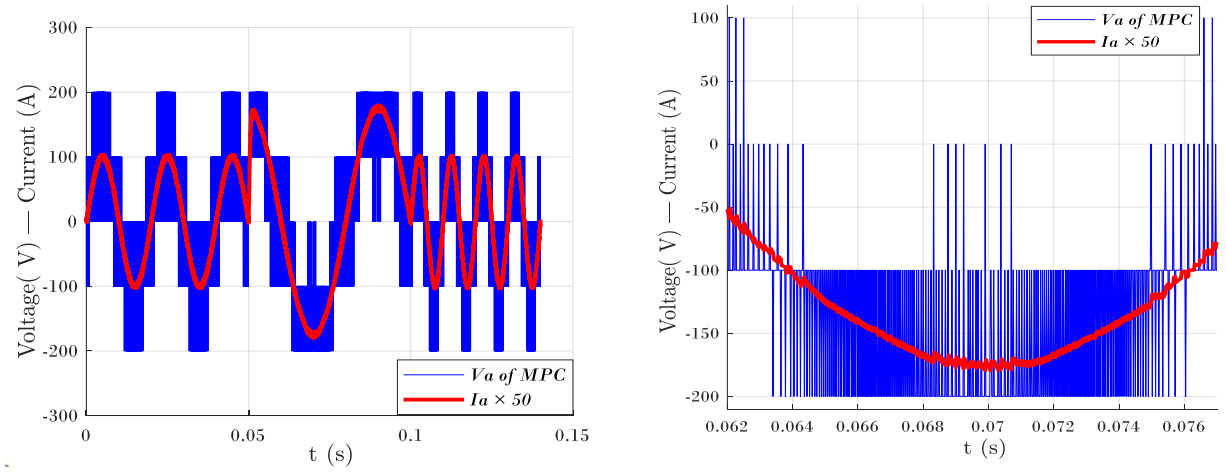

(a)

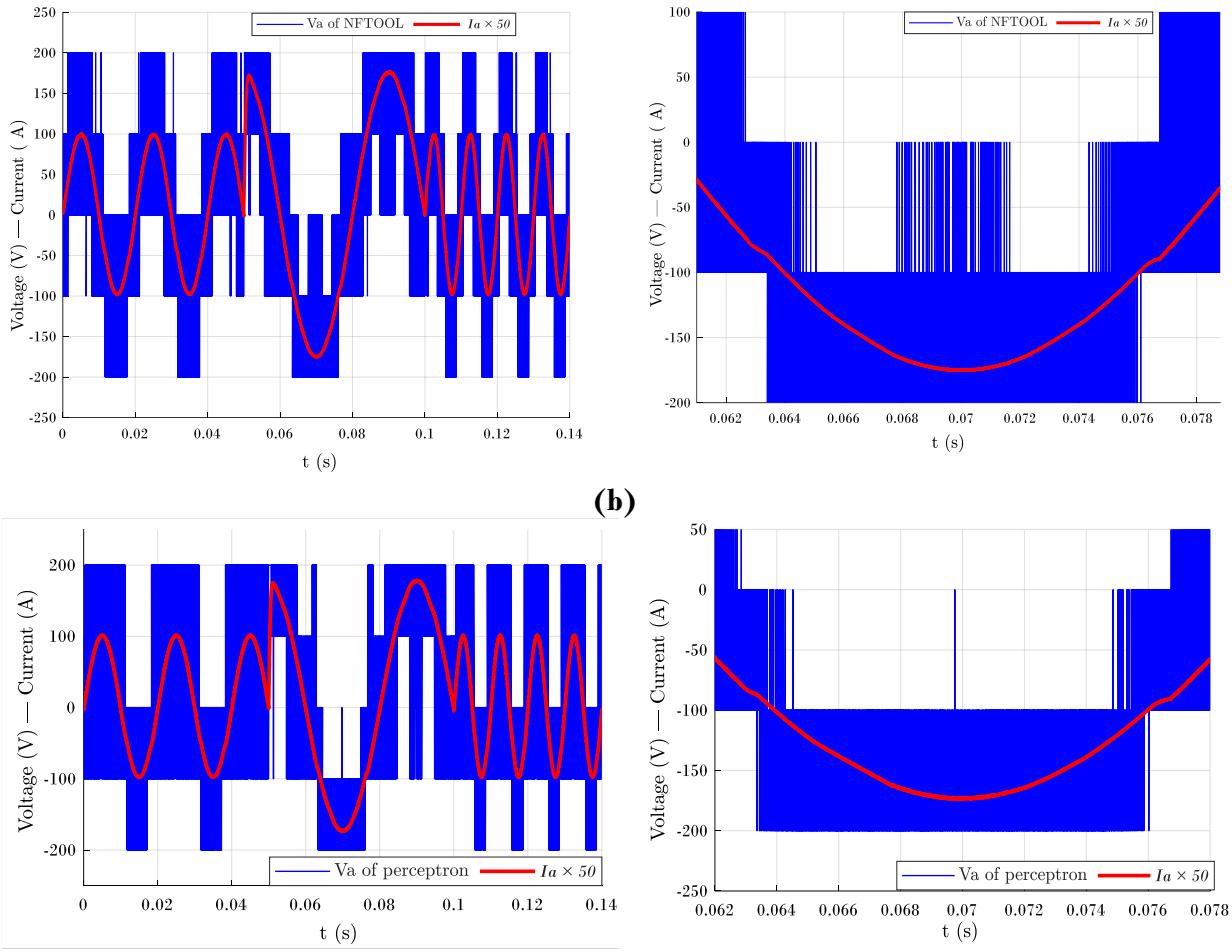

Figure II- 11: Simulation results of current control of a two-level inverter-fed RL-load: Output voltage of the inverter and 50 ×the load current of phase A with: (a) MPC, (b) fitnet, (c) PNN

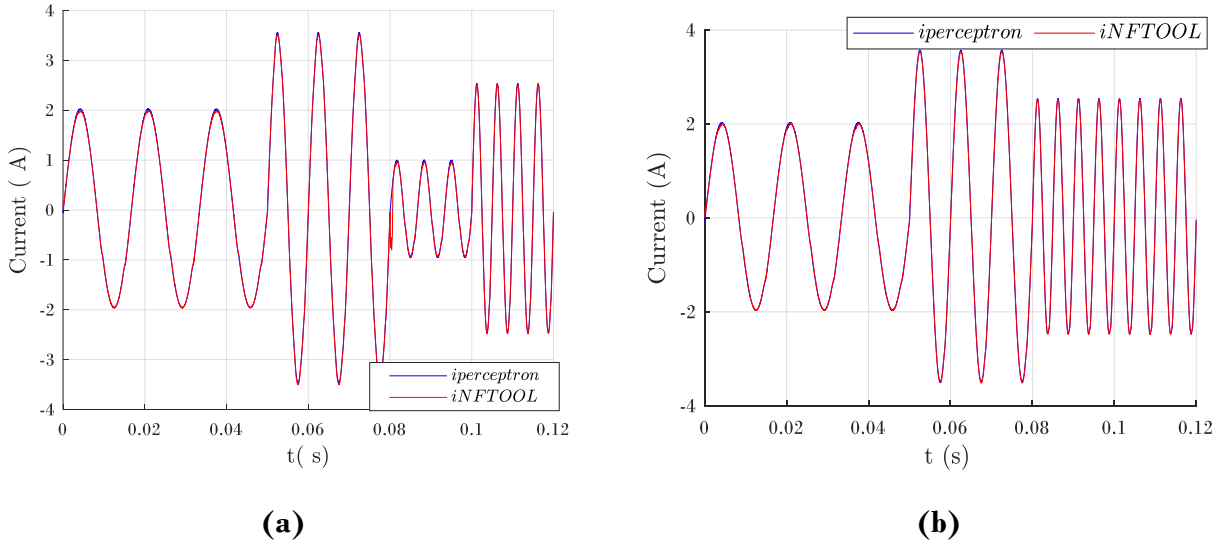

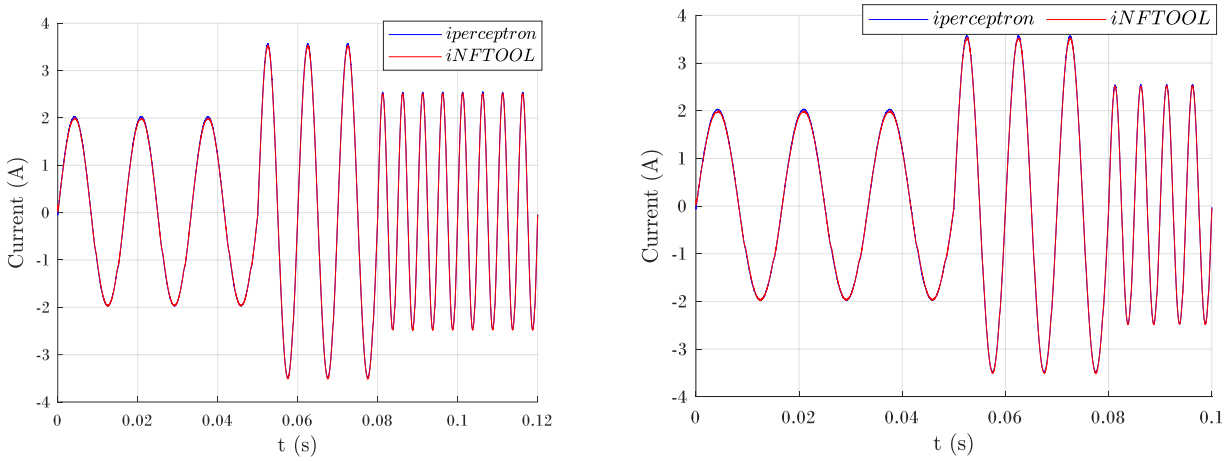

Figure II- 12: Simulation results of current control of a two-level inverter-fed RL-load: output current of phase A with PNN and fitnet (NFTOOL) for different magnitude and different frequencies

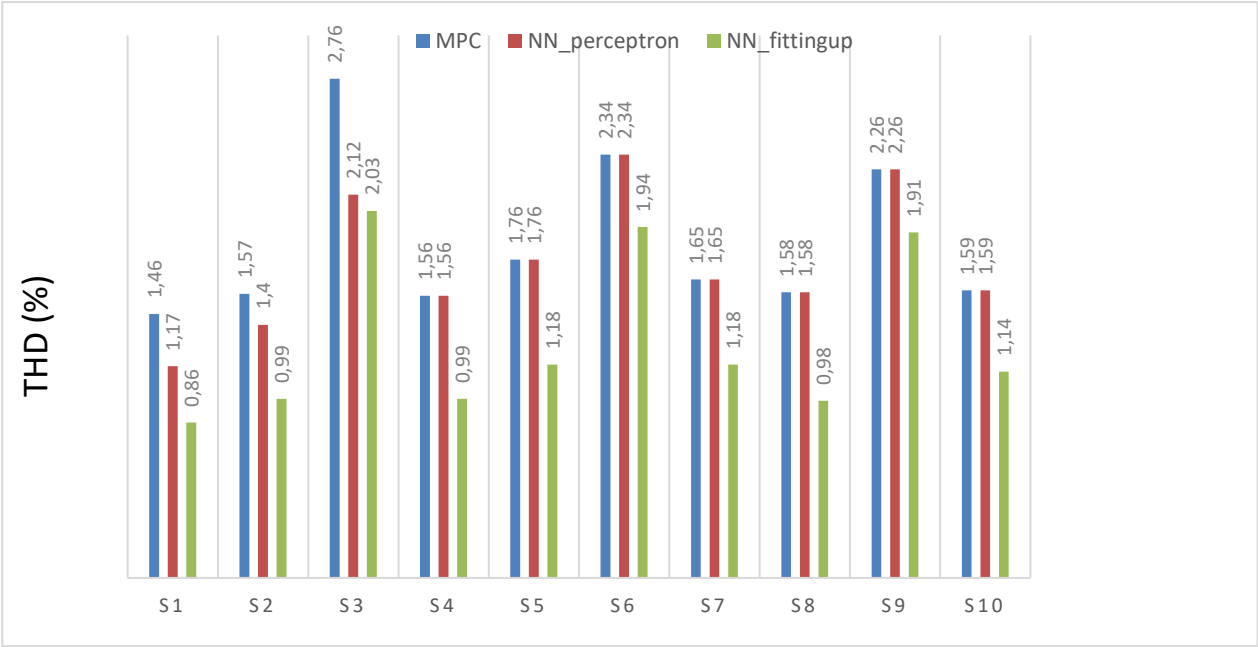

Figure II- 13 : Comparison of the THD of the output current obtained by the three proposed control strategies, for some cases given in Table below, under different operating conditions.

Table II- 4 : A comparison between the two proposed control strategies under different operating conditions

	V_{DC}	R	I	THD	THD	
				MPC	PERCEPTRON	FITNET
S1	300	10	4	1.46	1.17	0.86
S2	300	20	3.5	1.57	1.40	0.99
S3	300	30	2	2.76	2.12	2.03
S4	300	40	3.5	1.56	1.56	0.99
S5	300	50	3	1.93	1.76	1.18
S6	300	60	2	2.55	2.34	1.94
S7	350	40	3	2.08	1.65	1.18
S8	350	50	3.5	1.93	1.58	0.98
S9	350	60	2	2.67	2.26	1.91
S10	500	50	3	2.88	1.59	1.14

Figure II-9 shows the simulation steady performance of the MPC controller, PNN, and fitnet controller. For Fig II-9((a), (b), (c)), the outputs currents are controlled to track their references (different magnitudes and frequencies), the output current of MPC oscillates around its reference forming a ripple, or a band, around the reference while in the ANN-controllers almost are superimposed. The output current ranges from (2A, 50Hz) to (3A, 25Hz) then (2A, 100Hz). The ANN-controllers can track theirs references with fast dynamic response. In addition, both of the ANN-controllers have good wave form current effect compared to the MPC. Also, it can be noticed that current of fitnet is smoother than PNN.

Figure II-10 represents the output current and output voltage harmonic spectrum of the MPC, PNN, and fitnet controllers expressed as percentages of fundamental magnitude with a fixed reference frequency and magnitude. This figure clearly shows that ANN-controllers can achieve good THD results compared to MPC, it can be seen that the output current quality of ANN-based approach is improved significantly, with a current THD of 1.7737% for PNN, 1.3039% for fitnet compared to 2.3738% for MPC.

Figure II-11 represents the output voltage of the inverter and 50 ×the load current of phase A of the MPC, PNN and fitnet controllers. This figure clearly shows that the form of output voltages obtained using MPC is better than that obtained using the ANN-controllers but in some conditions, it can be noticed that fitnet controller achieves better results.

Figure II-12 is a comparison of the output current of the two strategies, the comparison did on different conditions : magnitudes (1A ,2A, 2.5A, 3.7A), different frequencies (60Hz, 100Hz, 200Hz), different values of Vdc (300V, 250V, 400V, 500V) and different values of resistance (50Ω, 20Ω ,40Ω) shown in Figure II-12 (a,b,c,d) following . We can see that the current follows its new reference quickly after any change in its magnitude and frequency despite the variations of the resistance and Vdc value. This result proves the flexibility, efficiency of proposedd strategies.

Figure II-13 is a Histogram gives statistical information about the THD of the current output of the three controls strategies. The histogram was created using information shown in Table II-4. It is observed that THD current obtained by proposed strategy improvesits performance to outperform that of MPC particularly that's obtained by fitnet strategy. For example, (THD) ANN-fitnet of cases S3, S5, S8, is decreased to be 2.03%, 1.18%, 0.98%, 2.35%, 3.86%, respectively.

As anticipated, the performance of the ANN-based MPC outperforms that of MPC, which can be noticed in lower THD and less settling time to reach steady-state particularly shown on fitnet. Moreover, in sample (10), it is noticed that THD of ANN-controllers achieves a good result in Vdc= 500V although when the range of data Vdc value fixed on 300 V.

II.6Comparison of the three methods

The advantages and disadvantages of the proposed methods are summarized as follow: regarding the computation burden, the ANN-controllers method has the lowest computation, this is the key advantage of the ANN compared to the MPC method. For the control performance, the THD of output current of the fitnet is the best. However, ANN-controllers have a better ability to handle the input variables, which beyond the training

data range. The waveform of output voltages obtained using MPC are better than that obtained using the ANN-controller.

II.7Implementation of ANN-MPCC

In order to verify the theoretical developments, emphasize the appeal of the proposal ANN control based on model predictive control, and to study how the technique can reduce the burden calculation and how the technique can operate with frequency as well as in power converters. An implementation test have been done in CDER laboratory.

II.7.1.1 Materials and Methods

We used the following hardware equipment to design the test bench developed for this project:

- The C2000 DIMM100 Experimenter's Kit “DSP card “

- Laptop with MATLAB/Simulink

- Oscilloscope

- Cables

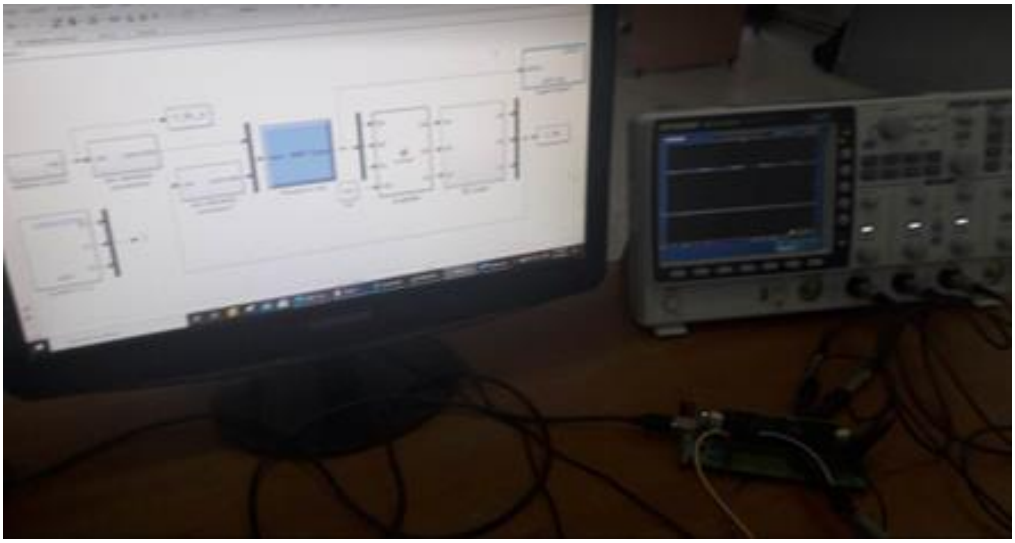

Figure II- 14 : laboratory materials

For neural network implementation, we used the software Matlab/Simulink with TI (Texas Instrument) development tools. First, it is necessary to make a Simulink model which will be compiled and then loaded to the DSP card.It is important to design the following blocks (algorithms): neural network block (the same as the one used in simulation), digital output (GPO blocs), current references.

II.7.1.2 Results

To obtain Implementation, results in DSP card, theused frequency was 40 KHz.

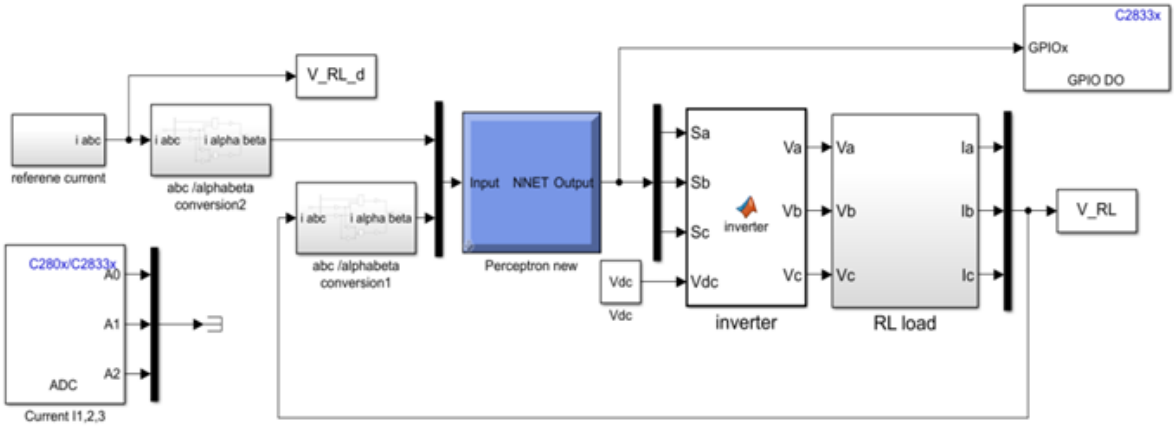

Figure II- 15 : The blocs used for implementation Test

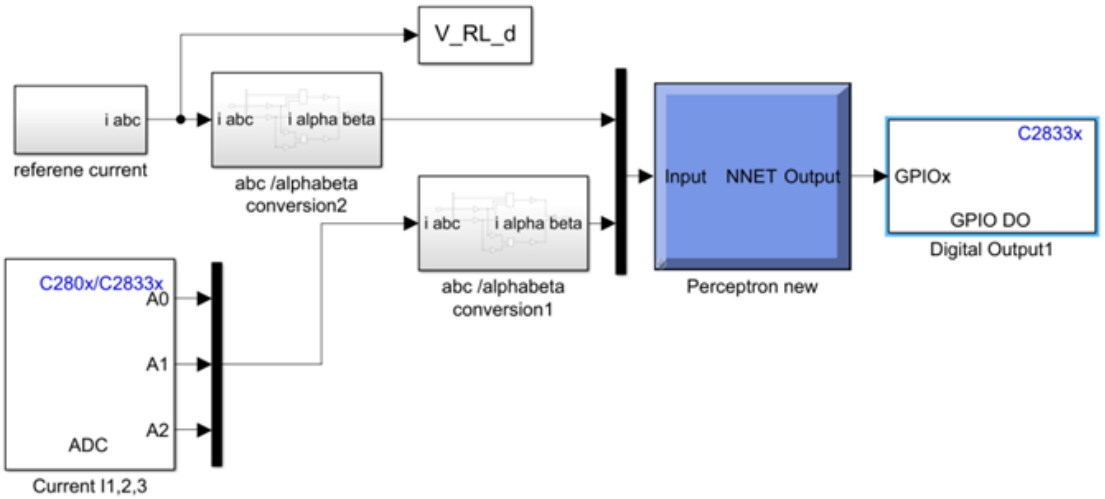

Figure II- 16 :the blocs that will be used for real implementation

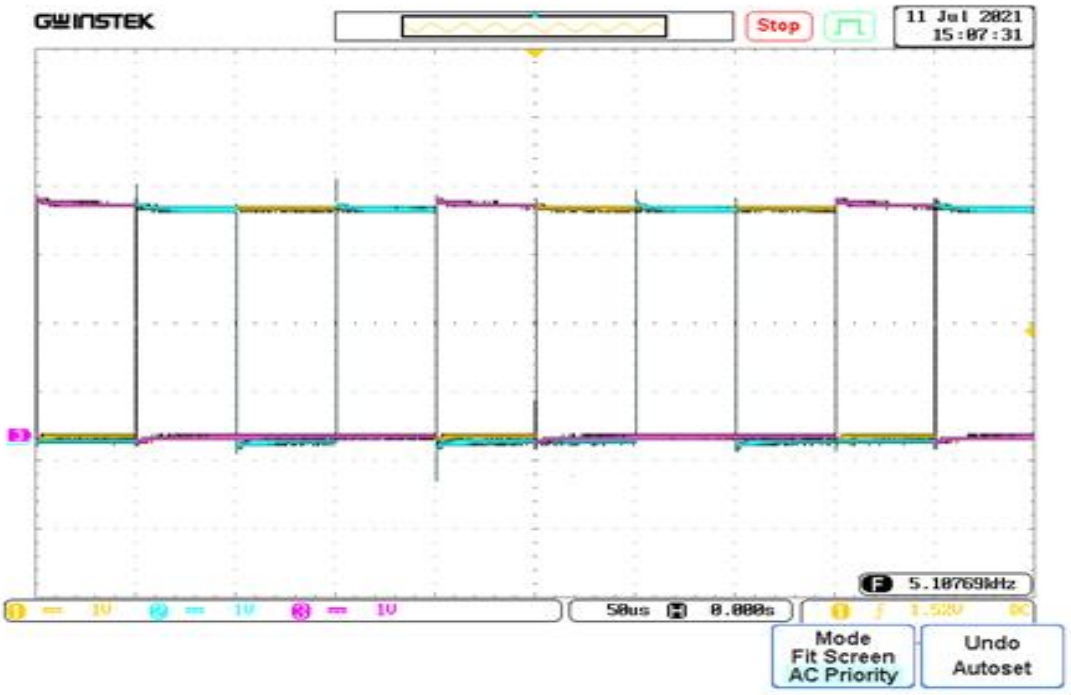

Figure II- 17 : the PWM signals (a)

The Implementation results of neural network (type perception) show that the controller can be easily implemented in the DSP and it can work even beyond 40 KHz.

II.8Conclusion

In this chapter, a novel control strategy using an artificial neural network control using two methods, to generate a high-quality sinusoidal output current of a three-phase inverter with an RL load has been successfully developed and simulated, under various operating conditions.

The output current of the inverter is directly controlled, without the need for the mathematical model of the inverter, considering the whole system as a black box. In this work, MPC has been used for two main purposes: (i) generating the data required for the off-line training of the proposed ANN, and (ii) comparing its performance with the proposed ANN-based controller for various conditions. Simulation results, based on a test with different references beyond the training data range, shows that the proposed ANN-based controllers give better performances than MPC in terms of a lower THD. Fitnet provides a better control performance compared to PNN.

Chapter three

Artificial neural network based on Model Predictive Torque Control a Three-Phase, Two Level, Inverter-Fed induction machine

CHAPTER THREE

Introduction

The induction machine is currently the most used machine in industrial field and gradually replacing the DC machine. However, the induction machine is a multivariate system. It is characterized by a nonlinear model, which makes the control very complicated. The Model Predictive Torque Control (MPTC) strategy is a developed drive control technique of induction machines. It is characterized by a fast dynamic response, simple implementation and robustness essentially to the rotor parameter variation. However, the MPC has the main disadvantages such as electromagnetic torque, stator flux ripples and the burden calculation. Therefore, many methods are used to overcome these disadvantages, for example, replacing it with a neural block. The artificial neural networks are capable to explore multivariate correlations between the outputs and inputs variables without knowing the mathematical model of the system [73][74]

In this chapter, the proposed strategy: Artificial neural network-based Model Predictive Torque Control (MPTC) scheme has been applied to the system (inverter + machine), which is one of the most common electrical motor drive. The control scheme is described in details from machine modeling to simulating the system along with inverter model that is described in the previous chapter.

III.1 Artificial neural network based MPTC

In this chapter we developed a strategy of an intelligent control based on neural network for induction motor control-based model predictive torque control (MPTC). The proposed control consists of an estimation of stator flux vector and electromagnetic torque, with the aim of getting a better dynamic performance of the system. First, MPTC is a selection of a voltage vector which results in a stator flux φ_s and electromagnetic torque T_{em} that satisfies the objective of the control. To do so, the control scheme uses models of the converter and the machine to calculate predictions of the controlled variables which are then compared to their references at each sampling period. The voltage vector is selected based on predefined conditions that are implemented in the cost function. This strategy of

control is used, as an expert, in the training phase to generate data required for training the proposed neural network. Then, once the neural network is fine-tuned, it can be successfully used online for controlling, without the need of using MPTC. The proposed ANN-based control strategy is validated through simulation, using MATLAB/Simulink tools, taking into account different conditions.

III.2 System modeling

In the control of any power electronics drive system to start with a mathematical model of the plant is required. This model should have a structure that fully describes the behavior of the machine and, on the other hand, it should be practical for the implementation of the MPC algorithm.

As shown in the Figure below, the three-phase induction machine has basically two parts: fixed part, called a stator,built up of high-grade alloy steel laminations to reduce eddy current losses. It has three main parts, namely the outer frame, the stator core, and a stator winding. A mobile part, called rotor, is not powered, it is short-circuited and it can be of two kinds:

- Wire-wound (with rings), is used when variable speed is required. The rotor carries a 3-phase insulated winding. Depending upon the requirement any external resistance can be added in the rotor circuit.

- Squirrel cage, almost 90% of induction motors have squirrel cage rotors. The rotor consists of a cylindrical laminated core with axially placed parallel slots for carrying the conductors. As the rotor bar ends are permanently short circuited, it is not possible to add any external resistance in the rotor circuit.

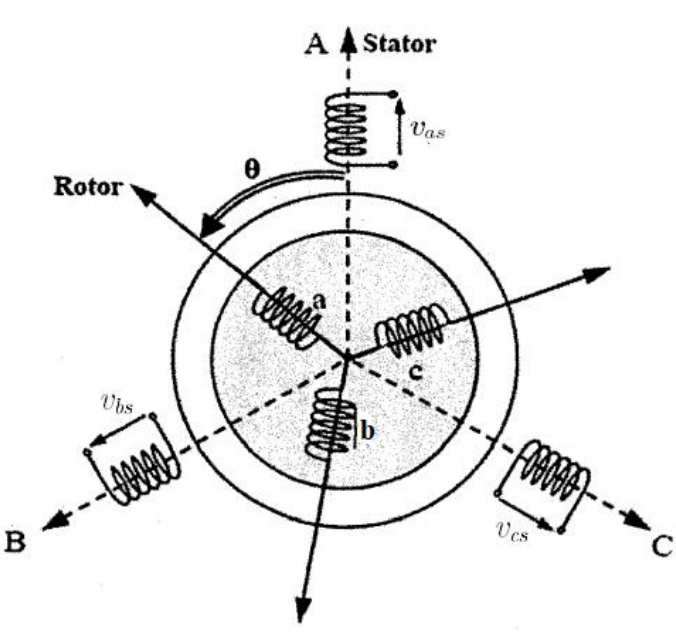

Figure III- 1 : Schematic representation of the three-phase asynchronous machine

We are interested in the squirrel cage asynchronous motor; this is because the squirrel cage rotor has a simple and rugged construction. In order to establish a simple relation between the supply voltage of motor and its currents, simplifying assumptions must be introduced as:

- The air gap is of uniform thickness and the notching effect is negligible;
- We neglect the eddy current and the saturation of the magnetic circuit and its hysteresis, which leads to a sinusoidal magnetic field;
- The resistance of the windings does not vary with the temperature and we neglect skin effect (uniform current density in the conductor section);
- We only consider the first space harmonic created by each of the phases of the two frames (neglecting space harmonics that do not contribute to the average torque. This assumption entails a sinusoidal magneto-motive force (MMF) distribution)

Among the important consequences of these hypotheses, we can cite:

- The flux is additive;
- Self-inductance is constant;

- The law of sinusoidal variation of mutual inductances between the windings of the stator and rotor as a function of the electrical angle of their magnetic axes.

III.2.1 Electrical equations

The electric equations of the asynchronous squirrel cage machine (short-circuited rotor), are written as follows:

$$\text{Stator: } \begin{cases} v_{as} = R_s I_{as} + \frac{d\varphi_{as}}{dt} \\ v_{bs} = R_s I_{bs} + \frac{d\varphi_{bs}}{dt} \\ v_{cs} = R_s I_{cs} + \frac{d\varphi_{cs}}{dt} \end{cases} \quad \text{(III.1)}$$

$$\text{Or in vector form: } [V_{sabc}] = [R_s][I_{sabc}] + \frac{d[\varphi_{sabc}]}{dt}$$

$$\text{Rotor: } \begin{cases} v_{ar} = R_r I_{ar} + \frac{d\varphi_{ar}}{dt} = 0 \\ v_{br} = R_r I_{br} + \frac{d\varphi_{br}}{dt} = 0 \\ v_{cr} = R_r I_{cr} + \frac{d\varphi_{cr}}{dt} = 0 \end{cases} \quad \text{(III.2)}$$

$$\text{Or in vector form: } [V_{rabc}] = [R_r][I_{rabc}] + \frac{d[\varphi_{rabc}]}{dt} = \begin{bmatrix} 0 \\ 0 \\ 0 \end{bmatrix}$$

Where:

- $v_{as}, v_{bs}, v_{cs}, v_{ar}, v_{br}$ and v_{cr} are the three stator and rotor voltages
- $i_{as}, i_{bs}, i_{cs}, i_{ar}, i_{br}$ and i_{cr} are the three stator and rotor currents
- $\varphi_{as}, \varphi_{bs}, \varphi_{cs}, \varphi_{ar}, \varphi_{br}$ and φ_{cr} are the fluxes through the three phases of the stator and the rotor

III.2.2 Magnetic equations

The magnetic equations of the asynchronous squirrel cage machine are written as follows:

$$\text{Stator: } \begin{cases} \varphi_{as} = L_s I_{as} + M_s I_{bs} + M_s I_{cs} + M_1 I_{ar} + M_3 I_{br} + M_2 I_{cr} \\ \varphi_{bs} = M_s I_{as} + L_s I_{bs} + M_s I_{cs} + M_2 I_{ar} + M_1 I_{br} + M_3 I_{cr} \\ \varphi_{cs} = M_s I_{as} + M_s I_{bs} + L_s I_{cs} + M_3 I_{ar} + M_2 I_{br} + M_1 I_{cr} \end{cases} \quad \text{(III.3)}$$

$$\text{Rotor: } \begin{cases} \varphi_{ar} = L_r I_{ar} + M_r I_{br} + M_r I_{cr} + M_1 I_{as} + M_2 I_{bs} + M_3 I_{cs} \\ \varphi_{br} = M_r I_{ar} + L_r I_{br} + M_r I_{cr} + M_3 I_{as} + M_1 I_{bs} + M_2 I_{cs} \\ \varphi_{cr} = M_r I_{ar} + M_r I_{br} + L_r I_{cr} + M_2 I_{as} + M_3 I_{bs} + M_1 I_{cs} \end{cases} \quad \text{(III.4)}$$

Where:

$M_1 = M_{sr}\cos(\theta)$

$M_2 = M_{sr}\cos(\theta - 2\pi/3)$

$M_3 = M_{sr}\cos(\theta + 2\pi/3)$

- L_s : stator inductance
- R_s : stator resistance
- L_r : rotor inductance
- R_r : rotor resistance
- M_s : mutual inductance between two stator windings
- M_r : mutual inductance between two rotor windings
- M_{sr} : magnitude of the inductance between the stator and the rotor

III.2.3 Mechanical equation

The mechanical equations of the asynchronous squirrel cage machine are written as follows:

$$\frac{d\Omega}{dt} = \frac{1}{J}\,(T_{em} - T_L - k_f\Omega) \qquad \text{(III.5)}$$

Where:

- Ω : mechanical speed
- J : moment of inertia of the mechanical shaft
- T_{em} : electromagnetic torque
- T_L : load torque
- k_f : dry friction coefficient

The problem with this model established so far (systems (III.1), (III.2), (III.3) and (III.4)) is the linear dependence of the system which can be presented a three-axis coordinate system. Thought we will have a number of equations, inputs and outputs, makes the model inappropriate for implementation.

A linearly dependent system allows to describe three physical quantities by only two variables. Hence, a complex variable can replace the three-phase systems as shown in Figure III- 2

For example, instead of representing the stator currents by a three-equation system, we can represent it using only one equation

$$i_s = \frac{2}{3}(i_{as} + a i_{bs} + a^2 i_{cs}) \text{ where: } a = e^{\frac{j2\pi}{3}} \quad \text{(III.6)}$$

Instead of:

$$\begin{cases} i_{as} = I_s \sin(\theta) \\ i_{bs} = I_s \sin(\theta - 2\pi/3) \\ i_{cs} = I_s \sin(\theta + 2\pi/3) \end{cases} \quad \text{(III.7)}$$

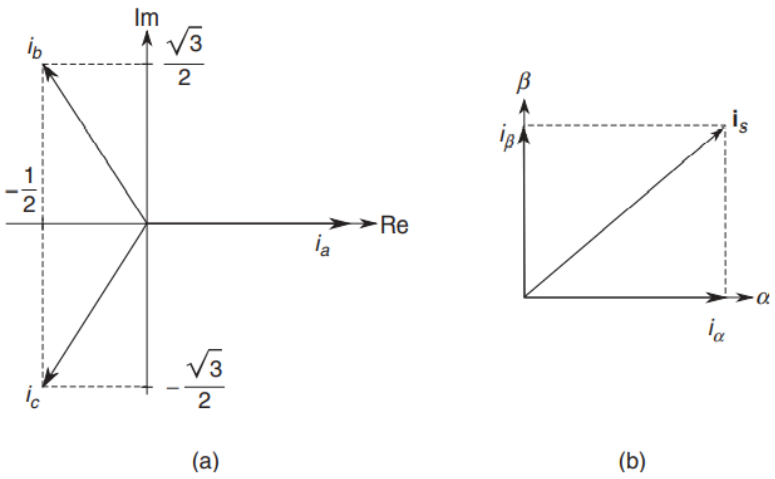

Figure III- 3 : Coordinate transformation

This coordinate transformation shown above is used for the other electrical and electromagnetic variables. Thus, the equations of an induction machine can be represented in any arbitrary reference frame rotating at an angular pulse ω_k. The variable ω denotes the rotor angular speed:

$$v_s = R_s i_s + \frac{d\varphi_s}{dt} + j\omega_k \varphi_s \quad \text{(III.8)}$$

$$v_r = R_r i_r + \frac{d\varphi_r}{dt} + j(\omega_k - \omega)\varphi_r = 0 \quad \text{(III.9)}$$

$$\varphi_s = L_s i_s + L_m i_r \quad \text{(III.10)}$$

$$\varphi_r = L_m i_s + L_r i_r \quad \text{(III.11)}$$

$$T_{em} = \frac{3}{2} pRe(\overline{\varphi_s} i_s) = -\frac{3}{2} pRe(\overline{\varphi_r} i_r) = \frac{3}{2} pIm(\overline{\varphi_r} i_s) \quad \text{(III.12)}$$

Where:

- ω : rotor angular speed $(\omega = p\Omega)$
- p : number of pole pairs
- $\bar{\varphi}$: the complex conjugate value of φ

In order to develop an appropriate control strategy, it is convenient to write the equations of the machine in terms of state variables[75][39]. The stator current $i_s$and the rotor flux vectors φ_r are selected as state variables.

From (III.11) we have:

$$i_r = \frac{\varphi_r - L_m i_s}{L_r} \quad \text{(III.13)}$$

By replacing (III.13) in (III.9) and by putting:

$$\tau_r = \frac{L_r}{R_r}$$

We get:

$$\varphi_r + \tau_r \frac{d\varphi_r}{dt} = -j(\omega_k - \omega)\tau_r \varphi_r + L_m i_s \quad \text{(III.14)}$$

For the other equation, we replace φ_s in (III.8) by $(L_s i_s + L_m i_r)$:

$$v_s = R_s i_s + \frac{d(L_s i_s + L_m i_r)}{dt} + j\omega_k (L_s i_s + L_m i_r)$$

Replacing (III.13) in (III.10) yields to:

$$v_s = R_s i_s + L_s \frac{di_s}{dt} + L_m \frac{di_r}{dt} + j\omega_k \left(L_s i_s + \frac{L_m}{L_r}\varphi_r - \frac{L_m^2}{L_r} i_s\right)$$

By putting:

$\tau_s = \frac{L_s}{R_s}$

$$\sigma = 1 - \frac{L_m^2}{L_s L_r}$$

$$k_r = \frac{L_m}{L_r}$$

$$R_\sigma = R_s + R_r k_r^2$$

$$\tau_\sigma = \sigma L_s / R_\sigma$$

We get:

$$i_s + \tau_\sigma \frac{di_s}{dt} = -j\omega_k \tau_\sigma i_s + \frac{k_r}{R_\sigma}\left(\frac{1}{\tau_r} - j\omega\right)\varphi_r + \frac{v_s}{R_\sigma} \quad \text{(III.15)}$$

Equations (III.12), (III.14) and (III.15) form the model of the induction machine used in this thesis. It has two inputs and two outputs that are mandatory for the control scheme to work.

$$\begin{cases} i_s + \tau_\sigma \dfrac{di_s}{dt} = -j\omega_k \tau_\sigma i_s + \dfrac{k_r}{R_\sigma}\left(\dfrac{1}{\tau_r} - j\omega\right)\varphi_r + \dfrac{v_s}{R_\sigma} \\ \varphi_r + \tau_r \dfrac{d\varphi_r}{dt} = -j(\omega_k - \omega)\tau_r \varphi_r + L_m i_s \\ T_{em} = \dfrac{3}{2} pIm(\overline{\varphi_r} i_s) \end{cases} \quad \text{(III.16)}$$

Other outputs can be extracted from the model, such as stator flux, rotor flux and electromagnetic torque because these variables are calculated inside the block of the induction machine. However, for experimental purposes, the stator flux and the rotor flux are estimated using estimators.

III.2.4 Cost function

The aim of the MPC is to maintain the actual value of torque and flux with its reference value and reduce the ripple, by the selection of an appropriated voltage vector that will derive the system variables $T_{em}(k+1)$and $\varphi_s(k+1)$ as close as possible to the desired reference value. The selection of a cost function usually dependents on absolute error between the predictions and the reference value. Therefore, the cost function can be expressed as:

$$J = \frac{|T_{em}^{p} - T^{*}|}{T_{nom}} + \frac{|\varphi_{s}^{p} - \varphi_{s}^{*}|}{\varphi_{s\,nom}} \qquad \text{(III.17)}$$

Where:

- T_{em}^{p} : the predicted value of the electromagnetic torque
- T^{*} : the reference value of the electromagnetic torque
- T_{nom} : the nominal value of the electromagnetic torque
- φ_{s}^{p} : the predicted value of the stator flux
- φ_{s}^{*} : the reference value of the stator flux
- $\varphi_{s\,nom}$: the nominal value of the stator flux

III.2.5 Working principle

The execution of the MPTC algorithm can be divided in three main steps: Estimation of the variables that cannot be measured, Prediction of the future plant behavior and Optimization of the single cost function according to a reference condition. The MPTC scheme is shown in figure bellow

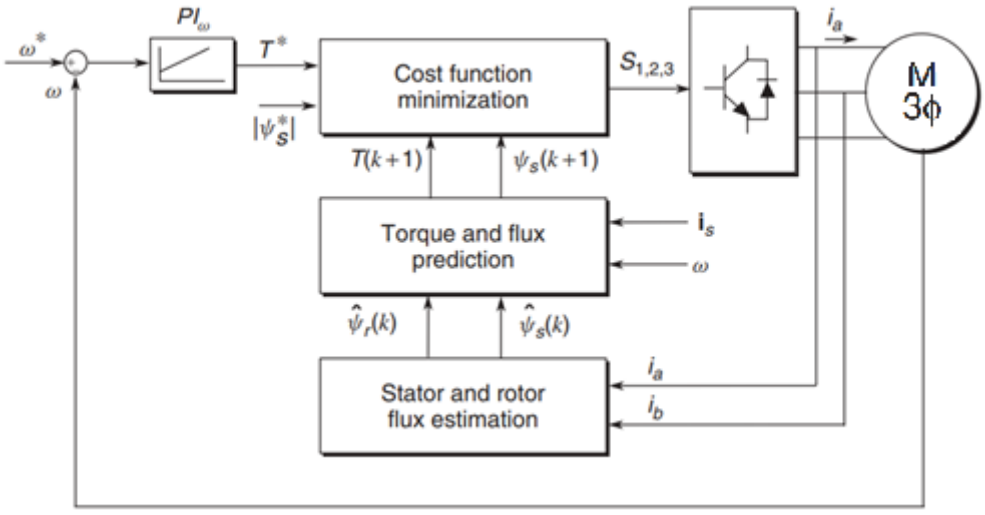

Figure III- 4 : MPTC scheme

Firstly, it computes the current values of the variables that cannot be measured, as the rotor flux and the stator flux. The predictive model computes the future values of

controlled variables, the electromagnetic torque and stator flux, in the next sampling period$(k+1)T_s$. These predictions are calculated for every actuating possibility given by the inverter topology. Then the model chooses the optimum switching statex_{opt}, which minimizes the corresponding cost function. The function contains the control law to reach the torque and stator flux references according to the references.

In order to further reduce the computational effort, only one out of two nil vectors of the 2LVSI is considered (the possible switching states of the converter are listed in Table II-1

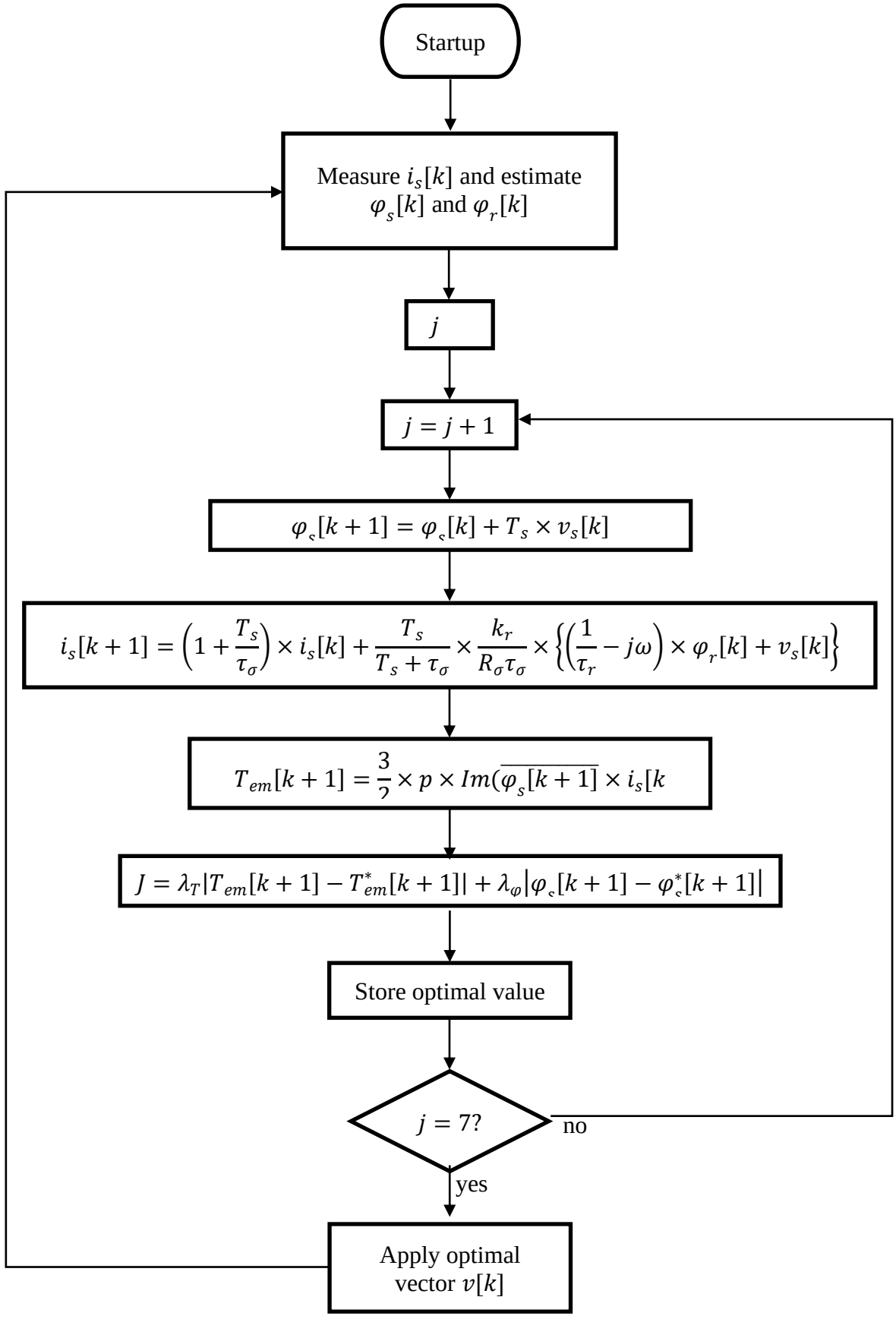

Figure III- 5 : Flow diagram of the MPTC

III.3 Implementation

Due to the discrete nature of digital controllers, probably the most common and simple method to obtain a discrete-time representation for a continuous-time system is the Euler approximation of time derivatives. The obtained model corresponds to a first order Taylor expansion

Choosing the stationary reference frame, $\omega_k = 0$, eliminates both multipliers in the internal feedback loops of the rotor winding and the stator winding [76].

After discretization and some arrangements of (III.12), (III.14), (III.15), and (III.16) we get:

We introduce the weighting factorsλ_T and λ_φ

Where: $\lambda_T = \frac{1}{T_{nom}}and\lambda_\varphi = \frac{1}{\varphi_{s\,nom}}$

The cost function, thus, becomes:

$$J = \lambda_T \left| T_{em}[k+1] - T_{ref} \right| + \lambda_\varphi ||\varphi_s[k+1]| - \varphi_{s\,ref}| \qquad \text{(III.18)}$$

The model used to estimate the stator flux is derived from the equation (III.8), given that the reference frame is stationary we get:

$$\frac{d\varphi_s}{dt} = v_s - R_s i_s \qquad \text{(III.19)}$$

We can estimate the rotor flux φ_r by replacing i_r by its expression from (III.10) in (III.11), we get:

$$\varphi_r = \frac{L_r}{L_m}\varphi_s + \left(L_m - \frac{L_r L_s}{L_m}\right) i_s \qquad \text{(III.20)}$$

As shown in **Figure III- 4,**the Proportional-Integral (PI) controller receives the error signal of the mechanical speed and computes the torque reference for the predictive controller.

By transforming (III.5) to Laplace domain we get:

$$\frac{\Omega}{T_{em} - T_l} = \frac{1}{Js + k_f} \qquad \text{(III.21)}$$

Where: s is the Laplace operator

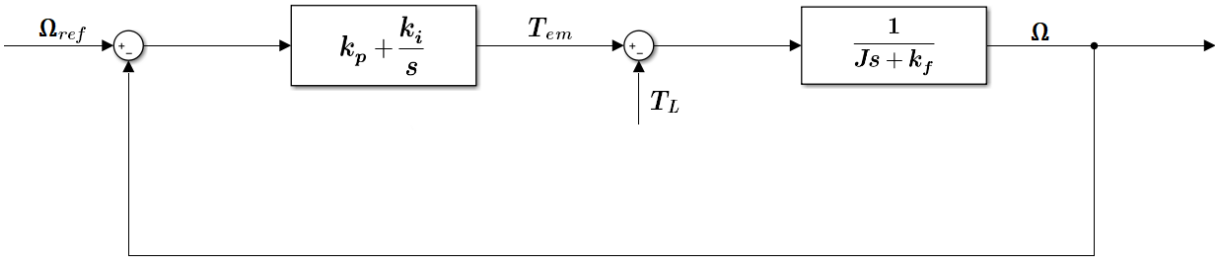

Figure III- 6 : PI speed controller

By considering the load torque T_L as a nil disturbance [77] , the transfer function (III.21), in closed loop, becomes:

$$\Omega = \frac{k_p}{J} \times \frac{s + \frac{k_i}{k_p}}{s^2 + \frac{k_p + k_f}{J} s + \frac{k_i}{J}} \Omega_{ref} \qquad \text{(III.22)}$$

The denominator of (III.22) is a second order system of the form:

$$s^2 + 2\xi\omega_n s + \omega_n^2$$

By identification we get:

$$\begin{cases} k_i = J\omega_n^2 \\ k_p = 2\xi\omega_n - k_f \end{cases}$$

Where:

- ξ : damping coefficient
- ω_n : natural circular pulse

III.4 Artificial neural network training principle

Artificial neural networks use a dense interconnection of computing nodes to approximate nonlinear functions. Each node constitutes a neuron, performs the

multiplication of its input signals by constant weights, sums up the results, and maps the sum to a nonlinear activation function: the result is then transferred to its output.

NN have self- adapting compatibilities which makes them well suited to handle non-linarites, uncertainness and parameter variations. A multilayered feed forward neural network constructs a global approximation to non-linear input-output mapping [15]. Neural networks are capable of generalization in regions of the input space, where little or no training data are available.

The ANN is trained by a learning algorithm which performs the adaptation of weights of the network iteratively until the error between target vectors and the output of the ANN is less than an error goal.

The most popular learning algorithm for nonlinear systems is the back propagation algorithm and its variants. The latter is implemented by many ANN software packages such as the neural network toolbox from MATLAB. In the case presented in this chapter, the MPTC control strategy has been implemented as a basic control to train our neural network

Neural network has been devised having as inputs the measured variables which are the speed motor ω, electromagnetic torqueT_{em}, the estimate variable which is stator flux represented in real and imaginary parts, and the references variables which are flux, speed and the torque reference that obtained from the proportional integral (PI) speed controller, bringing the total number of input features to seven i.e., *inputs* =7. The outputs of the ANN are the three control signals Sa, Sb, Sc.

The training data, which have been collected by MPTC, comprises a different experimental condition. The sweeping range for the variables was selected as follows: ψ^*= [0. 62, 0.82], T_{nom}= [7, 15] and different form signals of reference speed. For each experimental condition, the simulation is run using MPTC. Then, the input features of the neural network and their targets are stored for training. As a consequence, the total dataset consists of 1805043 instances.

The structure of the ANN proposed is as follows: 7 neurons in the first hidden layer, 9 neurons in the second hidden layer, 10 neurons in the third hidden layer, 9 neurons in the fourth hidden layer and 3 neurons in the output layer.

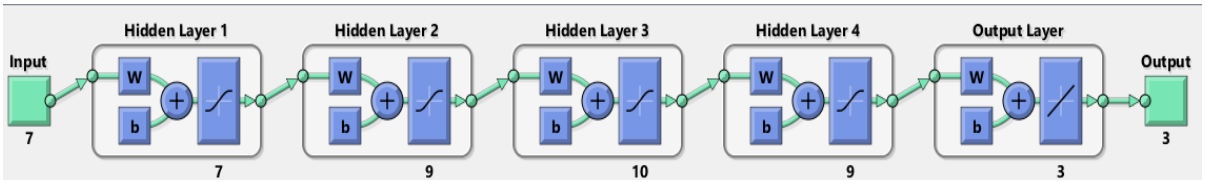

Figure III- 7 : General topology of multilayer Feed Forward Back-propagation neural networkof MPC

As mentioned above that torque reference obtained from the proportional integral (PI) speed controller, hence replacing it with a block of neural network, may further reduce computation burden. The ANN based PI block was implemented as follows:

- The ANN takes as input the error between speed measured and its reference while the output of the ANN is the reference signal torque.

- The training data, which have been collected by MPC, by varying the speed reference, the simulation is run using MPC. Then, the input features of the neural network and their targets are stored for training. The structure of the proposed ANN is as follows: one neuron in the first hidden layer, 2 neurons in the second hidden layer and one neuron in the output layer.

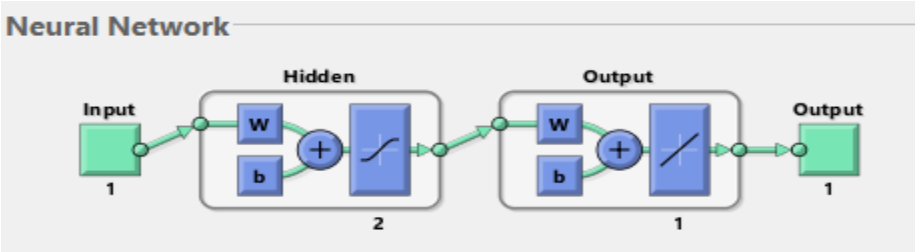

Figure III- 8 : General topology of multilayer Feed Forward Back propagation neural network of PI

At the end of the training, we get the performance plot and regression plot of the two training ANN-PI, ANN-MPTC which are shown below

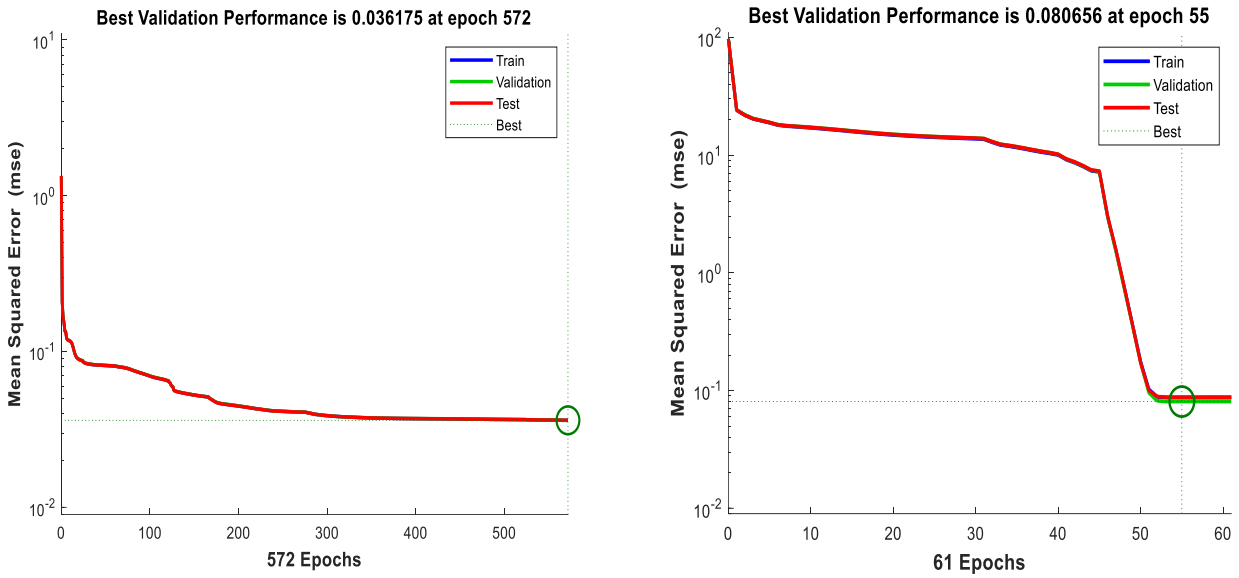

(a) **(b)**

Figure III- 9 : performance of Feed forward back-propagation neural network based

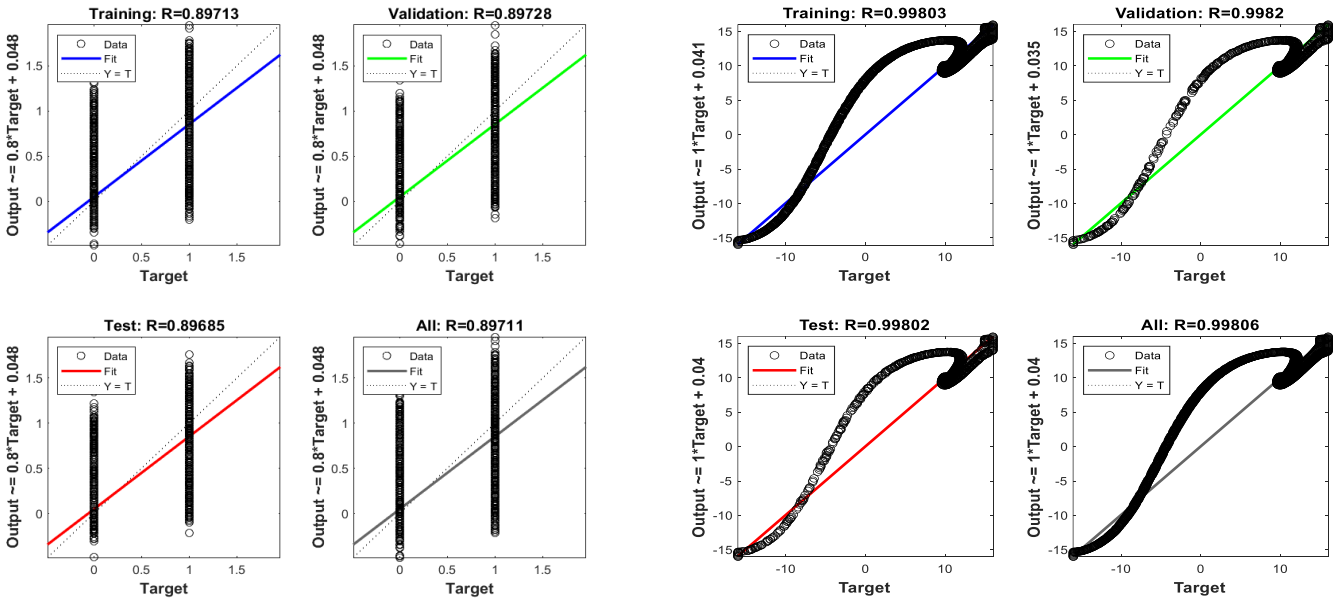

(a) **(b)**

Figure III- 10 : Regression training of: (a) MPC, (b) PI

Figure III-8 shows the best validation performance for both controllers, for NN-MPTC best performance is saved on epoch 572 with the lowest validation error of 0.036175 while the lowest validation error of NN-PI was 0.080656 on the 55th epochs.The diversity of these results goes back to the nature of the two trained systems. The PI is a simple linear system that has been trained with few data while the MPTC is a non-linear system that needed huge data to achieve these results.

Figure III- 9 represents the final regression plot training which shows a very good accuracy for the two training; thus, regression plot will generally have four graphs, training, validation, test and combining all. We can observe in Figure III- 9 (a) that all data sets are nearly fitted to the target. For a perfect fit, the data should fall along a 45-degree line (dash line), where the network outputs are equal to the targets [4]. For this study, the fits are found to be very good for all data sets, with the R = 0.99 for ANN-PI and R= 0.89 in each of the outputs.

Table III- 1: training parameters

	MPTC	PI
Epochs	1000	1000
iterations	572	61
Training time	12H 52mn 04sec	18 sec
MSE	0.036175	0.080656
regression	0.89713	0.9982
Hidden layers	4 hidden layers (7, 9 , 10,9 nodes respectively)	One hidden layer (2 nodes)

III.5 Simulation and results

The ANN-MPTC and the MPTC techniques were simulated with an Induction Machine fed by a two-level inverter. The ANN-MPTC and MPTC had been simulated in the MATLAB/Simulink environment with different values of the speed reference and the load torque in order to justify the performance of this control scheme in both transient and steady states. The parameters used in the simulation are given in Table B.1 and Table B.2 in Appendix B.

As for the stator flux reference, it is taken around its nominal value (0.82 Wb). The reference torque is generated from an external PI regulator loop.

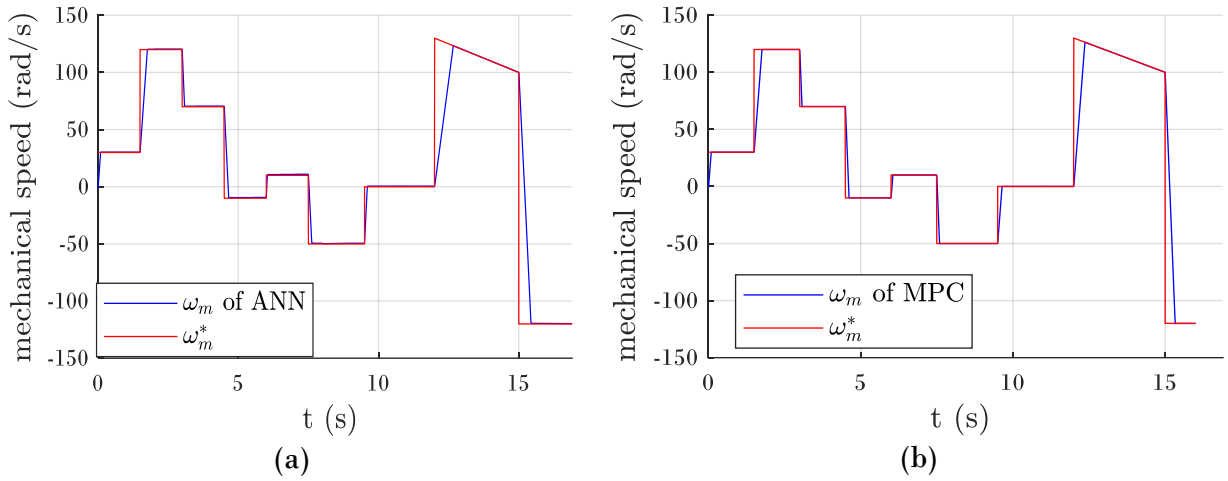

Figure III- 11: Simulation results (rotor speed and its reference) of an inverter-fed induction machine with: (a) ANN-MPTC, (b) MPTC

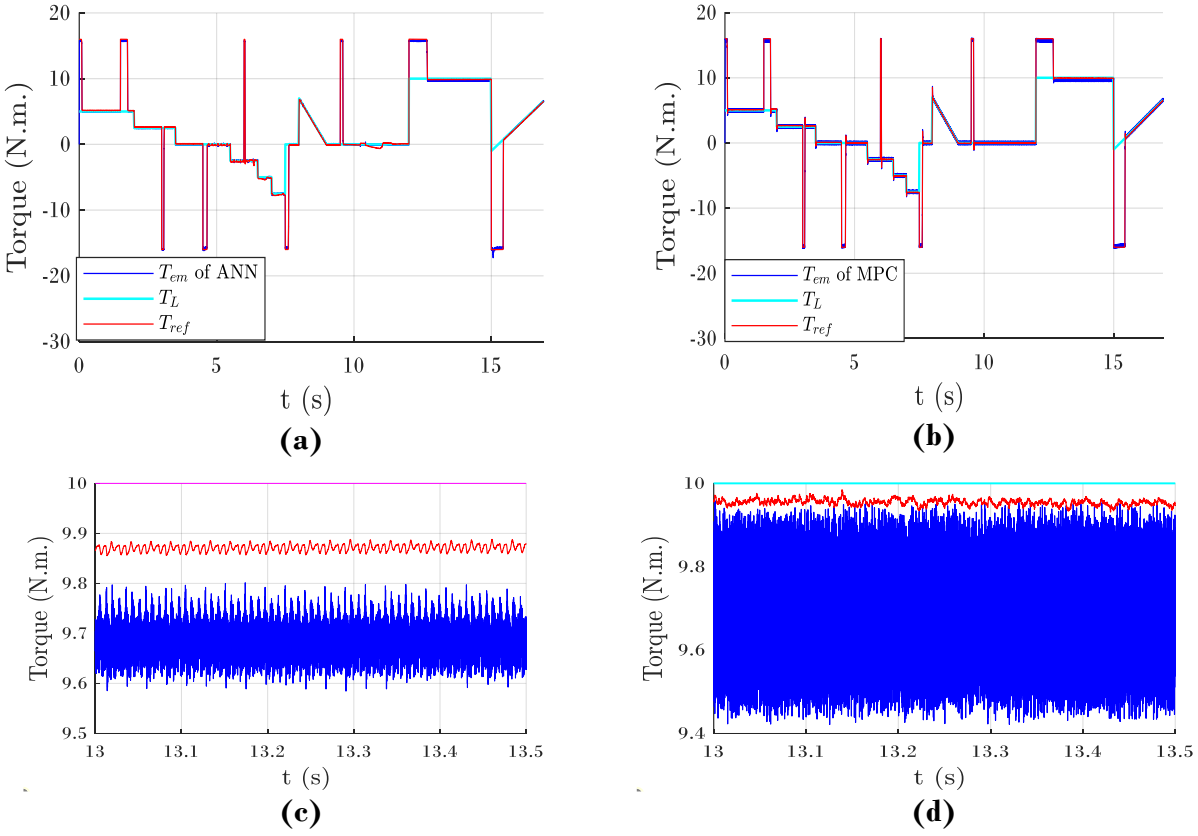

Figure III- 12: Simulation results (rotor speed and its reference) of an inverter-fed induction machine with: (a) ANN-MPTC, (b) MPTC and theirs zoom
(c) ANN-MPTC, (d) MPTC

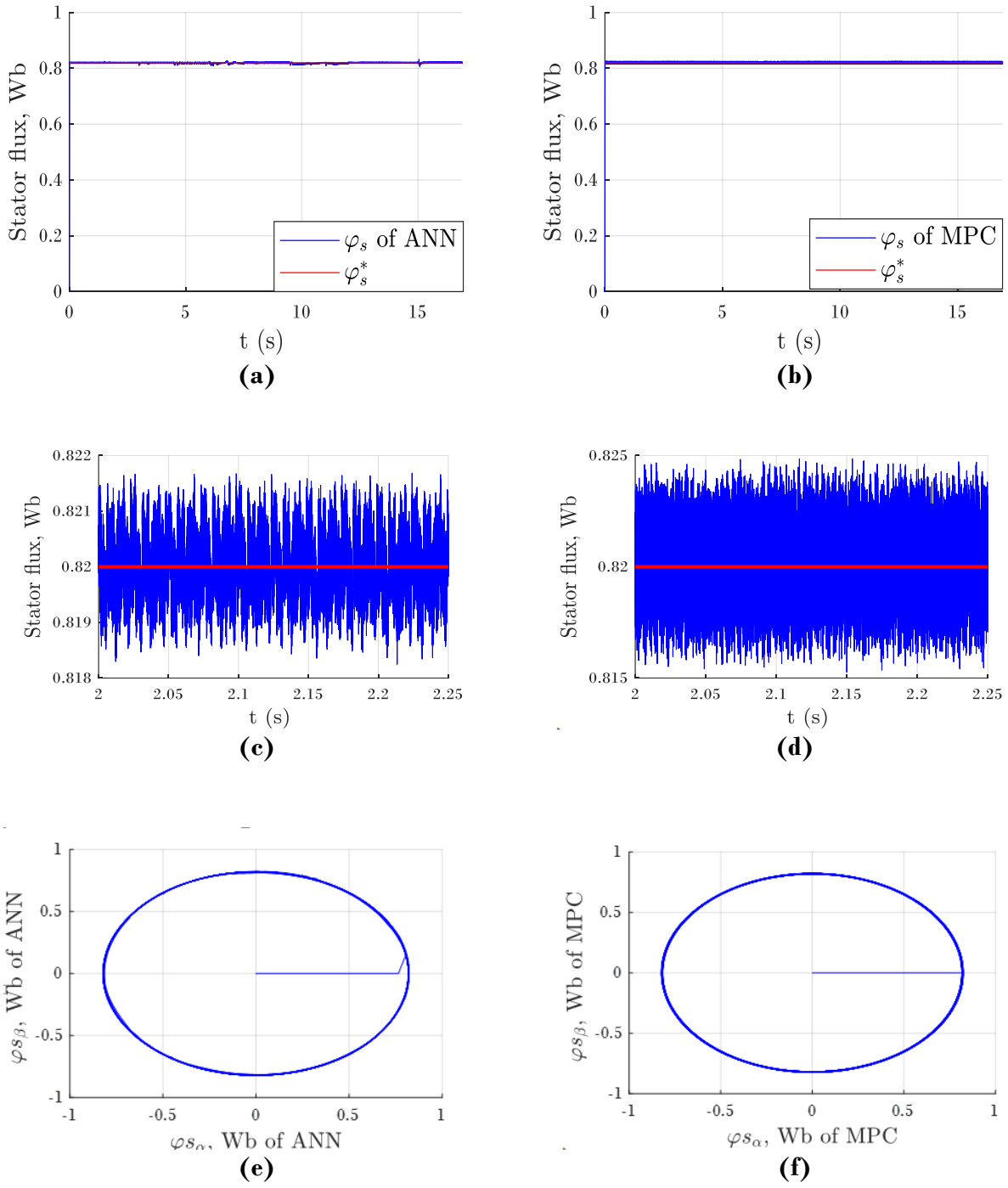

Figure III- 13: Simulation results of stator flux of an inverter-fed induction machine with (a) ANN-MPTC, (b) MPTC and theirs zoom (c) ANN-MPTC, (d) MPTC

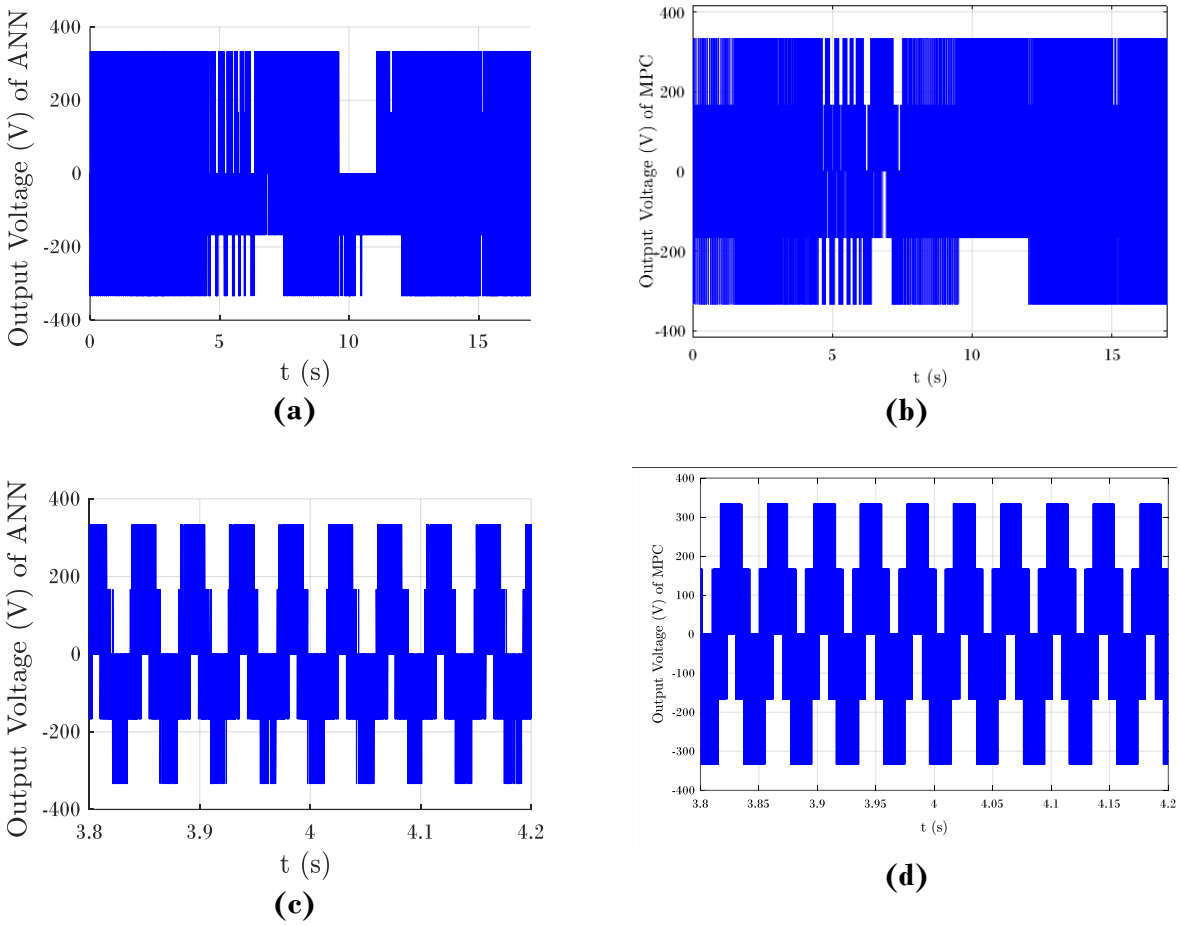

Figure III- 14: Simulation results of output voltage of an inverter-fed induction machine with (a) ANN-MPTC, (b) MPTC and theirs zoom (c) ANN-MPTC, (d) MPTC

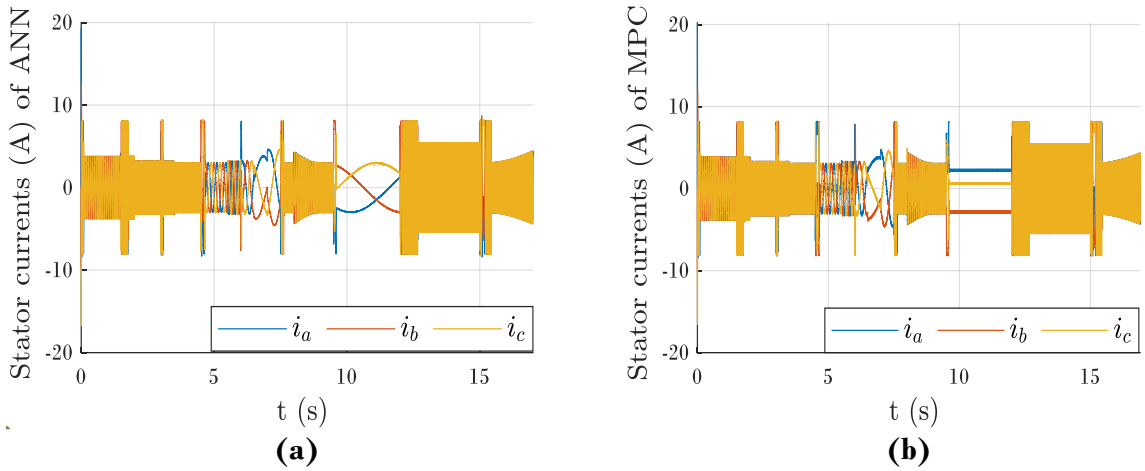

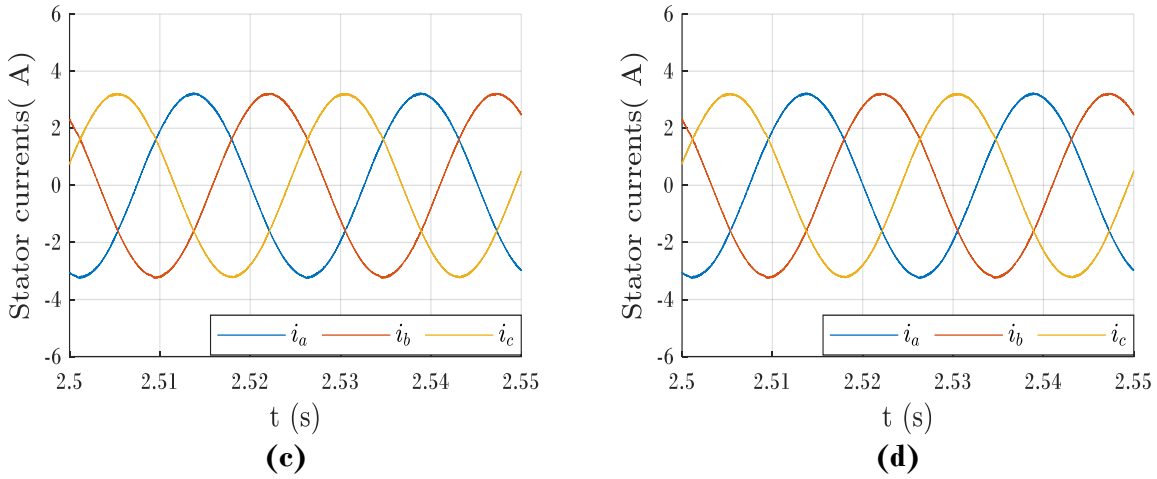

Figure III- 15 : Simulation results of stator current of an inverter-fed induction machine with (a) ANN-MPTC, (b) MPTC and theirs zoom (c) ANN-MPTC, (d) MPTC

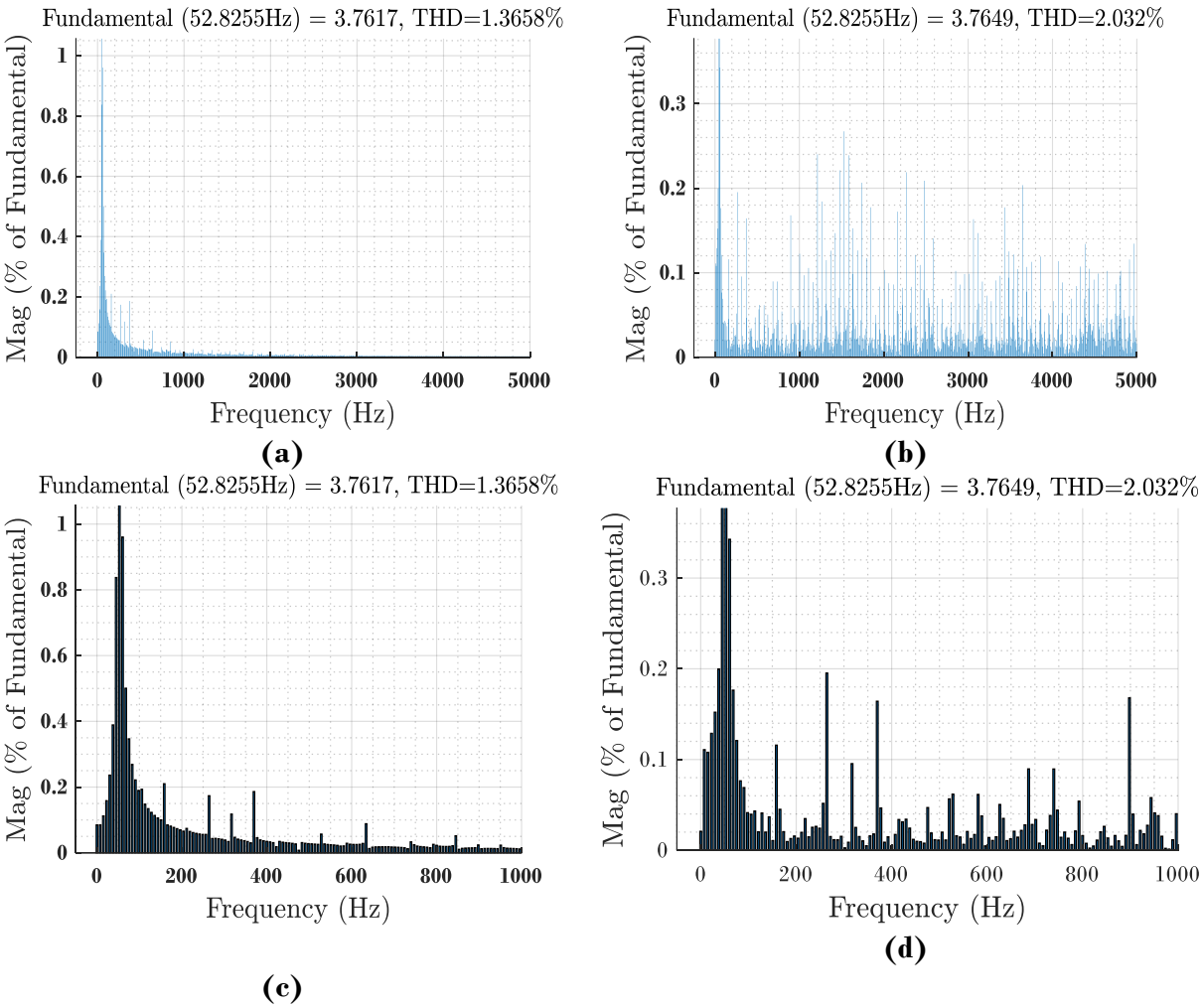

Figure III- 16: Simulation results of the THD of the stator current of an induction machine: (a) ANN-MPTC, (b) MPTC and theirs zoom (c) ANN-MPTC, (d) MPTC

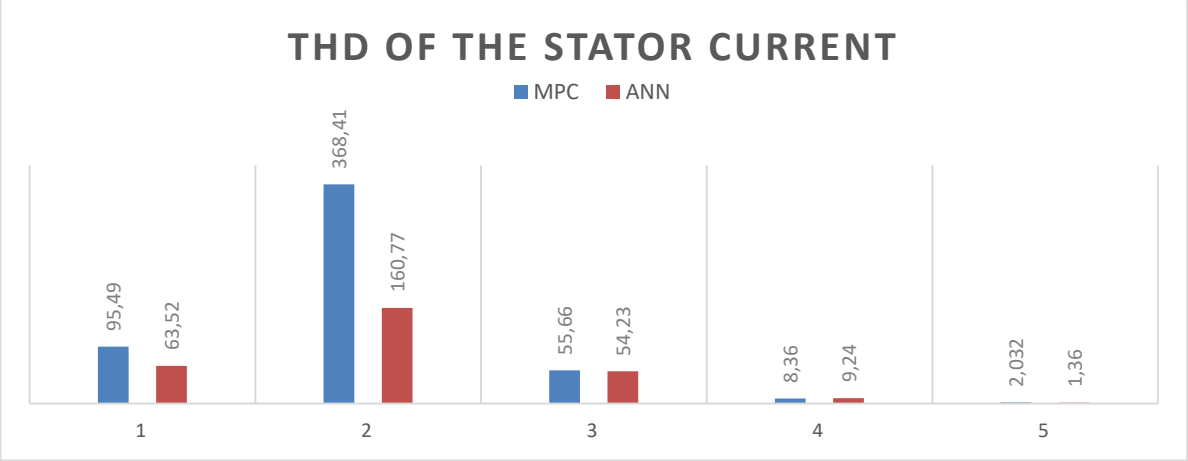

Figure III- 17 : Comparison of the THD of the stator current obtained by the two proposed control strategies, for some cases given in Table below, under different operating conditions.

Table III- 2 : Comparison of the THD of the stator current obtained by the two proposed control strategies, for some cases

Samples	ω (rad/s)	THD MPC	THD ANN-MPC
S1	110	95.45%	63.52%
S2	70	368.41%	160.78%
S3	130	55.66%	54.23%
S4	145	8.36%	9.24%
S5	157	1.36%	2.032%

Figure III- 11 shows simulation results of mechanical speed and its reference of (a) ANN-MPTC and (b) MPTC of a 1.5 kW squirrel-cage induction machine fed by a two-level inverter, it's observed that mechanical speed track their reference for both of the controllers. Similarly, they have the same response time in same conditions. In the first case, thespeed reference is set to 30 rad/s from 0 rad/s during 0.094 s. The variation of the response time depends on two factors, which are the reference speed and the load torque

Figure III-12 shows simulation results of electromagnetic torque and its reference with (a) ANN-MPTC and (b) MPTC.The electromagnetic torque is controlled to track its reference. We noticed that the electromagnetic torque of the system at each variation, follows its

reference andrapidly returns to its stability.When the IM reaches its steady state, the speed becomes constant whereas the electromagnetic torque settles at final value, which is the load torque. In figure III- 12 (c) and (d), and in the same operating conditions, the ripples in the conventional MPTC torque are about 0.4 N.m while they are around 0.2 N.m in NN-MPTC, this result proves the robustness of the ANN-MPTC.

Figure III-13 illustrates the response of stator flux magnitude of both methods (a) NN-MPTC, (b) conventional MPTC and theirs zoom (c) and (d) respectively. The results of NN-MPTC show a reduction in ripples compared with MPTC where the stator flux presents high ripples around 0.010 Wb compared to ANN-MPTC where the stator flux is approximately 0.04 Wb as shown in Figure III-13 (b) and (c) respectively, however we observe overshoots in some on ANN-MPTC flux magnitude. The trajectory of the stator flux vector, which is almost circular, is described in figure III- 13 (e) for ANN-MPTC and figure III- 13 (f) for MPTC strategy.

The steady-state current response of both strategies is presented in figure III-15. The quality of the waveform of the stator current is improved with a reduction in ripples. Thus the control proposed is efficient compared to the MPTC because it presents fewer ripples as indicated in the Figure III-15 (b) and (c).

The THD is one of the ways to prove the effectiveness of a controller, Figure III- 16 and Figure III-17present the THD of the stator current obtained by the proposed control strategies. As expected, the results of ANN-MPTC are improved by a lowerTHD value.

III.6 Conclusion

The study of this chapter have discussed the simultaneous control of the torque and stator flux of induction machine using neural network based MPTC method. The obtained results have shown that the ANN-MPTC was well trained according to the obtained results, furthermore, it gave better results than MPTC in most cases.

The use of ANN-MPTC controller was proposed in this work to increase the accuracy of speed results in addition to the ability of ANN-MPTC controller to react against sudden changes and non-linearity of the system. It has proved its efficiency by given good results and its ability to keep trackingthe desired speed and torque values with minimum ripples. In addition, in terms of a lower THD of stator current,NN-MPTC shows a better control performance compared to the conventional strategy

From the obtained results, we can conclude that NN-MPTC method is a very good choice for the control of induction machines in term of better performance, simplicity, and efficiency. The control has shown the ability of this method to track different speed values with good tracking performances.

Chapter four

Artificial neural network based Model Predictive Current Control of a Matrix Converter-fed RL-load

CHAPTER FOUR

Introduction

As mentioned in Chapter I, Matrix converters (MCs) are one of the most attractive families of converters in the power electronics field. The matrix converter is a set of controlled bidirectional power switches that connects a voltage source directly to a load without using any DC-link or other energy storage element.[79]

This chapter presents an ANN-MPCC scheme of an RL-load fed by a matrix converter with direct and indirect topologies. The modeling of both converters is presented alongside with the modeling of the input filter. The working principle of the MPCC and the load model are explained in detail in Chapter 2.

The control scheme is simulated using the two topologies in MATLAB/Simulink for different references of the output current and reactive power.

IV.1 Modeling of the input filter

In the design of matrix converters, the use of electronic power devices such as bidirectional switches requires input filters. This reduces the high harmonic content in the input current, increasing the system protection against transitory effects coming from the power supply. Furthermore, the ripple in the waveform and excessive currents or voltages in the converter will be reduced. A low-pass filter can be employed to avoid these unwanted harmonic signals in the input[80]. A second-order low-pass filter (Figure IV.1) at the input is considered to avoid over-voltages and harmonics distortions in the source current.

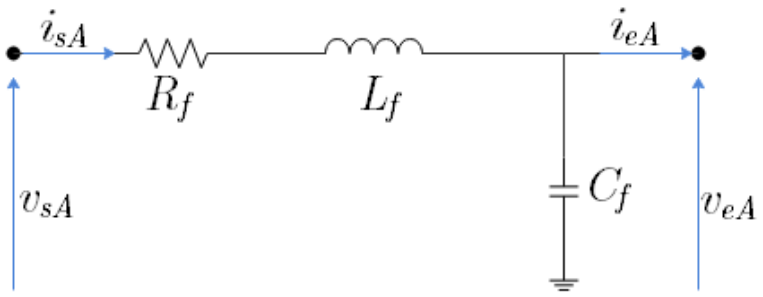

Figure IV- 1: Input filter

In order to obtain the dynamic model of the filter, Kirchhoff's first and second law are applied to the power circuit in Figure IV-1

We get :

$$v_s = R_f i_s + L_f \frac{di_s}{dt} + v_e \tag{IV. 1}$$

$$i_s = i_e + C_f \frac{dv_e}{dt} \tag{IV. 2}$$

With:

$$\begin{cases} v_s = \frac{2}{3}(v_{sA} + a v_{sB} + a^2 v_{sC}) \\ v_e = \frac{2}{3}(v_{eA} + a v_{eB} + a^2 v_{eC}) \\ i_s = \frac{2}{3}(i_{sA} + a i_{sB} + a^2 i_{sC}) \\ i_e = \frac{2}{3}(i_{eA} + a i_{eB} + a^2 i_{eC}) \end{cases}$$

By considering the vector $[v_e i_s]^T$ as a state variable and the vector $[v_s i_e]^T$ as an input variable, we end up with a continuous-time state space representation of the filter.

$$\underbrace{\begin{bmatrix} \dot{v}_e \\ \dot{i}_s \end{bmatrix}}_{\dot{X}} = \underbrace{\begin{bmatrix} 0 & 1/C_f \\ -1/L_f & -R_f/L_f \end{bmatrix}}_{A_f} \underbrace{\begin{bmatrix} v_e \\ i_s \end{bmatrix}}_{X} + \underbrace{\begin{bmatrix} 0 & -1/C_f \\ 1/L_f & 0 \end{bmatrix}}_{B_f} \underbrace{\begin{bmatrix} v_s \\ i_e \end{bmatrix}}_{U} \tag{IV. 3}$$

IV.2 Modeling of the Direct Matrix Converter (DMC)

The power circuit of the DMC is presented in Figure IV-2. It uses a set of bidirectional switches to directly connect the three-phase power supply to a three-phase load, or in this case, through an input filter.

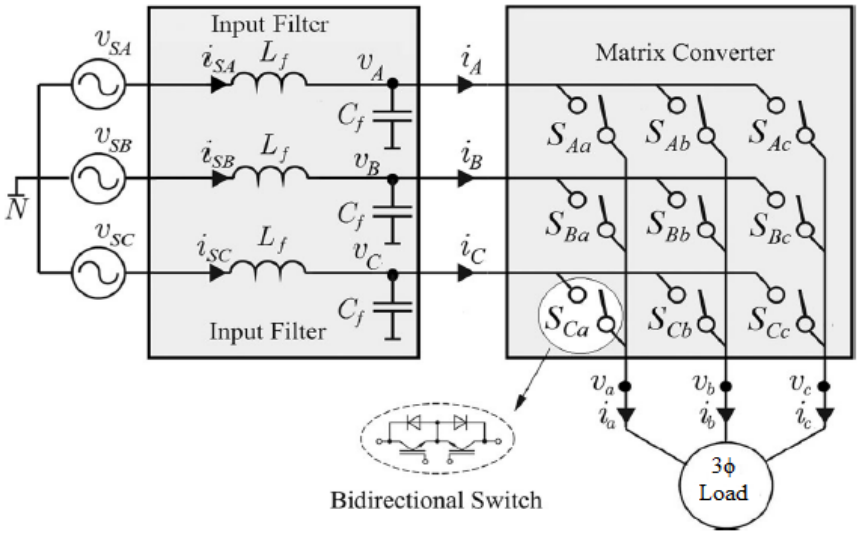

Figure IV- 2 : topology of (3×3) direct matrix converter

The behavior of the modulation function for an output phase is defined by the activation and deactivation of the switches that are connected to each input phase, as indicated in Expression (IV.1):

$$S_{xy} = \begin{cases} 0, \text{if} S_{xy} \text{is open} \\ 1, \text{if} S_{xy} \text{is close} \end{cases} \qquad \text{(IV. 4)}$$

Where:

$y \in \{a, b, c\}$: The output phases

$x \in \{A, B, C\}$: The input phases

S_{xy} : The connection function

Two switches should not be activated at the same time to avoid short circuits in the input phases. In the same way, it should be avoided that at any moment of operation, all the switches are deactivated, since it would cause a high voltage differential at the output

This operation constraint is expressed in (IV. 5)

$$S_{Ay} + S_{By} + S_{Cy} = 1, \qquad \forall y \in \{a, b, c\} \tag{IV. 5}$$

The voltages and the input and output currents referred to the neutral line can be expressed with their vector representation, as developed in (IV. 6) and (IV. 7) respectively

$$\begin{bmatrix} v_a \\ v_b \\ v_c \end{bmatrix} = \underbrace{\begin{bmatrix} S_{Aa}(t)S_{Ba}(t)S_{Ca}(t) \\ S_{Ab}(t)S_{Bb}(t)S_{Cb}(t) \\ S_{Ac}(t)S_{Bc}(t)S_{Cc}(t) \end{bmatrix}}_{S} \times \begin{bmatrix} v_{eA} \\ v_{eB} \\ v_{eC} \end{bmatrix} \tag{IV.6}$$

$$\begin{bmatrix} i_A \\ i_B \\ i_C \end{bmatrix} = \begin{bmatrix} S_{Aa}(t)S_{Ba}(t)S_{Ca}(t) \\ S_{Ab}(t)S_{Bb}(t)S_{Cb}(t) \\ S_{Ac}(t)S_{Bc}(t)S_{Cc}(t) \end{bmatrix}^T \times \begin{bmatrix} i_a \\ i_b \\ i_c \end{bmatrix} \tag{IV.7}$$

- v_a,$v_b$and$v_c$are the load voltages referenced to the load neutral point;
- v_{eA},$v_{eB}$and$v_{eC}$are the filter capacitor voltages, also input voltages of the DMC;
- i_a,$i_b$and$i_c$are the load currents;
- i_A,$i_B$and$i_C$are the input currents of the DMC.

The power filters located at the input of each of the lines of the converter mitigate the high-frequency components, generating current signals from input and sinusoidal output voltages, avoiding the generation of over-voltages. The over-voltage is caused by the fast switching in the input currents due to the presence of the short-circuit reactance of any real power supply. An adequate design of these filters is very important in the operation of matrix converters [80][81].

IV.3 Modeling of the Indirect Matrix converter (IMC)

The power circuit of the IMC is presented in Figure IV.3. The converter can be divided into two stages: the rectifier stage and the inverter stage.

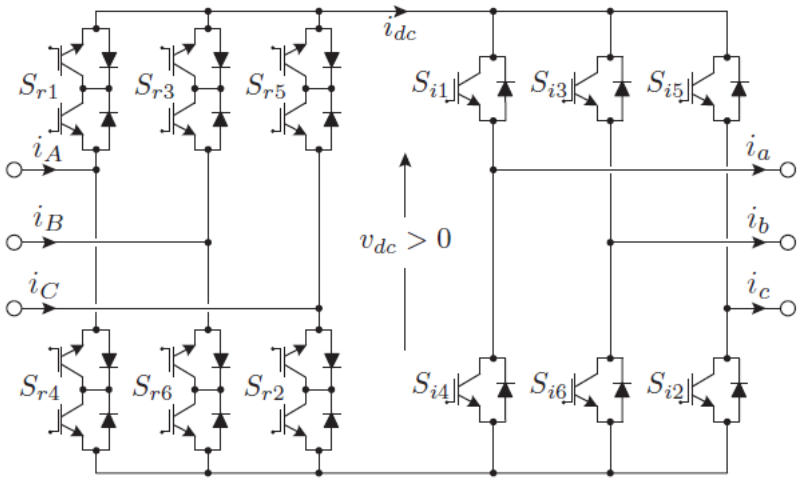

Figure IV- 3 : (3×3) Indirect Matrix Converter

The rectifier stage is a current source rectifier that consists of six bidirectional switches, which makes it capable of operating in all four quadrants. The inverter stage is a conventional voltage source inverter. This topology helps extend the control technique of the inverter on the previous two chapters.

The model of the converter can be described as the product of two instantaneous transfer matrices of the rectifier and the inverter.

$$\begin{bmatrix} v_a \\ v_b \\ v_c \end{bmatrix} = \underbrace{\begin{bmatrix} S_{i1}(t)S_{i4}(t) \\ S_{i3}(t)S_{i6}(t) \\ S_{i5}(t)S_{i2}(t) \end{bmatrix}}_{S_{inv}} \times \underbrace{\begin{bmatrix} S_{r1}(t)S_{r3}(t)S_{r5}(t) \\ S_{r4}(t)S_{r6}(t)S_{r2}(t) \end{bmatrix}}_{S_{rec}} \times \begin{bmatrix} v_{eA} \\ v_{eB} \\ v_{eC} \end{bmatrix} \qquad \text{(IV.8)}$$

The input current of the IMC is given by:

$$\begin{bmatrix} i_A \\ i_B \\ i_C \end{bmatrix} = \begin{bmatrix} S_{r1}(t)S_{r3}(t)S_{r5}(t) \\ S_{r4}(t)S_{r6}(t)S_{r2}(t) \end{bmatrix}^T \times \begin{bmatrix} S_{i1}(t)S_{i4}(t) \\ S_{i3}(t)S_{i6}(t) \\ S_{i5}(t)S_{i2}(t) \end{bmatrix}^T \times \begin{bmatrix} i_a \\ i_b \\ i_c \end{bmatrix} \qquad \text{(IV.9)}$$

Where:

- v_a,$v_b$and$v_c$are the load voltages referenced to the load neutral point.
- v_{eA},$v_{eB}$and$v_{eC}$are the filter capacitor voltages, also input voltages of the IMC.
- i_a,$i_b$and$i_c$are the load currents.
- i_A,$i_B$and$i_C$are the input currents of the IMC.

The two conditions of operation of the IMC are translated to the following equations:

$$\begin{cases} S_{r1} + S_{r3} + S_{r5} = 1 \\ S_{r2} + S_{r4} + S_{r6} = 1 \end{cases} \quad \text{(IV.10)}$$

$$S_{ij} + S_{i(j+3)} = 1, \;\; j = \{1,2,3\} \quad \text{(IV.11)}$$

According to (IV.10) and (IV.11), there are 72 possible switching states of the 3×3 IMC, 9 for the rectifier and 8 for the inverter.

Table IV- 1: Possible switching states for the rectifier stage

Vectors		S_{r1}	S_{r2}	S_{r3}	S_{r4}	S_{r5}	S_{r6}	i_A	i_B	i_C	v_{dc}
Active	I_1	1	1	0	0	0	0	i_{dc}	0	$-i_{dc}$	v_{AC}
	I_2	0	1	1	0	0	0	0	i_{dc}	$-i_{dc}$	v_{BC}
	I_3	0	0	1	1	0	0	$-i_{dc}$	i_{dc}	0	$-v_{AB}$
	I_4	0	0	0	1	1	0	$-i_{dc}$	0	i_{dc}	$-v_{AC}$
	I_5	0	0	0	0	1	1	0	$-i_{dc}$	i_{dc}	$-v_{BC}$
	I_6	1	0	0	0	0	1	i_{dc}	$-i_{dc}$	0	v_{AB}
Nil	I_0	1	0	0	1	0	0	0	0	0	0
		0	1	0	0	1	0	0	0	0	0
		0	0	1	0	0	1	0	0	0	0

Table IV- 2: Possible switching states for the inverter stage

Vectors		S_{i1}	S_{i2}	S_{i3}	S_{i4}	S_{i5}	S_{i6}	v_{ab}	v_{bc}	v_{ca}	i_{dc}
Active	V_1	1	1	0	0	0	1	v_{dc}	0	$-v_{dc}$	i_a
	V_2	1	1	1	0	0	0	0	v_{dc}	$-v_{dc}$	$i_a + i_b$
	V_3	0	1	1	1	0	0	$-v_{dc}$	v_{dc}	0	i_b
	V_4	0	0	1	1	1	0	$-v_{dc}$	0	v_{dc}	$i_b + i_c$
	V_5	0	0	0	1	1	1	0	$-v_{dc}$	v_{dc}	i_c
	V_6	1	0	0	0	1	1	v_{dc}	$-v_{dc}$	0	$i_a + i_c$
Nil	V_0	1	0	1	0	1	0	0	0	0	0
		0	1	0	1	0	1	0	0	0	0

IV.4 Working principle of MPCC

The working principle of the MPCC is explained in detail in Chapter 2. As mentioned before, it is possible to operate in unity power factor, which means the minimization of the instantaneous input reactive power. The reactive power in the $\alpha\beta$reference frame is given by the following equation.

$$Q = v_{s\alpha} i_{s\beta} - v_{s\beta} i_{s\alpha} \qquad \text{(IV.12)}$$

At each sampling period, the control scheme calculates predictions of the reactive power and selects the actuation that minimizes it. Hence the need of prediction values of supply current. The supply current is predicted using the filter model

For minimizing the reactive power, a term must be added to the cost function in (II.1) to penalize the switching states that produce higher values of reactive power predictions. Since the goal is to control the output current and operate in the input unity factor mode, the cost function then becomes:

$$J = \left|i_a^* - i_a^p\right| + \left|i_b^* - i_b^p\right| + \left|i_c^* - i_c^p\right| + \lambda|Q^p| \quad \text{(IV.13)}$$

Where:

- i^* : The reference value of the current;
- i^p : The predicted value of the current;
- Q^p :The predicted value of the input reactive power;
- λ : The weighting factor.

IV.5 Implementation of the MPC

The control scheme has been implemented in MATLAB/Simulink using the models (II.6), (IV.3), (IV.6),(IV.7),(IV.8) and (IV.9)The filter, load and simulation parameters are given in Table C.2, Table A.1 and Table C.1 respectively.

The discrete-time model of the load is given in equation (II.1) and the discrete-time model of the filter is given as follows[82]:

$$\begin{bmatrix} v_e[k+1] \\ i_s[k+1] \end{bmatrix} = A_{fd} \begin{bmatrix} v_e[k] \\ i_s[k] \end{bmatrix} + B_{fd} \begin{bmatrix} v_s[k] \\ i_e[k] \end{bmatrix} \quad \text{(IV.14)}$$

Where:

$$A_{fd} = e^{A_f T_s}$$

$$B_{fd} = \int_0^{T_s} e^{A_f (T_s - \tau)} B_f d\tau$$

In order to minimize computation time, only active vectors of the rectifier are used and only one nil vector of the inverter is used, totalling in 42 possible of the IMC instead of 72.

IV.6 Training procedure

The training principle of the neural is explained in detail in precedent Chapters, each topology of matrix converter direct and indirect trained with its own Data and each neural has its own architecture.

In the following paragraph, the training procedure of neural network based MPCC fed direct and indirect matrix converter will be explained:

For the neural network based MPCC fed direct matrix converter , the ANN takes as inputs the measured variable of the three phases currentand it's the references that fixe the total number of input features to six i.e., *inputs* = 6. The outputs of the ANN are the nine control signals$S_{Aa}, S_{Ba,}S_{Ca}, S_{Ab}, S_{Bb}, S_{Cb,}S_{Ac,}S_{Bc}, S_{Cc}$.

We entered the reactive power output and reference reactive power as inputs as well, then we trained an ANN with rich data, but the results of training and simulation were not good at all, due to the complexity of the system, thus in this chapter, we controlled only the current without reactive power

The training data, which have been collected by MPCC, derived in different experimental conditions , in each experience we choose a specific conditions, at the first one, we choosed different values of (Q^*= 0, 50,100 , 200 ,300,350) with different values of reference currenti^*, by keeping a constant value of R=50 for each experimental condition, then we kept the same variation of current but we considered more variation of Q^*which takes its values from 0 to 400 VAR with different values of the resistor (R= 25,30,35,40,45) , the simulation is run using MPCC , then the input features of the neural network and their targets are stored for training.

As a consequence, the total dataset consists of 400006 for IMC training and 1000010 for DMC training instances. The neural is implemented by nntool toolbox from MATLABusing back propagation feed forward as type of network and trainlm as training algorithm for both topologies. The structure and training parameters are mentioned in table bellow

Table IV- 3 : Training parameters of DMC and IMC

	MPCC (DMC)	MPCC (IMC)
Epochs	1000	1000
iterations	263	231
Training time	6H 10mn 09sec	5H 32mn 36sec
MSE	0.11253	0.10474
regression	0.70211	0.76278
Hidden layers	2 hidden layers 8 ,12 nodes respectively)	3 hidden layers (10,13,8 nodes respectively)

At the end of the training, the performance plot, regression plot, testing plot and validation plot are shown below for the two training of the two topologies

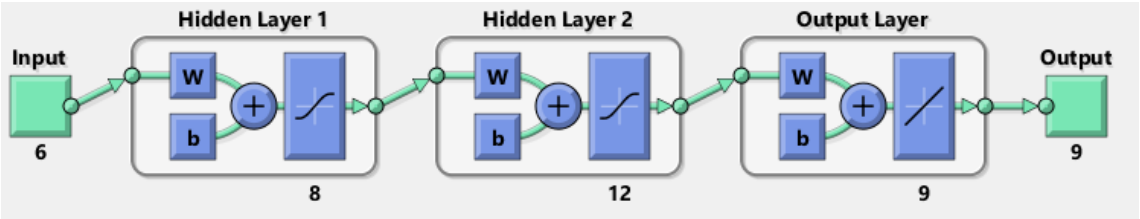

(a)

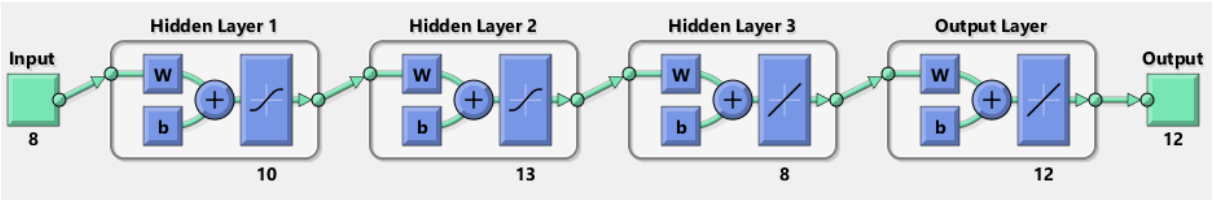

(b)

Figure IV- 4 : General topology of multilayer Feed Forward Back-propagation neural network of MPCC of : (a) DMC , (b) IMC

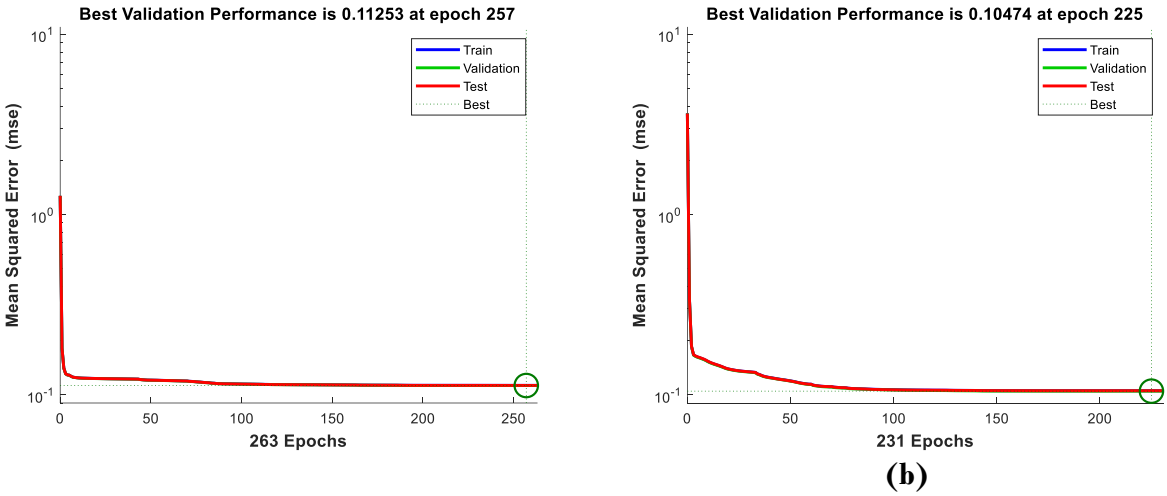

Figure IV- 5: Performance of Feed forward back-propagation neural network based MPCC of: (a) DMC, (b) IMC

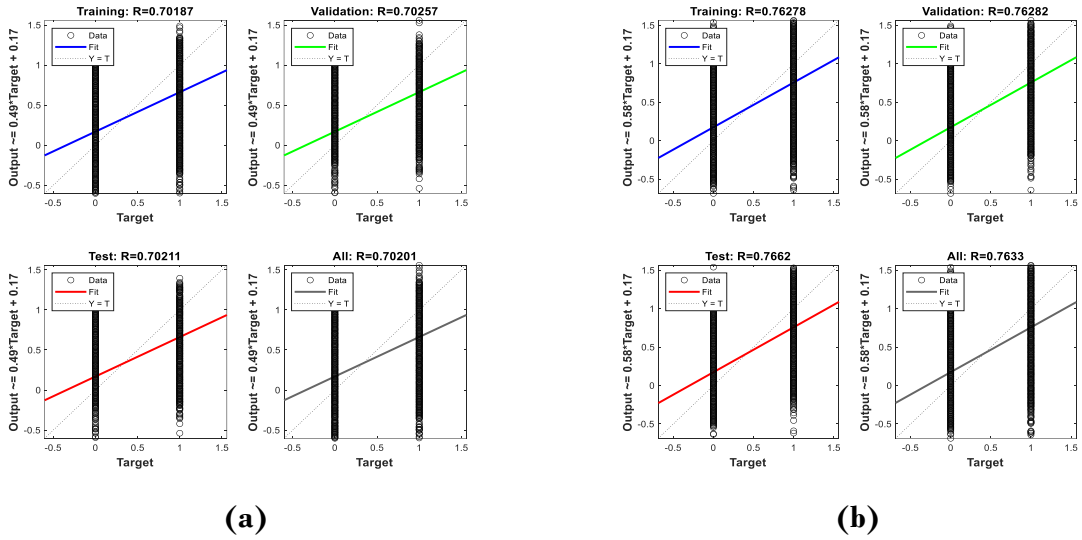

Figure IV- 6: Regression of Feed forward back-propagation neural network based MPCC of: (a) DMC, (b) IMC

IV.7 Simulation and results

This section provides a comprehensive study and evaluation of the proposed control strategies fed to the two topologies direct and indirect Matrix converter with load RL.

As it is mentioned above, the inputs of neural network are references currents and their outputs of the three phases, it means that the reactive power is not controllable compared to the MPC strategy.

To verify the proposed ANN-based control strategy (model predictive current control) fed DMC-fed RL-load, IMC-fed RL-load and compare their performance with the conventional MPC, we used MATLAB (R2020a)/SIMULINK software components to implement the SIMULINK model and the simulations of the system shown in figures bellow

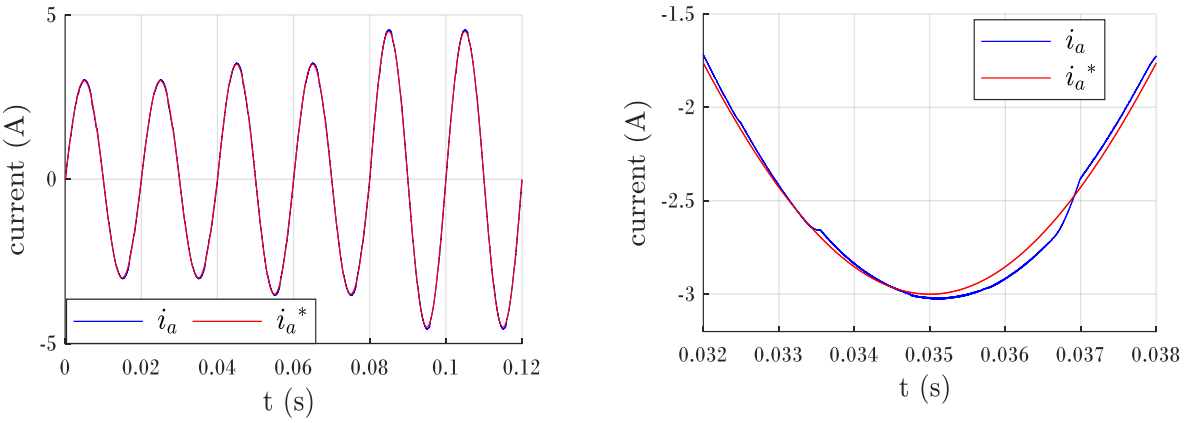

(a)

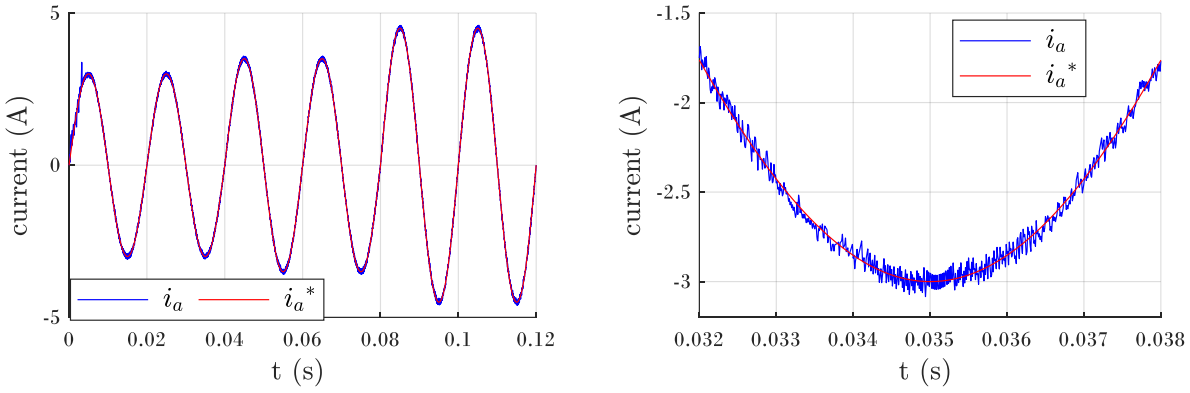

(b)

Figure IV- 7 : Simulation results of a DMC-fed RL-load: Reference and output current of phase A and their zoom with: (a) ANN-MPCC, (b) MPC

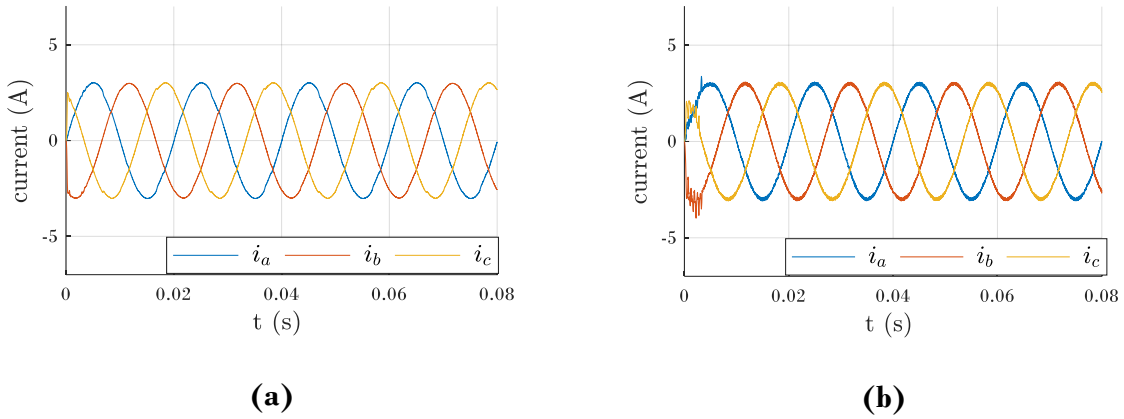

Figure IV- 8 : Simulation results of a DMC-fed RL-load of load currents with: (a) ANN-MPCC, (b) MPC

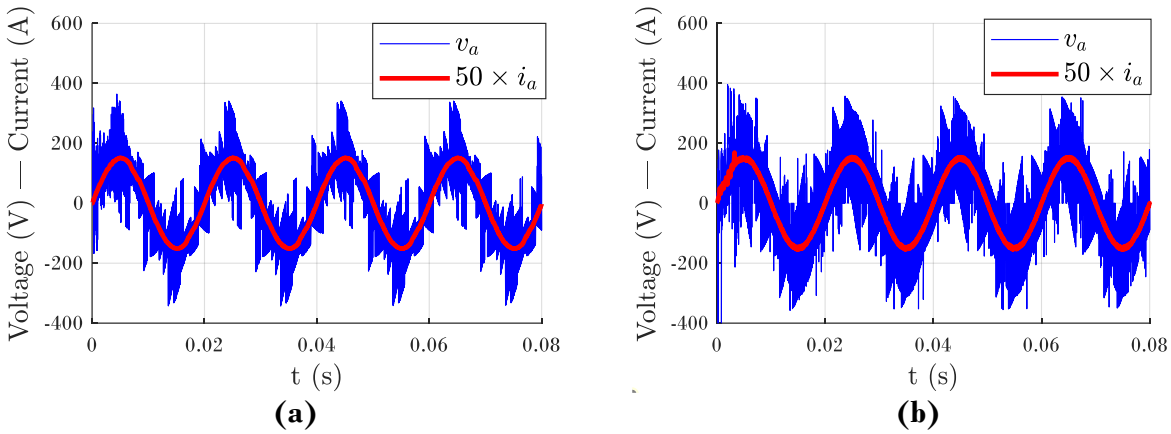

Figure IV- 9 : Simulation results of a DMC-fed RL-load of load voltage and currents of phase A with: (a) ANN-MPCC, (b) MPC

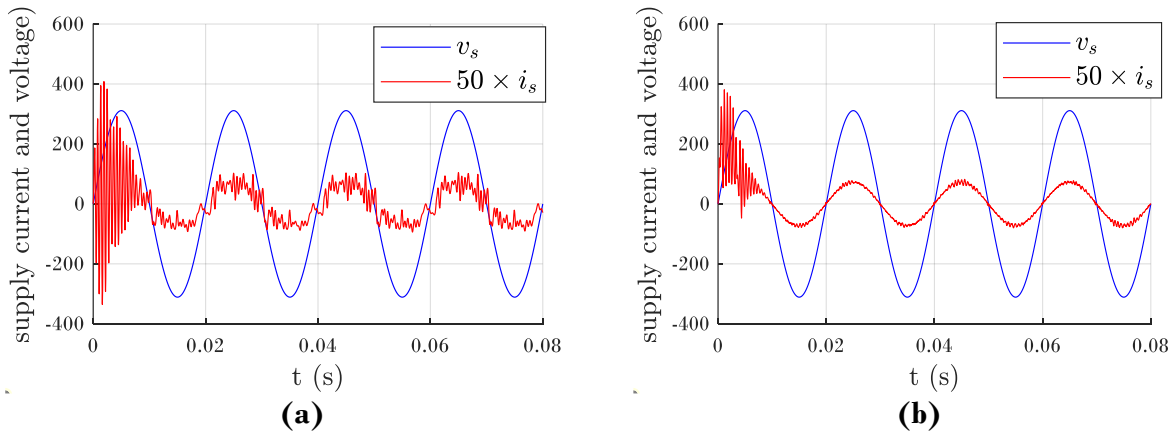

Figure IV- 10 : Simulation results of a DMC-fed RL-load of supply current and of phase A with: (a) ANN-MPCC, (b) MPC

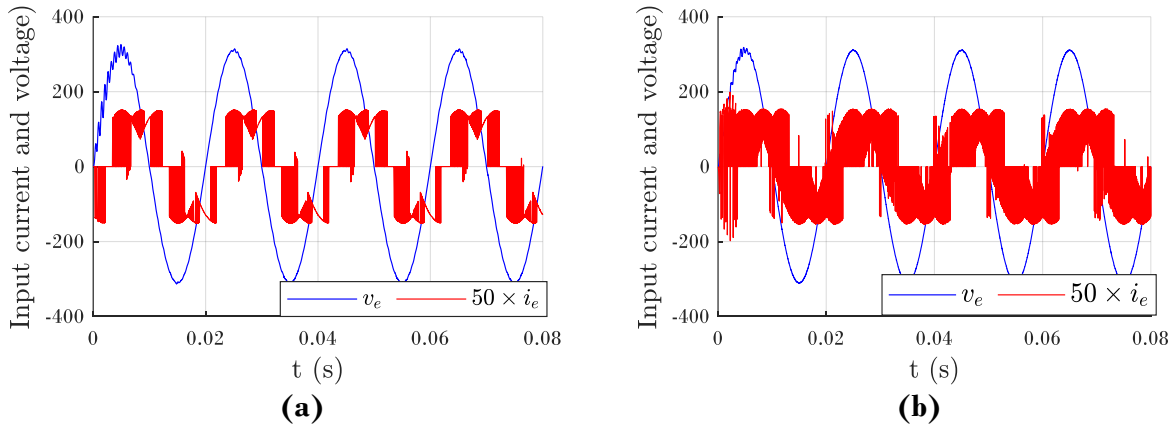

Figure IV- 11 : Simulation results of a DMC-fed RL-load of input current and voltage of DMC of phase A with: (a) ANN-MPCC, (b) MPC

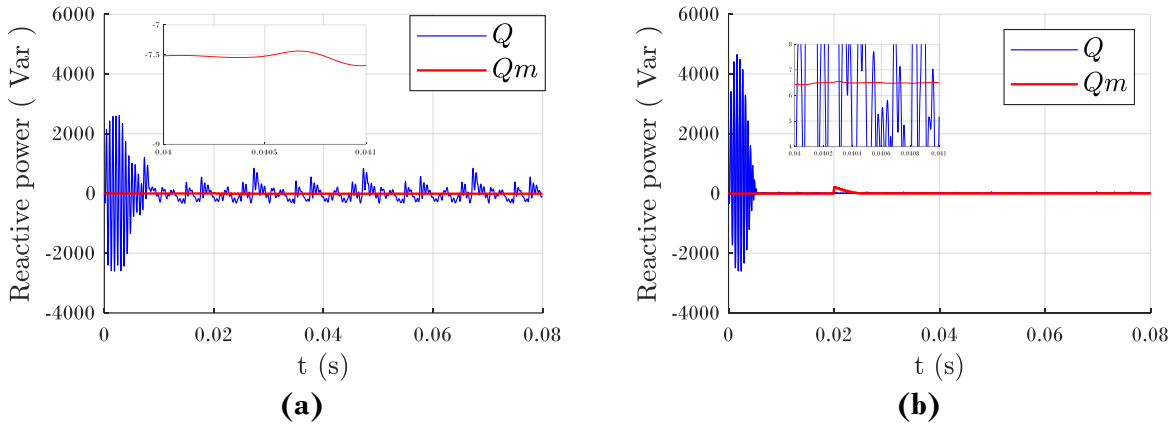

Figure IV- 12: Simulation results of a DMC-fed RL-load of the input reactive power and its moving average value with: (a) ANN-MPCC, (b) MPC

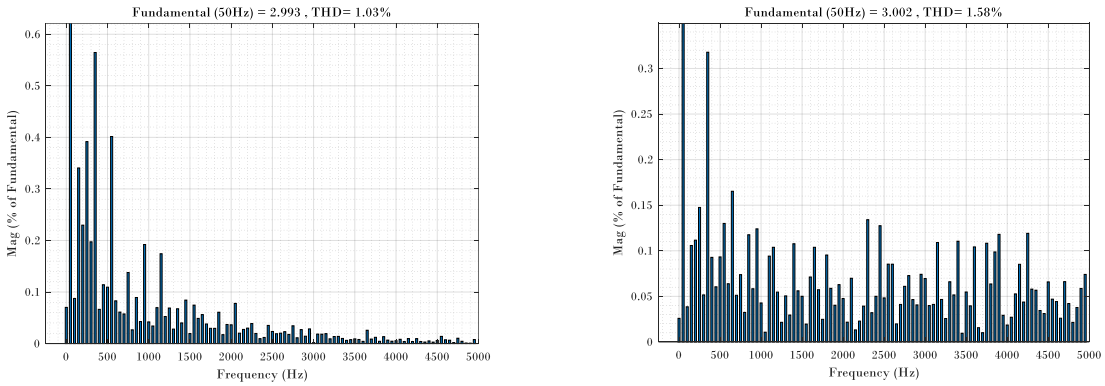

Figure IV- 13 : Simulation results of a DMC-fed RL-load of Output current spectra expressed as percentages of fundamental magnitude with: (a) ANN-MPCC, (b) MPCC

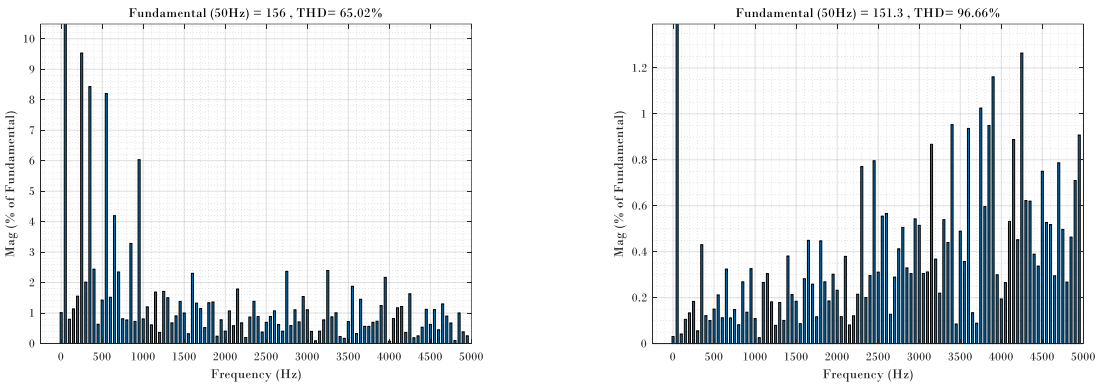

(a) **(b)**

Figure IV- 14: Simulation results of a DMC-fed RL-load of Output voltage spectra expressed as percentages of fundamental magnitude with: (a) ANN-MPCC, (b) MPCC

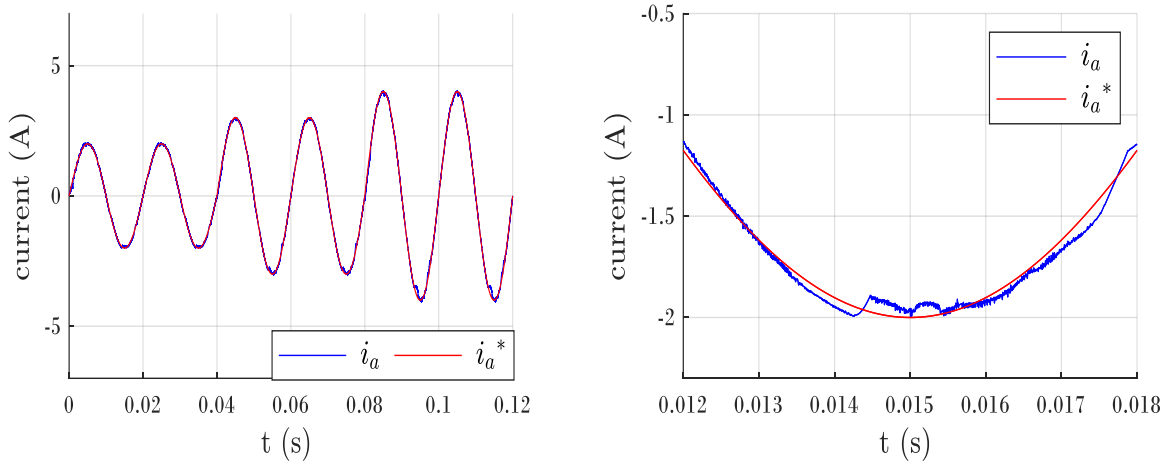

(a)

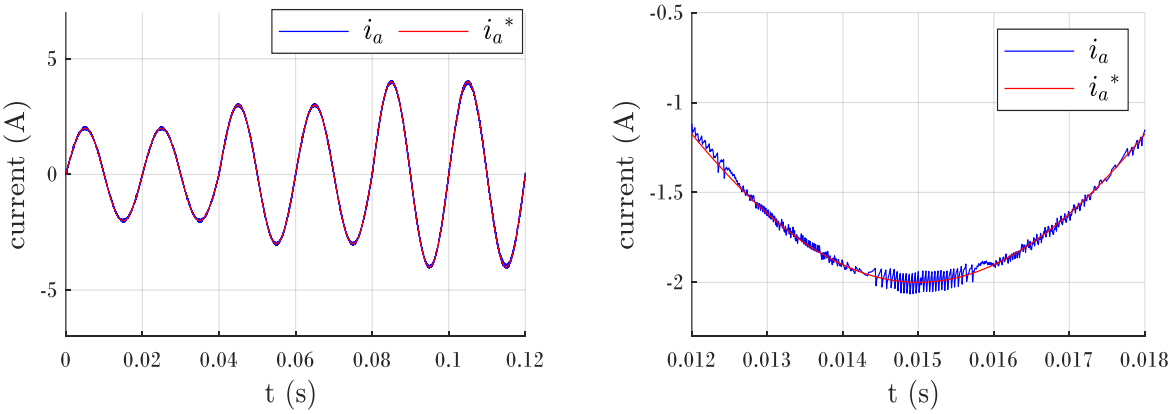

(b)

Figure IV- 15 : Simulation results of an IMC-fed RL-load: Reference and output current of phase A and their zoom with: (a) ANN-MPCC, (b) MPC

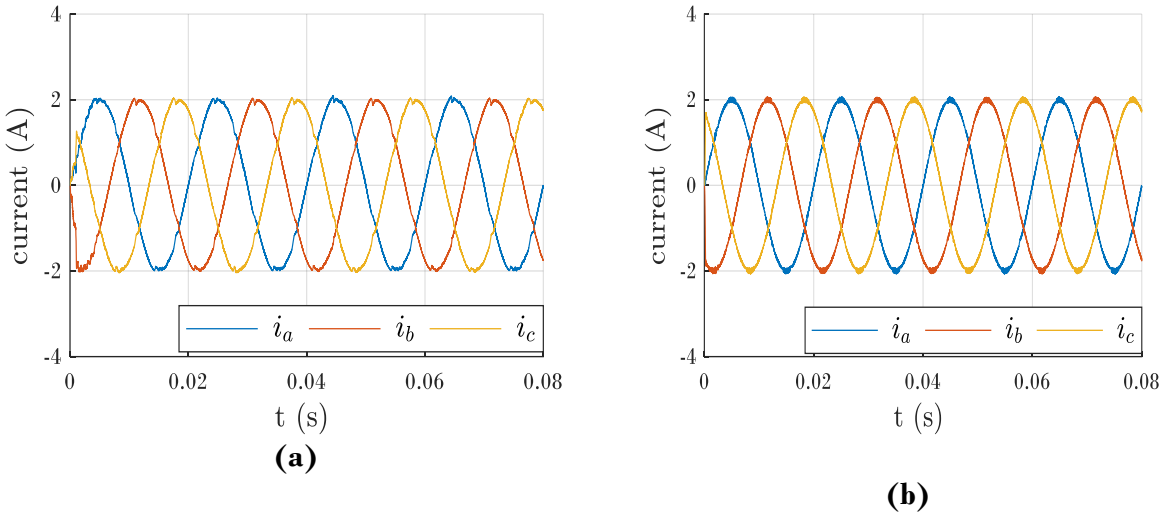

Figure IV- 16: Simulation results of an IMC-fed RL-load of load currents with: (a) ANN-MPCC, (b) MPC

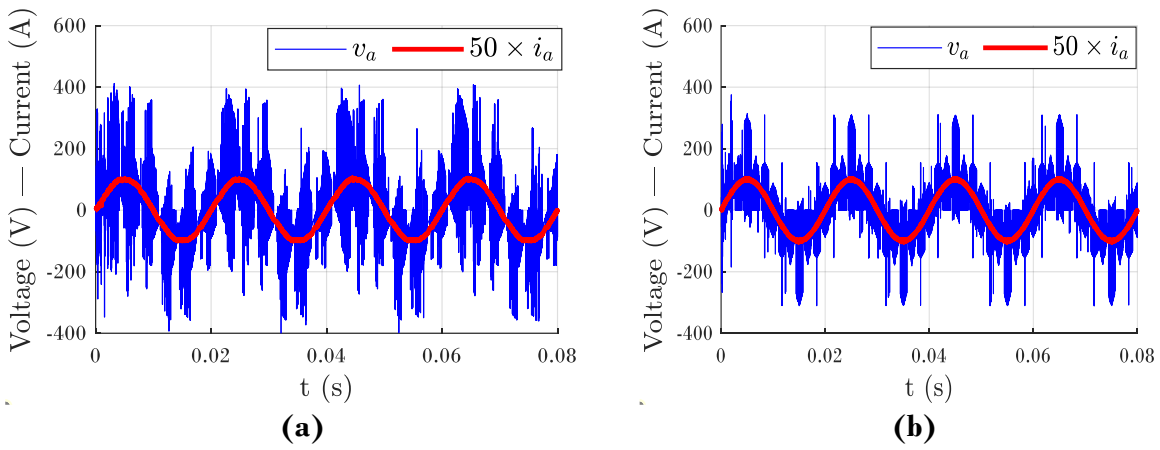

Figure IV- 17: Simulation results of an IMC-fed RL-load of load voltage and currents of phase A phase A with: (a) ANN-MPCC, (b) MPC

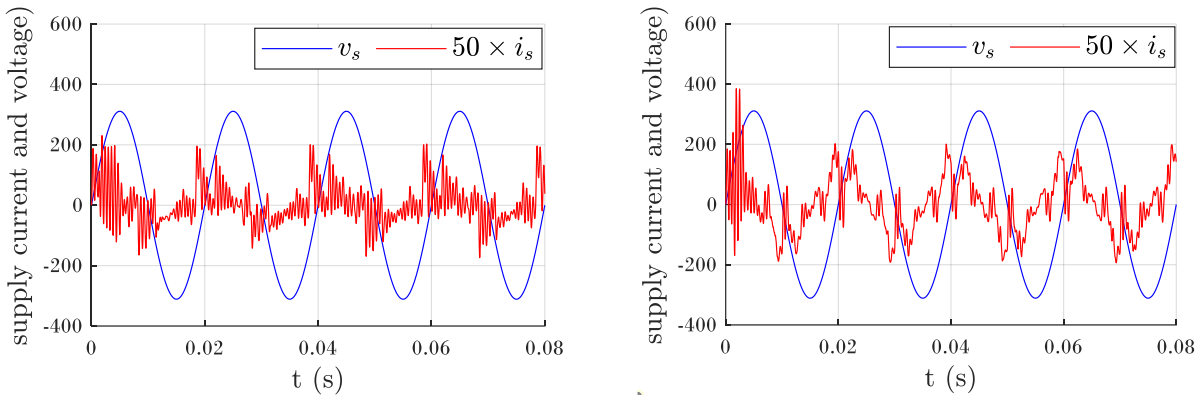

Figure IV- 18 : Simulation results of an IMC-fed RL-load of supply current and of phase A with: (a) ANN-MPCC, (b) MPC

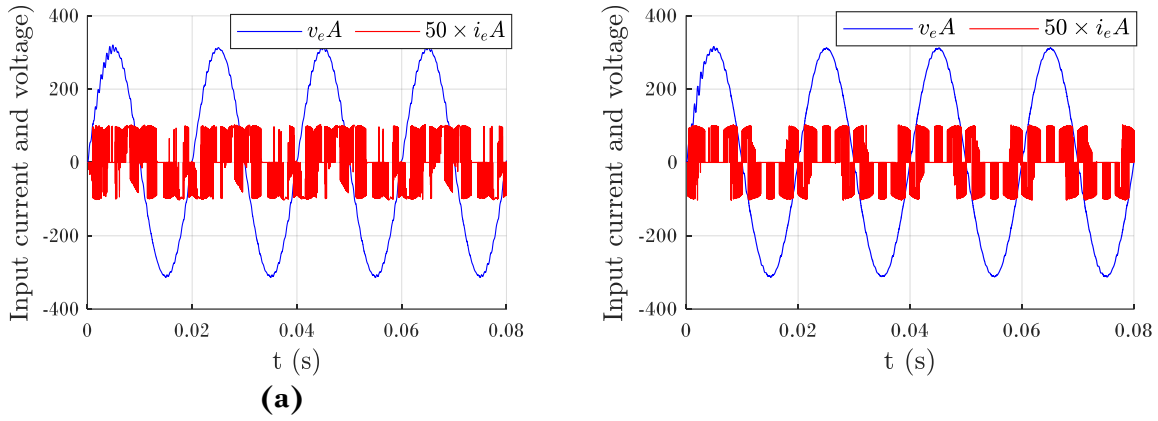

Figure IV- 19 : Simulation results of an IMC-fed RL-load of input current and voltage of DMC of phase A with: (a) ANN-MPCC, (b) MPC

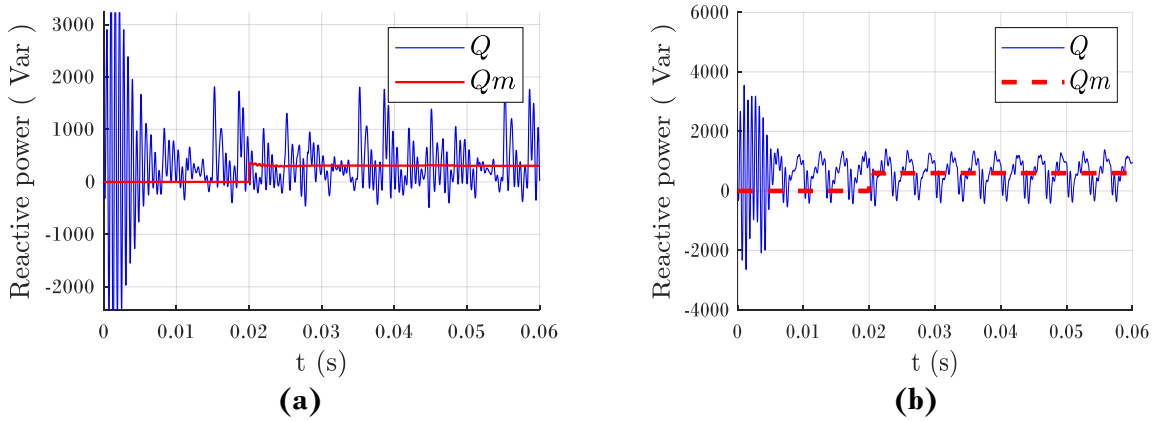

Figure IV- 20: Simulation results of an IMC-fed RL-load of the input reactive power and its moving average value with: (a) ANN-MPCC, (b) MPC

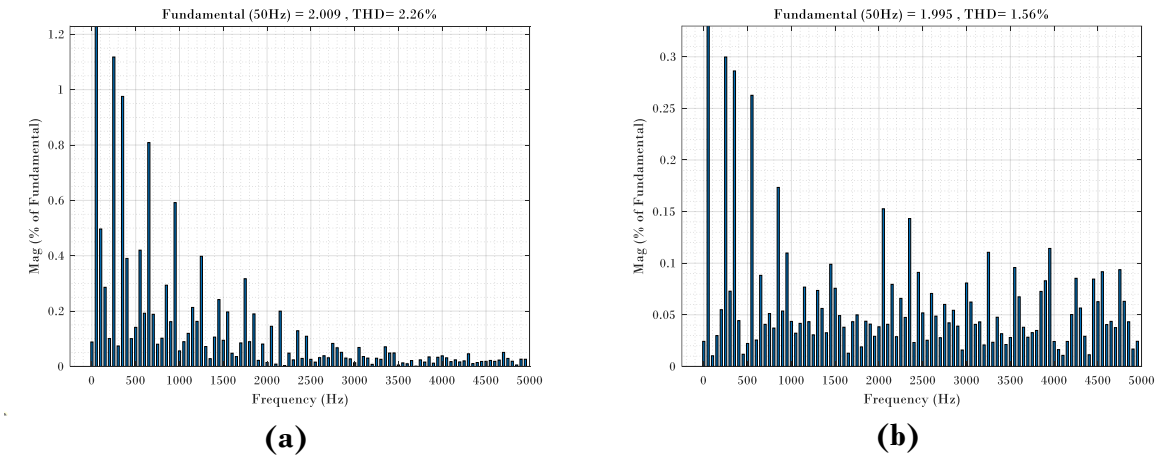

Figure IV- 21 : Simulation results of an IMC-fed RL-load of Output current spectra expressed as percentages of fundamental magnitude with: (a) ANN-MPCC, (b) MPCC

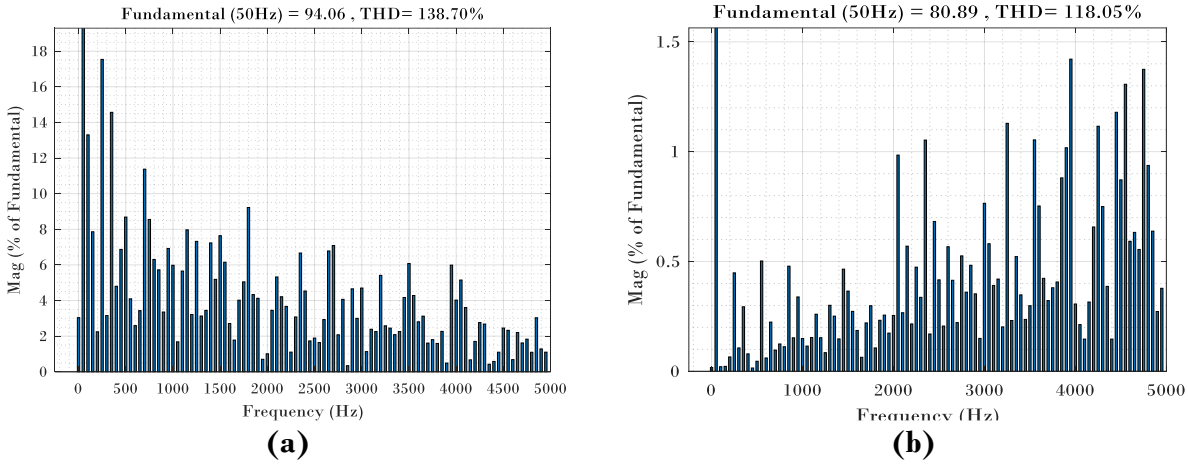

Figure IV- 22: Simulation results of an IMC-fed RL-load of Output voltage spectra expressed as percentages of fundamental magnitude with: (a) ANN-MPCC, (b) MPCC

Figures from Figure IV-7 to Figure IV-14 present the simulation results of ANN-MPCC of DMC fed RL load and from Figure IV-15 to Figure IV-22 present the simulation results of ANN-MPCC of IMC-fed RL-load

Figure IV-7 and Figure IV-15show the simulation steady performance of ANN-MPC controller of DMC-fed RL-load, IMC-fed RL-load respectively.From Figure IV-7 (a) and Figure IV-15 (a), the outputs currents of the two topologies are controlled to track their references (different magnitudes). From their zoom, it observed that the output current properly fitted on its reference with a smooth wave form, minimum ripples with ANN-MPC

while in theFigure IV-7 (b) and Figure IV-15 (b), the output current of MPC oscillates around its reference forming a ripple, or a band, around the reference

In term of comparison between the two topologies controlled by ANN-MPC,it can be observed that the oscillations of the output current are more important with the indirect topology compared to direct one.

Figure IV-8 to Figure IV-11 and from Figure IV-16 to Figure IV-19 present the behaviour of the system of both converters, with the control of the input reactive power on MPCC, compare to AN-MPCC where the input reactive power is incontrollable.

A phase shift between the supply voltage and current plus an almost chaotic behaviour of the supply current and the input reactive power.

The noticeable difference in the supply current and in the input reactive power at transient state is due the different simulation components. In the DMC topology, the models (II.1), (IV.5) and (IV.6) have been used. Whereas in the IMC topology, components from the *SimPowerSystems* library in Simulink, which are more reliable because they take into account phenomena that have been neglected in this thesis such as the magnetic saturation of the power switches and diode forward voltage drop, which gives more reliable results.

In term quality of wave-form and for voltage and current output, the proposed strategy for the two topologies gives better results than conventional MPCC, particularly results given byANN-MPC of DMC-fed RL-load.

Figure IV.12 and Figure IV.20, show the reactive power and its average value of the ANN-MPCC and MPCC fed DMC-fed RL-load, IMC-fed RL-load respectively, as mentioned above, reactive power is not controllable by the proposed strategy, as expected the conventional strategy have better average value and better shape with minimum ripples.

Figure IV-13, Figure IV-14, Figure IV-21 and Figure IV-22 present the output current and voltage spectra expressed as percentages of the fundamental magnitude of both topologies with the two controllers. The THD of the output current of the proposed strategy of DMC-fed RL-load decreased to 1.03 compared to MPCC while in ANN-MPCCof

IMC-fed RL-load, THD increase compared to MPCC. Same thing for the THD of output voltage of DMC and IMPC the results of PMCC is better than the ANN-MPCC

IV.8 Conclusion

The work and study done in this chapter have discussed the control of matrix converter of two topologies direct and indirect fed RL load, using neural network based MPCC method. The obtained results have shown that the use of ANN-MPCC control method is improved ,in term lower THD of output current and voltage in ANN-MPCC of direct matrix converter compared to MPCC .While in ANN-MPCC of indirect matrix converter, results appeared the non-efficiently of proposed strategy compared to conventional strategy . From the obtained results we can conclude that ANN-MPCC of matrix converter particularly ANN-MPCC of DMC is improved. The use of ANN-MPCC could be improved by ranging maximum samples of data with different conditions or adding another features as inputs to train neural network.

General conclusion

GENERAL CONCLUSION

In power electronics, the control system has always been a key issue since they influence drastically the overall system performances. In order to achieve the necessary regulation, a controller in a feedback loop is needed.The main drawback of MPC is that the computational time necessary to calculate a control signal at each sampling time can be much greater than the amount of time that is available in a real time setting, the major drawback is the low computation efficiency [48] and the huge amount of real-time calculations [13]. For this reason, most of the methods used to overcome these disadvantages are accomplished by replacing another strategy more efficient.

In this work, and in order to solve the problem discussed in chapter I, a neural network based Model Predictive Control schemes have been applied to power converters associated with a RL-load and with an induction machine, namely the 2LVSI, the DMC and the IMC. The study was done by simulation in the MATLAB/Simulink environment.

Our work is summarized in four chapter, it began with a state of art which introduced a general description of power converters, a description of the most famous topologies of matrix converters. Then followed by brief description of the MPC, working principle, its applications and its major drawback. The first chapter ended with an overview of a novel proposed strategy of control such as artificial neural network. This bibliographic study has shown that this topic is contemporary and promising, attracting the attention of researchers around the world.

In the second chapter, the proposed strategy “neural network based on predictive current control” was introduced. Both the converter and the load have been modeled and a training procedure was explained with two different algorithms. The ANN-MPCC proved its performance in term of quality and lower THD compared to the conventional strategy control in many experience conditions. The inverter allows, thanks to the NN-MPCC, to control the output current in magnitude and frequency. In order to improve the efficient of the control proposed in term of burden time reduction.The chapter was concluded by a real time implementation of the ANN-MPC .

The non-linearity of 2LVSI make the ANN-MPCC of a 2LVSI-fed RL-load one of the simplest control schemes, in terms of training, complexity of neural architecture and of calculation power.

In the third chapter, the neural network based on MPTC control applied to an induction motor that is fed by a 2LVSI has been introduced, the induction machine has been modeled in a way that suits the control scheme and a cost function has been expressed in order to satisfy the objective of the MPTC control. MPTC was used, as an expert, in the training phase to generate data required for training the proposed neural network. Then, once the neural network is fine-tuned, it can be successfully used online for controlling, without the need of using MPTC.

Simulation results demonstrate the excellent performance of the proposed ANN-MPTC for induction machine fed 2LVSI, while the good responses of the flux, torque, and speed also has the good robustness when the load torque TL is changed. Moreover, that under identical conditions the results obtained by the use of proposed method, are improved compared to classical MPTC, which is especially true for the torque, flux and stator current ripple. Torque ripple is reduced by a considerable ratio due to soft interpolation property of ANN. Furthermore,the proposed ANN-based controller performs better than MPTC, in terms of a lower THD of stator current.

The last chapter presents an ANN-MPCC scheme of an RL-load fed by a matrix converter with both topologies direct and indirect. The modeling of both converters was presented alongside with the modeling of the input filter. The phase shift at the input of the converter between the current and the voltage is also controllable for the both topologies.

Furthermore, both topologies did not allow the control of the input reactive power, although the use of reference and output reactive power as inputs, hence just the current output of three phases was controlled.

In addition, in terms of a lower THD of output voltage, ANN- MPCC shows a better control performance in term of lower voltage output THD compared to conventional strategy for the two topologies while current output THD is improved only in ANN- MPC of DMC fed RL load.

Human comportment and thinking form the basis of intelligent control techniques. By adopting techniques based on artificial intelligence, the performance of linear and nonlinear control systems can be further improved. Neural network controllers are proposed for MPC

for linear and non-linear loads under different operating conditions fed different topologies of power converter. The simulations results discussed in precedent thesisprove the efficient robustness of proposed strategy.

According to the studies conducted in this thesis, the neural network based on predictive control has the following advantages:

- A great capacity in predicting model (even with different situations of those used for training phase).
- Appealing attributes of nonlinear identification and control.
- Suitable for non-mathematical models.
- Able to manage abundant number of data and input variables.
- Trustworthy predictions.

Although this advantages a neural network has the following disadvantages

- Operating a neural network needs to be trained and need a good database.
- Takes long time to process of a large neural network
- Expending a lot of time for off-line training.
- Quality of the predictions need a large amount of data.

As a perspective to this work, we plan to:

- Improving the results of ANN-MPCC fed matrix converter in order to control the reactive power also.
- Study NN-MPTC for induction machine fed a matrix converter, direct and indirect topologies.
- Study other MC topologies; multilevel IMC, sparse IMC and five phases MC in particular.
- Implement the control strategy on a Field-Programmable Gate Array (FPGA) card to control an induction machine for the experimental validation.

References

References

[1] B. K. Bose, « Energy, environment, and advances in power electronics », 2000, vol. 1, p. TU1-T14.

[2] S. Kouro, M. A. Perez, J. Rodriguez, A. M. Llor, et H. A. Young, « Model predictive control: MPC's role in the evolution of power electronics », *IEEE Ind. Electron. Mag.*, vol. 9, nº 4, p. 8-21, 2015.

[3] J. Petrovcic et S. Strmcnik, « A microcomputer-based speed controller for lift drives », *IEEE Trans. Ind. Appl.*, vol. 24, nº 3, p. 487-498, 1988.

[4] C. Buccella, C. Cecati, et H. Latafat, « Digital control of power converters—A survey », *IEEE Trans. Ind. Inform.*, vol. 8, nº 3, p. 437-447, 2012.

[5] J. J. Rodríguez-Andina, M. D. Valdes-Pena, et M. J. Moure, « Advanced features and industrial applications of FPGAs—A review », *IEEE Trans. Ind. Inform.*, vol. 11, nº 4, p. 853-864, 2015.

[6] A. Fathy Abouzeid *et al.*, « Control strategies for induction motors in railway traction applications », *Energies*, vol. 13, nº 3, p. 700, 2020.

[7] A. M. El-Refaie, « Motors/generators for traction/propulsion applications: A review », *IEEE Veh. Technol. Mag.*, vol. 8, nº 1, p. 90-99, 2013.

[8] S. J. Qin et T. A. Badgwell, « A survey of industrial model predictive control technology », *Control Eng. Pract.*, vol. 11, nº 7, p. 733-764, 2003.

[9] B. Schenker et M. Agarwal, « Predictive control of a bench-scale chemical reactor based on neural-network models », *IEEE Trans. Control Syst. Technol.*, vol. 6, nº 3, p. 388-400, 1998.

[10] S.-F. Mo et J. Billingsley, « Fast-model predictive control of multivariable systems », 1990, vol. 137, nº 6, p. 364-366.

[11] S. Gdaim, N. Slama, A. Mtibaa, et M. F. Mimouni, « Direct Torque Control based on Artificial Neural Networks of Induction Machine ».

[12] L. Romeral, A. Arias, E. Aldabas, et M. G. Jayne, « Novel direct torque control (DTC) scheme with fuzzy adaptive torque-ripple reduction », *IEEE Trans. Ind. Electron.*, vol. 50, nº 3, p. 487-492, 2003.

[13] I. S. Mohamed, S. Rovetta, T. D. Do, T. Dragicević, et A. A. Z. Diab, « A Neural-Network-Based Model Predictive Control of Three-Phase Inverter With an Output LC Filter », *IEEE Access*, vol. 7, p. 124737-124749, 2019, doi: 10.1109/ACCESS.2019.2938220.

[14] M.-K. Nguyen, « Power Converters in Power Electronics: Current Research Trends », 2020.

[15] J. W. Kolar, T. Friedli, F. Krismer, et S. Round, « The essence of three-phase AC/AC converter systems », 2008, p. 27-42.

[16] A. Tsoupos et V. Khadkikar, « A novel SVM technique with enhanced output voltage quality for indirect matrix converters », *IEEE Trans. Ind. Electron.*, vol. 66, nº 2, p. 832-841, 2018.

[17] E. Ibarra *et al.*, « New fault tolerant matrix converter », *Electr. Power Syst. Res.*, vol. 81, nº 2, p. 538-552, 2011.

[18] M. Hosseini Abardeh et R. Ghazi, « A Dynamic Model for Direct and Indirect Matrix Converters », *Adv. Power Electron.*, vol. 2014, p. 864203, avr. 2014, doi: 10.1155/2014/864203.

[19] S. Ansari et A. Chandel, « Simulation based comprehensive analysis of direct and indirect matrix converter fed asynchronous motor drive », in *2017 4th IEEE Uttar*

Pradesh Section International Conference on Electrical, Computer and Electronics (UPCON), oct. 2017, p. 9-15. doi: 10.1109/UPCON.2017.8251014.

[20] O. Abdel-Rahim, H. Abu-Rub, A. Iqbal, et A. Kouzou, « Five-to-three phase direct matrix converter with model predictive control », in *4th International Conference on Power Engineering, Energy and Electrical Drives*, mai 2013, p. 204-208. doi: 10.1109/PowerEng.2013.6635607.

[21] M. Y. Lee, « Three-level neutral-point-clamped matrix converter topology », 2009.

[22] J. Zhang, L. Li, et D. G. Dorrell, « Control and applications of direct matrix converters: A review », *Chin. J. Electr. Eng.*, vol. 4, nº 2, p. 18-27, 2018.

[23] L. Huber et D. Borojevic, « Space vector modulated three-phase to three-phase matrix converter with input power factor correction », *IEEE Trans. Ind. Appl.*, vol. 31, nº 6, p. 1234-1246, 1995.

[24] M. Hamouda, H. F. Blanchette, et K. Al-Haddad, « Indirect Matrix Converters' Enhanced Commutation Method », *IEEE Trans. Ind. Electron.*, vol. 62, nº 2, p. 671-679, févr. 2015, doi: 10.1109/TIE.2014.2341583.

[25] C. Klumpner, « An indirect matrix converter with a cost effective protection and control », in *2005 European Conference on Power Electronics and Applications*, sept. 2005, p. 11 pp.-P.11. doi: 10.1109/EPE.2005.219558.

[26] H. J. Cha, « Analysis and design of matrix converters for adjustable speed drives and distributed power sources », 2004.

[27] L. Rmili, S. Rahmani, H. Vahedi, et K. Al-Haddad, « Comprehensive analysis of Matrix Converters: Indirect topology », in *2014 15th International Conference on Sciences and Techniques of Automatic Control and Computer Engineering (STA)*, déc. 2014, p. 679-684. doi: 10.1109/STA.2014.7086728.

[28] L. Rmili, S. Rahmani, et K. Al-Haddad, « Sparse matrix converter: Modeling and PWM control », in *2015 IEEE 24th International Symposium on Industrial Electronics (ISIE)*, juin 2015, p. 411-416. doi: 10.1109/ISIE.2015.7281503.

[29] Yong Shi, Xu Yang, Qun He, et Zhaoan Wang, « Research on a novel capacitor clamped multilevel matrix converter », *IEEE Trans. Power Electron.*, vol. 20, nº 5, p. 1055-1065, sept. 2005, doi: 10.1109/TPEL.2005.854027.

[30] P. C. Loh, F. Blaabjerg, F. Gao, A. Baby, et D. A. C. Tan, « Pulsewidth Modulation of Neutral-Point-Clamped Indirect Matrix Converter », *IEEE Trans. Ind. Appl.*, vol. 44, nº 6, p. 1805-1814, déc. 2008, doi: 10.1109/TIA.2008.2006321.

[31] Y. Sun, W. Xiong, M. Su, X. Li, H. Dan, et J. Yang, « Topology and Modulation for a New Multilevel Diode-Clamped Matrix Converter », *IEEE Trans. Power Electron.*, vol. 29, nº 12, p. 6352-6360, déc. 2014, doi: 10.1109/TPEL.2014.2305711.

[32] *Model Predictive Control System Design and Implementation Using MATLAB®*. London: Springer London, 2009. doi: 10.1007/978-1-84882-331-0.

[33] « Model Predictive Control by E. F. Camacho, C. Bordons (z-lib.org).pdf ».

[34] M. Grimble, « LQG predictive optimal control for adaptive applications », *Automatica*, vol. 26, nº 6, p. 949-961, 1990.

[35] D. Linkers et M. Mahfonf, « Advances in Model-based predictive control, chapter Generalised predictive control in clinical anaesthesia », 1994.

[36] S. Vazquez, J. Rodriguez, M. Rivera, L. G. Franquelo, et M. Norambuena, « Model Predictive Control for Power Converters and Drives: Advances and Trends », *IEEE Trans. Ind. Electron.*, vol. 64, nº 2, p. 935-947, févr. 2017, doi: 10.1109/TIE.2016.2625238.

[37] A. M. Dadu, S. Mekhilef, et T. K. Soon, « Lyapunov model predictive control to optimise computational burden, reference tracking and THD of three-phase four-leg inverter », *IET Power Electron.*, vol. 12, nº 5, p. 1061-1070, 2019.
[38] J. H. Lee, « Model predictive control: Review of the three decades of development », *Int. J. Control Autom. Syst.*, vol. 9, nº 3, p. 415-424, 2011.
[39] J. Rodriguez et P. Cortes, *Predictive control of power converters and electrical drives*, vol. 40. John Wiley & Sons, 2012.
[40] Y. Tan et R. De Keyser, « Neural network based adaptive control », in *Advances in model based predictive control*, Oxford University Press, 1994, p. 358-369.
[41] I. Škrjanc et D. Matko, *Fuzzy predictive controller with adaptive gain*. 1994.
[42] J. Rodriguez *et al.*, « State of the art of finite control set model predictive control in power electronics », *IEEE Trans. Ind. Inform.*, vol. 9, nº 2, p. 1003-1016, 2012.
[43] S. Vazquez *et al.*, « Model predictive control: A review of its applications in power electronics », *IEEE Ind. Electron. Mag.*, vol. 8, nº 1, p. 16-31, 2014.
[44] E. Fernandez-Camacho et C. Bordons-Alba, *Model Predictive Control in the Process Industry*. London: Springer London, 1995. doi: 10.1007/978-1-4471-3008-6.
[45] J. H. Lee, « Model predictive control: Review of the three decades of development », *Int. J. Control Autom. Syst.*, vol. 9, nº 3, p. 415-424, 2011.
[46] L. Yan et X. Song, « Design and Implementation of Luenberger Model-Based Predictive Torque Control of Induction Machine for Robustness Improvement », *IEEE Trans. Power Electron.*, vol. 35, nº 3, p. 2257-2262, mars 2020, doi: 10.1109/TPEL.2019.2939283.
[47] W. C. Wong et J. H. Lee, « Postdecision-state-based approximate dynamic programming for robust predictive control of constrained stochastic processes », *Ind. Eng. Chem. Res.*, vol. 50, nº 3, p. 1389-1399, 2011.
[48] Z. Liu *et al.*, « Recurrent Model Predictive Control », *ArXiv Prepr. ArXiv210210289*, 2021.
[49] S. Kwak, U. Moon, et J. Park, « Predictive-Control-Based Direct Power Control With an Adaptive Parameter Identification Technique for Improved AFE Performance », *IEEE Trans. Power Electron.*, vol. 29, nº 11, p. 6178-6187, nov. 2014, doi: 10.1109/TPEL.2014.2298041.
[50] H. Miranda, P. Cortes, J. I. Yuz, et J. Rodriguez, « Predictive Torque Control of Induction Machines Based on State-Space Models », *IEEE Trans. Ind. Electron.*, vol. 56, nº 6, p. 1916-1924, juin 2009, doi: 10.1109/TIE.2009.2014904.
[51] R. Vargas, P. Cortes, U. Ammann, J. Rodriguez, et J. Pontt, « Predictive Control of a Three-Phase Neutral-Point-Clamped Inverter », *IEEE Trans. Ind. Electron.*, vol. 54, nº 5, p. 2697-2705, oct. 2007, doi: 10.1109/TIE.2007.899854.
[52] P. Cortes, J. Rodriguez, D. E. Quevedo, et C. Silva, « Predictive Current Control Strategy With Imposed Load Current Spectrum », *IEEE Trans. Power Electron.*, vol. 23, nº 2, p. 612-618, mars 2008, doi: 10.1109/TPEL.2007.915605.
[53] X. Zhang, L. Zhang, et Y. Zhang, « Model Predictive Current Control for PMSM Drives With Parameter Robustness Improvement », *IEEE Trans. Power Electron.*, vol. 34, nº 2, p. 1645-1657, févr. 2019, doi: 10.1109/TPEL.2018.2835835.
[54] S. Hanke, S. Peitz, O. Wallscheid, J. Böcker, et M. Dellnitz, « Finite-Control-Set Model Predictive Control for a Permanent Magnet Synchronous Motor Application with Online Least Squares System Identification », in *2019 IEEE International Symposium on Predictive Control of Electrical Drives and Power Electronics (PRECEDE)*, juin 2019, p. 1-6. doi: 10.1109/PRECEDE.2019.8753313.

[55] T. Orłowska-Kowalska, F. Blaabjerg, et J. Rodríguez, Éd., *Advanced and Intelligent Control in Power Electronics and Drives*, vol. 531. Cham: Springer International Publishing, 2014. doi: 10.1007/978-3-319-03401-0.

[56] J.-F. Qiao et H.-G. Han, « Identification and modeling of nonlinear dynamical systems using a novel self-organizing RBF-based approach », *Automatica*, vol. 48, nº 8, p. 1729-1734, 2012.

[57] H. Han et J. Qiao, « Hierarchical neural network modeling approach to predict sludge volume index of wastewater treatment process », *IEEE Trans. Control Syst. Technol.*, vol. 21, nº 6, p. 2423-2431, 2013.

[58] H. Han, L. Zhang, Y. Hou, et J. Qiao, « Nonlinear Model Predictive Control Based on a Self-Organizing Recurrent Neural Network », *IEEE Trans. Neural Netw. Learn. Syst.*, vol. 27, nº 2, p. 402-415, févr. 2016, doi: 10.1109/TNNLS.2015.2465174.

[59] D. Sobajic et Y. Pao, « Associative computing with artificial neural networks in electric power systems engineering », présenté à First Workshop on Neural Networks, 1990.

[60] I. S. Mohamed, S. Rovetta, T. D. Do, T. Dragicević, et A. A. Z. Diab, « A Neural-Network-Based Model Predictive Control of Three-Phase Inverter With an Output LC Filter », *IEEE Access*, vol. 7, p. 124737-124749, 2019, doi: 10.1109/ACCESS.2019.2938220.

[61] S. M. Halpin et R. F. Burch, « Applicability of neural networks to industrial and commercial power systems: a tutorial overview », in *Proceedings of 1996 IAS Industrial and Commercial Power Systems Technical Conference*, mai 1996, p. 75-81. doi: 10.1109/ICPS.1996.533939.

[62] D. Pham et D. Karaboga, *Intelligent optimisation techniques: genetic algorithms, tabu search, simulated annealing and neural networks*. Springer Science & Business Media, 2012.

[63] S. Tiwari, R. Naresh, et R. Jha, « Neural network predictive control of UPFC for improving transient stability performance of power system », *Appl. Soft Comput.*, vol. 11, nº 8, p. 4581-4590, 2011.

[64] Z. Yan et J. Wang, « Robust Model Predictive Control of Nonlinear Systems With Unmodeled Dynamics and Bounded Uncertainties Based on Neural Networks », *IEEE Trans. Neural Netw. Learn. Syst.*, vol. 25, nº 3, p. 457-469, mars 2014, doi: 10.1109/TNNLS.2013.2275948.

[65] Y. Pan et J. Wang, « Model Predictive Control of Unknown Nonlinear Dynamical Systems Based on Recurrent Neural Networks », *IEEE Trans. Ind. Electron.*, vol. 59, nº 8, p. 3089-3101, août 2012, doi: 10.1109/TIE.2011.2169636.

[66] Z. Yan et J. Wang, « Model Predictive Control of Nonlinear Systems With Unmodeled Dynamics Based on Feedforward and Recurrent Neural Networks », *IEEE Trans. Ind. Inform.*, vol. 8, nº 4, p. 746-756, nov. 2012, doi: 10.1109/TII.2012.2205582.

[67] F. Murtagh et M. Hernández-Pajares, « The Kohonen self-organizing map method: an assessment », *J. Classif.*, vol. 12, nº 2, p. 165-190, 1995.

[68] S. Solla, « Generalization in feedforwad neural networks », présenté à Proc. the IEEE International Joint Conference on Neural Networks (Seattle), 1991, 1991.

[69] T. Sasakawa, J. Hu, et K. Hirasawa, « Self-organized function localization neural network », in *2004 IEEE International Joint Conference on Neural Networks (IEEE Cat. No.04CH37541)*, juill. 2004, vol. 2, p. 1463-1468 vol.2. doi: 10.1109/IJCNN.2004.1380168.

[70] P. Cortes, J. Rodriguez, C. Silva, et A. Flores, « Delay Compensation in Model Predictive Current Control of a Three-Phase Inverter », *IEEE Trans. Ind. Electron.*, vol. 59, nº 2, p. 1323-1325, févr. 2012, doi: 10.1109/TIE.2011.2157284.
[71] S. Sabzevari, R. Heydari, M. Mohiti, M. Savaghebi, et J. Rodriguez, « Model-free neural network-based predictive control for robust operation of power converters », *Energies*, vol. 14, nº 8, p. 2325, 2021.
[72] M. H. Beale, M. T. Hagan, et H. B. Demuth, « Neural network toolbox user's guide », *MathWorks Inc*, vol. 103, 1992.
[73] C. A. ROJAS MONRROY, « MULTIOBJETIVE FINITE CONTROL SET MODEL PREDICTIVE TORQUE AND STATOR FLUX CONTROL OF AN INDUCTION MACHINE », 2013.
[74] N. Vahdatifar, S. Mortazavi, et R. Kianinezhad, « Neural Network Based Predictive DTC Algorithm for Induction Motors », *Int. J. Electr. Comput. Eng.*, vol. 4, nº 11, p. 5, 2010.
[75] J. Holtz, « The representation of AC machine dynamics by complex signal flow graphs », *IEEE Trans. Ind. Electron.*, vol. 42, nº 3, p. 263-271, 1995.
[76] J. Holtz, « The representation of AC machine dynamics by complex signal flow graphs », *IEEE Trans. Ind. Electron.*, vol. 42, nº 3, p. 263-271, juin 1995, doi: 10.1109/41.382137.
[77] A. Benachour, « Commande sans capteur basée sur DTC d'une machine asynchrone alimentée par Convertisseur Matriciel », PhD, ENP, Algiers, 2017.
[78] M. Ndaliman, M. Hazza, A. Khan, et M. Ali, « Development of a new model for predicting EDM properties of Cu-TaC compact electrodes based on artificial neural network method », *Aust. J. Basic Appl. Sci.*, vol. 6, nº 13, p. 192-199, 2012.
[79] J. Andreu, I. M. de Alegria, I. Kortabarria, J. L. Martin, et S. Ceballos, « Improvement of the Matrix Converter Start-up Process », 2007, p. 1811-1816.
[80] S. F. Pinto et J. F. Silva, « Input filter design for sliding mode controlled matrix converters », 2001, vol. 2, p. 648-653.
[81] F. Fnaiech et K. Al-Haddad, « Input filter design for SVM dual-bridge matrix converters », 2006, vol. 2, p. 797-802.
[82] J. Rodriguez et P. Cortes, *Predictive control of power converters and electrical drives*, vol. 40. John Wiley & Sons, 2012.

Appendices

APPENDIX A

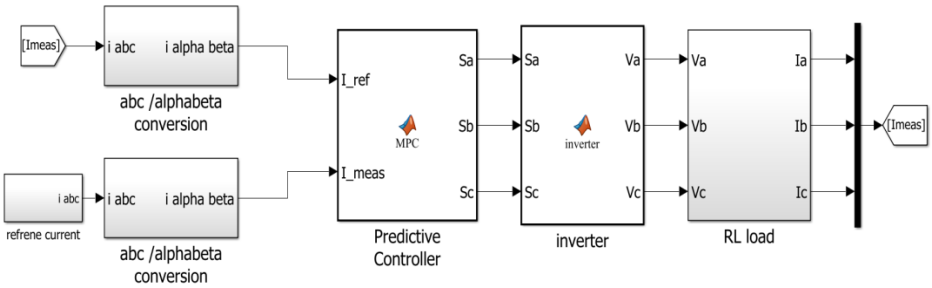

(a)

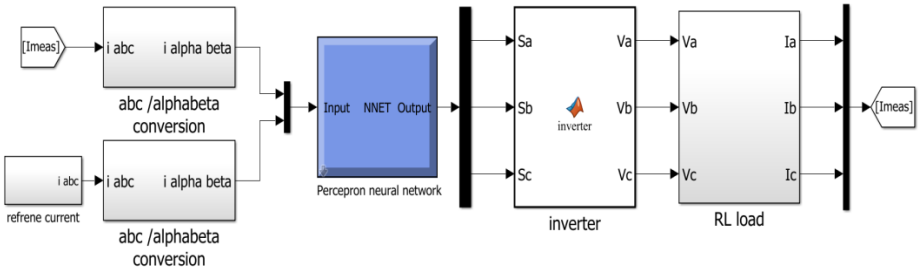

(b)

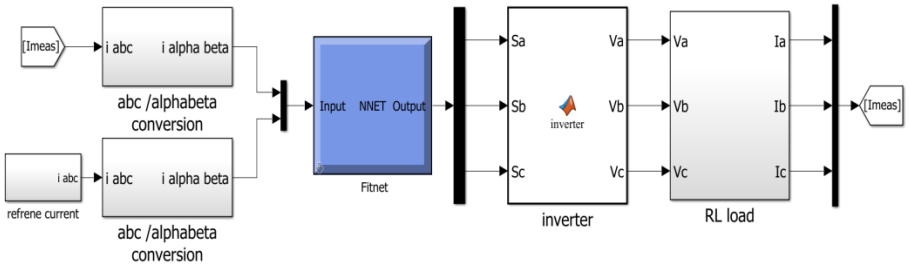

(c)

Figure A- 1 : Simulink model of a 2 level inverter fed RL load of: (a) MPC, (b) PNN, (c) Fitnet

Table A- 1 : Simulation parameters for the MPCC / PNN / Fitnet of an inverter fed RL load

Parameter	Value
Fixed-step size	5 μs
Solver	ode3
Tasking mode	SingleTasking
Resistance	50Ω
Inductance	20 mH
DC voltage	300 V

APPENDIX B

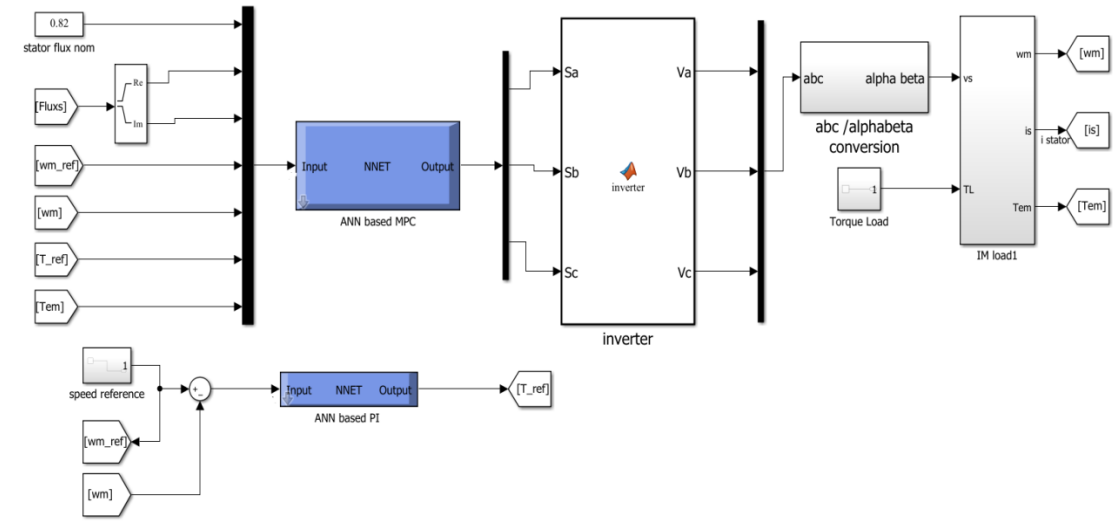

(a)

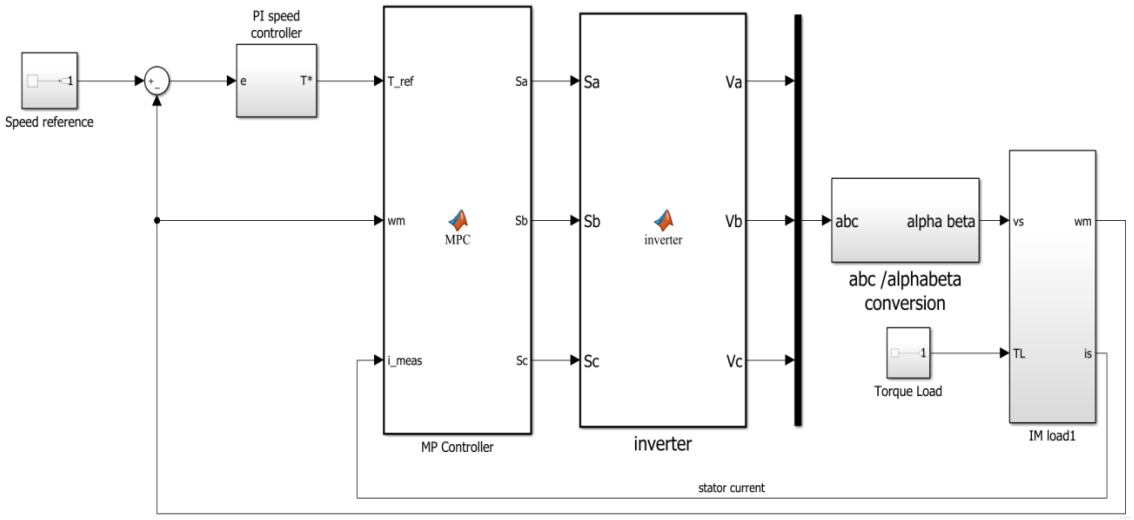

(b)

Figure B- 1 : Simulink model of a 2LVSI fed induction machine with: (a) ANN-MPTC (b) MPTC

Table B- 1: Machine parameters

Description	Variables	Values
Rated power	P_{nom}	1.5 kW
Rated torque	T_{nom}	15 N.m
Rated speed	Ω_{nom}	157 rad/s
Rated stator current (RMS)	I_{nom}	6.7 A
Stator resistance	R_s	4.85Ω
Stator inductance	L_s	0.274 H
Rotor resistance	R_r	6.3Ω
Rotor inductance	L_r	0.274 H
Magnetizing inductance	L_m	0.258 H
Pole pairs	p	2
Dry friction coefficient	k_f	N.m.s.rad^{-1}
Moment of inertia	J	0.031 kg.m^2

Table B- 2 : Simulation parameters for the MPTC of an inverter fed IM

Description	Variables	Values
Fixed-step size	-	5 μs
Solver	-	ode3
Tasking mode	-	SingleTasking
Supply voltage	V_{DC}	500 V
Damping coefficient	ξ	0.7
Natural circular pulse	ω_n	100π rad/s
Weighting factors	λ_T	0.0667 N^{-1}m^{-1}
	λ_φ (case 1)	1.2195 Wb^{-1}
	λ_φ (case 2)	3.6585 Wb^{-1}

APPENDIX C

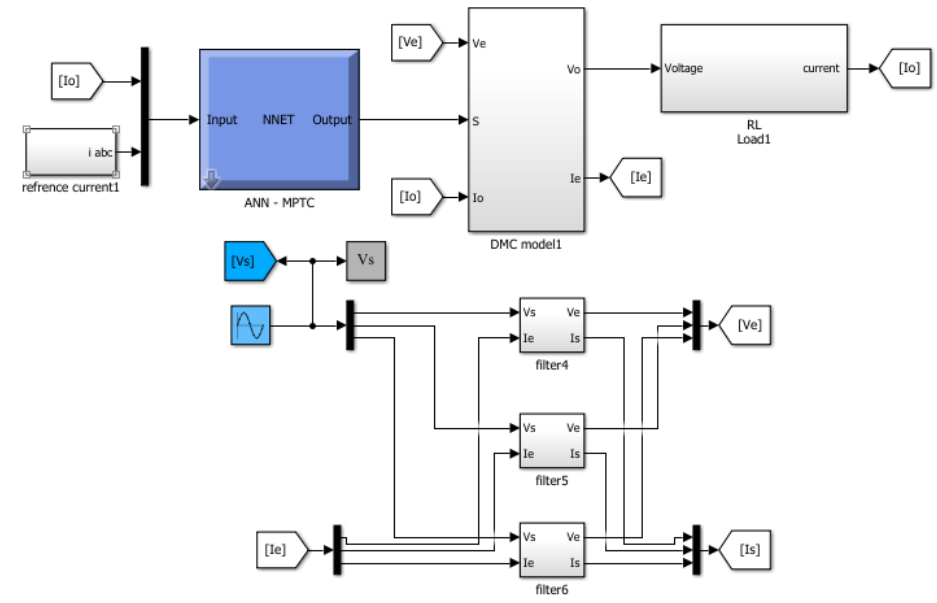

(a)

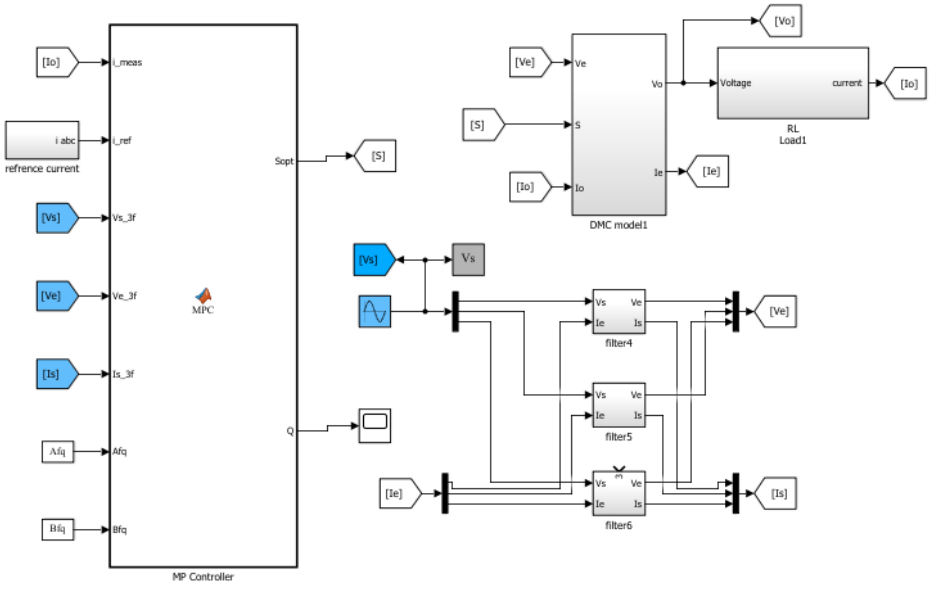

(b)

Figure C- 1 : Simulink model of a DMC-fed RL-load with: (a) ANN-MPCC, (b) MTCC

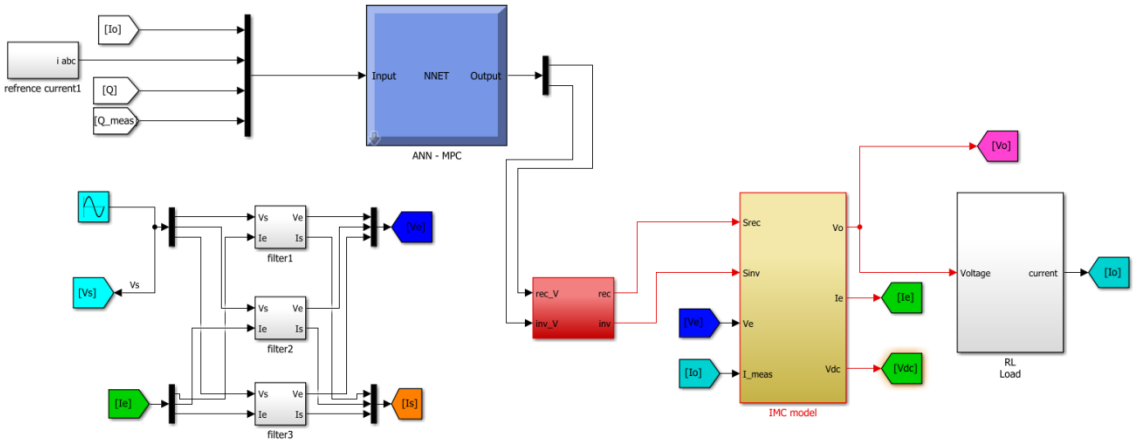

(c)

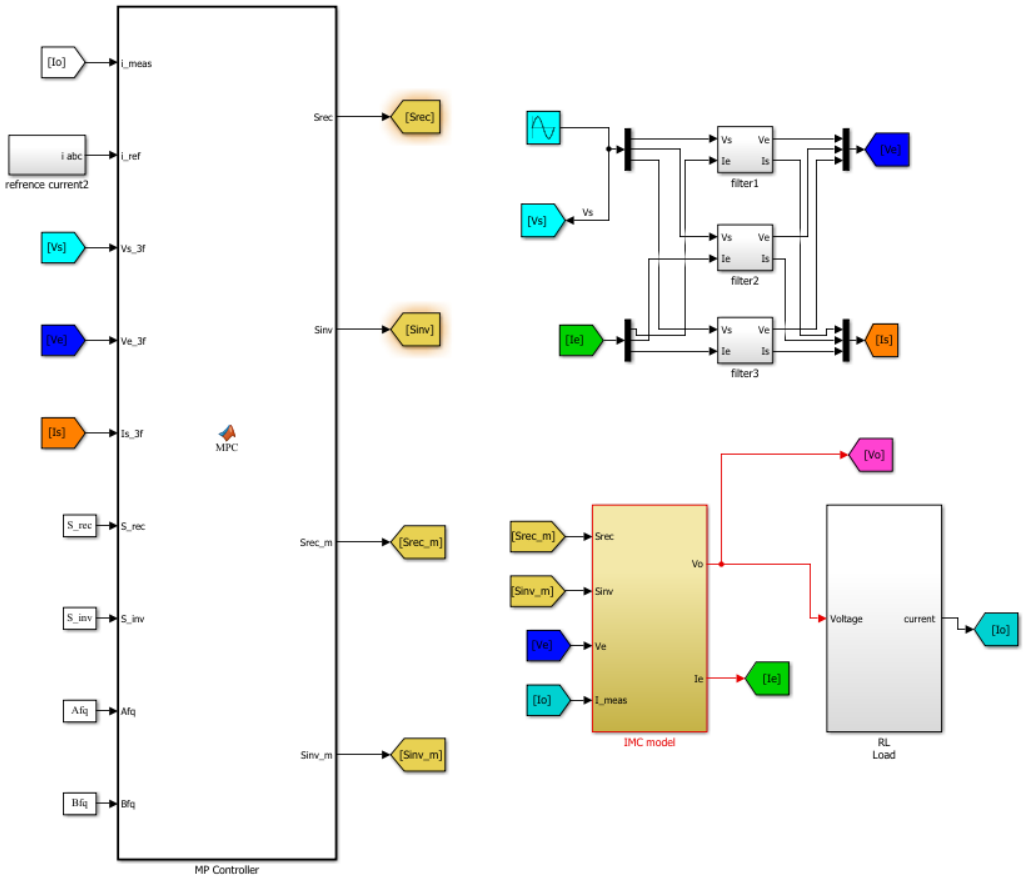

(d)

Figure C- 2 : Simulink model of IMC fed RL Load with (a): ANN-MPCC (b) MPCC

Table C- 1: Simulation parameters for the MPCC of a MC-fed RL-load

Description	Variables	Values
Fixed-step size	-	5 μs
Tasking mode	-	SingleTasking
Solver	-	ode3
Supply voltage (RMS)	v_s	220 V
Weighting factor	λ_Q	0.035

Table C- 2 : Filter parameters

Description	Variables	Values
Filter resistor	R_f	0.5 Ω
Filter inductor	L_f	400 µH
Filter capacitor	C_f	21 µF